

# Inter-American Photochemical Society Newsletter



I-APS Internet Address <http://www.chemistry.mcmaster.ca/~iaps>

This newsletter is available in pdf format from the web site.

**Volume 22 Number 2**

**November 1999**

I-APS Officers .....	
Letter from Linda Johnston, I-APS President.....	
Announcements.....	
Report on the XIXth International Confernece on Photochemistry.....	
International Conferneces on Photochemistry 1962-1999.....	
Light Compendium – Ultraviolet Principles and Applications.....	
Using Stark Spectroscopy to Probe Polymer and Organic Glass Matrices .....	
Tinkering with Stilbene.....	
Recent Noteworthy Articles in Organic Photochemistry and Photobiology .....	
Upcoming Meetings.....	
Registration Form for the I-APS	91

## I-APS Officers

### President

Linda J. Johnston  
Steacie Institute for Molecular  
Science  
National Research Council  
Ottawa, ON K1A 0R6  
ljj@ned1.sims.nrc.ca

### Vice President

Frederick D. Lewis  
Department of Chemistry  
Northwestern University  
Evanston, IL 60208-3113  
lewis@chem.nwu.edu

### Secretary

Russell H. Schmehl  
Tulane University  
Department of Chemistry  
New Orleans, LA 70118  
schmehl@mailhost.tcs.tulane.edu

### Treasurers

Lisa Kelly  
Department of Chemistry &  
Biochemistry  
1000 Hilltop Circle  
University of Maryland-Baltimore  
County  
Baltimore, MD 21250  
lkelly@umbc.edu

Cornelia Bohne  
Department of Chemistry  
University of Victoria  
P.O. Box 3055  
Victoria, B.C.  
Canada V8W 3P6  
bohne@uvic.ca

Miguel G. Neumann (South America)  
Instituto de Quimica e Fisicade Sao  
Carlos  
CP 369, Universidade de Sao Paulo  
Sao Carlos, Sao Paulo CEP 13560  
Brazil  
[neumann@iqsc.sc.usp.br](mailto:neumann@iqsc.sc.usp.br)

## Advisory Committee

Cornelia Bohne  
Department of Chemistry  
University of Victoria, B.C.  
P.O. Box 3055  
Victoria, B.C.  
CANADA V8W 3P6  
[bohne@uvphys.phys.uvic.c](mailto:bohne@uvphys.phys.uvic.c)

Frank H. Quina  
Instituto de Química  
Universidade de São Paulo  
São Paulo, Brazil  
frhquina@quim.iq.usp.br

Richard G. Weiss  
Department of Chemistry  
Georgetown University  
Washington, DC 20057  
[weissr@gusun.georgetown.edu](mailto:weissr@gusun.georgetown.edu)

Lisa McElwee-White  
Department of Chemistry  
P.O. Box 117200  
University of Florida  
Gainesville, FL 32611  
lmwhite@chem.ufl.edu

Ian R. Gould  
Department of Chemistry  
Arizona State University  
Box 871604  
Tempe, AZ 95287-1604  
igould@asu.edu

Irene E. Kochevar  
Department of Dermatology  
Massachusetts General Hospital  
WEL-224  
Harvard Medical School  
Boston, MA 02114  
[kochevar@helix.mgh.harvard.edu](mailto:kochevar@helix.mgh.harvard.edu)

### I-APS Webmaster

William Leigh  
Department of Chemistry  
McMaster University  
1280 Main St. West  
Hamilton, ON L8S 4M1 Canada  
Leigh@mcmaster.ca

October 15, 1999

Dear Colleagues,

Summer has come and gone. I hope that everyone enjoyed their summer and managed to find at least some time for a holiday.

This issue of the newsletter has announcements of this year's IAPS award winner (Peter Wagner) and IAPS Fellow (Tony Trozzolo). I am sure that everyone joins me in congratulating both Peter and Tony. Many thanks to the Awards Committee chaired by Fred Lewis for their efforts on the Society's behalf and to all members who took time to nominate colleagues for either the award or fellowship.

I expect that by now many of you have already made plans to attend the 11<sup>th</sup> I-APS Winter Conference. Full details on the meeting are available on the I-APS web site. Approximately seventy abstracts have already been received and there is still time to submit abstracts for poster presentations. For those of you have not yet booked your flights, time is getting short. Please also remember to book hotel rooms as soon as you can. The Society will get a better deal if we fill all the rooms that have been reserved.

Plans are in progress for a second South American I-APS meeting to be held in Argentina in the spring of 2001. Pedro Aramendia (University of Buenos Aires) and Miguel Garcia-Garibay (University of California, Los Angeles) will be the conference co-chairs. They are busy putting together an organizing committee and deciding on time and location for the meeting. Preliminary details will be available at the Winter Conference in Clearwater.

I hope to see many of you in Florida in January.

Linda Johnston

October 15, 1999

**2000 I-APS Award in Photochemistry: Peter J. Wagner**

Professor **Peter J. Wagner** of Michigan State University is the winner of the 2000 I-APS Award in Photochemistry. This Award recognizes Pete's outstanding contributions to the advancement of photochemical and photophysical sciences during the last ten years. The nomination materials note numerous contributions to the understanding of the mechanisms of photochemical reactions, particularly those reactions that originate in the excited states of aromatic ketones and involve biradical intermediates. While the award is based on contributions made during the past decade, the selection committee was clearly impressed by the breadth and depth of Pete's contributions to photochemistry during a career spanning well over three decades. An autobiographical sketch appears in the November 1998 I-APS Newsletter. MSU is clearly on a roll with this award and a gridiron victory over Michigan.

**2000 I-APS Fellowship: Anthony M. Trozzolo**

**Anthony M. Trozzolo**, Huisling Professor Emeritus of Chemistry at the University of Notre Dame has been elected to Fellowship of the Inter-American Photochemical Society. Fellowship is awarded on the basis of lifetime scientific achievements in photochemistry or contributions to the science of photochemistry as a discipline or service to the Society. Tony qualifies in all respects. The nomination notes his pioneering investigations of photochemically generated reactive intermediates in solution and solid states by a variety of spectroscopic techniques. Tony served as the Chair of the first Gordon Research Conference on Organic Photochemistry and has attended every meeting of that conference. He has also been a regular participant in the I-APS Winter Conference. He has served the broader chemical community in numerous ways. He is an honorary citizen of the town of Castrolibero, Italy and is affectionately known by his friends as the "Godfather of Organic Photochemistry."

**2000 Cilento Award: Ana Paola Prata Cione**

Ana Paola Prata Cione from the University of Sao Paulo, Brazil, is the winner of the first Cilento Award. This Award is presented to a scientist under the age of 35 working in Latin America in order to encourage participation in the IAPS Winter Conference. Ms. Cione is a graduate student in the Department of Physical Chemistry in the Institute of Chemistry and a member of the research group of Professor Fergus Gessner. She is investigating the effects of clay surfaces on the photo-physical and photochemical properties of organic molecules.

**I-APS Electronic Distribution Lists**

Electronic mail distribution lists have been created for general announcements to all I-APS members. The lists have been set up as one-way electronic mailings and are now being maintained by Professor Russ Schmehl at Tulane University. If you have an announcement of interest to the general membership (e.g., postdoc openings, job postings, conference announcements), please send an e-mail message to:

[schmehl@mailhost.tcs.tulane.edu](mailto:schmehl@mailhost.tcs.tulane.edu)

and the message will be sent to the membership.

If you have not been receiving these irregular mailings or have recently changed your e-mail address, please forward your new address to Professor Schmehl so that he may get you added to the list.

## **Eleventh Inter-American Photochemical Society Winter Conference**

Hilton Clearwater Beach Resort

Clearwater Beach, Florida

January 2-6, 2000

[http:// www.chem.fsu.edu/iaps2000](http://www.chem.fsu.edu/iaps2000)

### **Plenary Speakers**

A.Paul Alivisatos (University of California, Berkeley)  
Pedro F. Aramendia (Universidad Buenos Aires, Argentina)  
Gerald T. Babcock (Michigan State University)  
Irena Y. Bronstein (Tropix Inc.)  
Robert M. Dickson (Georgia Institute of Technology)  
Richard S. Givens (University of Kansas)  
F. Richard Keene (James Cook University, Queensland, Australia)  
Lisa A. Kelly (University of Maryland-Baltimore)  
David R. McMillin (Purdue University)  
Norbert F. Scherer (University of Chicago)  
Gary B. Schuster (Georgia Institute of Technology)  
Richard G. Weiss (Georgetown University)  
Francoise M. Winnik (McMaster University)

### **1999 I-APS Award in Photochemistry**

Douglas C. Neckers (Bowling Green State University)

### **2000 I-APS Award in Photochemistry**

Peter J. Wagner (Michigan State University)

### *Also*

Approximately ten of the abstracts submitted by October 1, 1999 will be selected for short talks. The winners (to be selected) of the following awards will give lectures: Cilento Award (scientist, age 35 or younger, working in Latin America) and Closs Award (graduate or undergraduate student). **Abstracts for poster presentations win continue to be accepted after October 1.** See the conference web site for details.

This Winter Conference will take place at a different hotel from that of the past conferences in Clearwater Beach. This site is located near the end of the causeway leading into Clearwater Beach: the Hilton Clearwater Beach Resort at 400 Mandalay Avenue, Clearwater Beach, Florida 33767. Please make your hotel reservations and travel plans as soon as possible.

Registration and a reception will take place in the evening on Sunday, January 2, 2000. The scientific sessions will begin the morning of January 3 and end at noon on January 6.

For more information about deadlines, hotel reservations and registration, please go to the Inter-American Photochemical Society web site at <http://www.chemistry.mcmaster.ca/~iaps/> and click on the link for this conference or contact one of the co-chairpersons:

Professor Edwin F. Hilinski  
Florida State University  
FAX: 850-644-8281  
E-mail: [hilinski@chem.fsu.edu](mailto:hilinski@chem.fsu.edu)

Professor Joseph T. Hupp  
Northwestern University  
FAX: 847-492-7713  
E-mail: [jthupp@chem.nwu.edu](mailto:jthupp@chem.nwu.edu)

## **Peter J. Wagner: 2000 I-APS Award in Photochemistry**



Peter Wagner is known world-wide for his contributions to organic photochemistry, in particular for his thorough study of the Norrish type II reaction and the creative use of this reaction to establish fundamental aspects of excited state reactivity, and for his additions to our understanding of intramolecular and intermolecular energy transfer processes. Insights gained from his studies pervade all areas of organic photochemistry.

Peter Wagner received his B.S. degree in Chemistry from Loyola University, Chicago, and his Ph.D. in chemistry from Columbia University where his mentor was Cheves Walling. After a postdoctoral stint with George Hammond, he joined the Chemistry faculty at Michigan State University in 1965. He was promoted to Professor in 1970 and is currently a University Distinguished Professor. To expand his research expertise, Peter received a fellowship from the Guggenheim Foundation and was a NSF Senior Postdoctoral. Peter Wagner has authored or coauthored almost 200 research publications. He has presented over 100 invited lectures on his research and has been a plenary lecturer at over 30 national and international conferences. He has served the chemical community as an Associate Editor for the *Journal of the American Chemical Society* for 11 years, as the American organizer for the 1980 IUPAC Conference on Organic Photochemistry and as the chairman of the 1985 Gordon Conference on Organic Photochemistry.

On a personal level, Peter Wagner is well known for the head-spinning speed of this Chicago-accented language while discoursing on topics from photoenolization of  $\alpha$ -diketones to *Phalaenopsis* subspecies to the under-appreciated merits of the Chicago Cubs. The fact that all of these topics arise in one conversation attests to his ever nimble mind and breadth of intense interests.

-Irene E. Kochevar

**Anthony M. Trozzolo: Fellow of the Inter-American  
Photochemical Society**



I am delighted to announce that Anthony M. Trozzolo, the Charles L. Huisking Professor Emeritus of Chemistry at the University of Notre Dame, has been elected a Fellow of the Inter-American Photochemical Society. This fellowship is awarded in recognition of both Tony's lifetime achievements in organic photochemistry and his leadership role in the photochemical field. Bell Laboratories and then the University of Notre Dame have been sites of Tony's research activities. His pioneering studies on the photochemical generation of reactive intermediates in low-temperature matrices and the characterization of these species - carbenes, nitrenes, carbonyl ylides, and azomethine ylides - by means of electron paramagnetic resonance (EPR), absorption, and fluorescence spectroscopies have shaped the way in which we think about these transient entities. Information from these investigations provides a foundation on which today's many time-resolved laser spectroscopic studies are based. Dicarbenes and dinitrenes which were prepared and detected revealed early on that this type of approach can lead to high-spin systems of interest. In work on the degradation and the stabilization of polymers, Tony performed experiments involving singlet oxygen and suggested the first mechanism involving singlet oxygen in the photodegradation of polyalkenes. Tony's excellent organizational skills along with his political astuteness allowed him to be a leader in establishing the variety of means by which we as scientists promote photochemistry. He was the driving force behind the founding of the Gordon Research Conference on Organic Photochemistry and served as its first organizer and chair. He has had important involvement in organizing international conferences, in strengthening photochemical organizations such as the Inter-American Photochemical Society, and in continued work with the Gordon Research Conferences as a Member of Council and as a Member of the Board of Trustees. Tony is an elected Fellow of the New York Academy of Sciences, the American Association for the Advancement of Science, and the American Institute of Chemists. He has been an active member of the American Chemical Society serving as National Councilor for the Division of Organic Chemistry and for the North

Jersey Section, as a member of the Joint Board-Council Committee on Chemistry and Public Affairs, as Associate Editor of the **Journal of the American Chemical Society**, as Editor of **Chemical Reviews**, as a member of the Editorial Board of **Accounts of Chemical Research**, and as a tour speaker. I am always happy to see Tony and his wife Dolly at conferences whether it is in my backyard of Clearwater Beach, Florida or a bit more distant locale such as Helsinki, Finland. I am looking forward to many more enjoyable discussions on topics ranging from science and history to the Fightin' Irish of Notre Dame.

-Edwin F. Hilinski

**Conference Report on the XIXth International Conference on  
Photochemistry, Duke University, Durham, NC USA, August 1-6, 1999**

by Cornelia Bohne, Department of Chemistry, University of Victoria, Victoria, BC  
and Cliff P. Kubiak, Department of Chemistry and Biochemistry, University of  
California-San Diego, La Jolla, CA

The conference started on a beautiful, but hot Sunday with a very lively reception. Serious business began on Monday morning with the welcoming words of the co-chairs (John Simon and Cliff Kubiak) and the provost of Duke University (Peter Lange). George M. Wyman got the conference off to an amusing start with an interesting account of the history of this conference. The scientific program covered a variety of traditional and emerging topics in the field of photochemistry. Morning and afternoon sessions started with plenary lectures that were followed by parallel sessions. The complete program and abstracts can be viewed at <http://www.chem.duke.edu/-icp99/>. The talks covered a variety of areas. The plenary lectures in the supramolecular photochemistry and the photochemistry on nanoscale materials were delivered by V. Balzani and M. A. EI Sayed. The plenary lecture by P.-S. Song covered phytochromes that belong to an important class of molecules in photobiology. The application of infra-red multiphoton photoselective photochemistry was covered by V.S. Letokov. The plenary lecture by W.E. Moerner showed some of the most recent studies using single molecule imaging. This topic was also covered in one of the parallel sessions with additional lectures by R. C. Dunn, Sunney Xie, R. M. Dickson, and J. Hofkens. J.T. Hynes presented an enlightening lecture on his theoretical work on proton transfer reactions. Also on the theoretical front, J. Troe talked about state specific photolysis rates. An extensive overview on the photochemistry of metal carbonyls was the topic of the plenary lecture by J.J. Turner. Finally, S Farid gave a lively account during his plenary lecture on how the fundamental knowledge of electron transfer reactions can be applied to develop the chemistry involved in photography. Other aspects of electron transfer such as reactions in DNA, changes in enthalpy, volume and entropy in electron transfer reactions, the effect of electric potential were covered in the parallel sessions. The parallel sessions often developed the topics covered in plenary lectures in more detail through invited and late-breaking contributed talks. In addition, several other areas of photochemistry were covered, such as ultrafast phenomena, photochemistry in solids and polymers, gas phase and atmospheric photochemistry, several aspects of inorganic photochemistry, spectroscopy, and dynamics of protein folding. The conference had two well-lubricated poster sessions, where participants had the opportunity to present and discuss in more detail their research findings. An extensive social program provided the participants with a sample of the attractions and local culture in the Durham area. These included an outing to a Durham Bulls baseball game and the reception at the Museum of Life and Science. In addition, on Wednesday afternoon participants were given an option to visit the Free Electron Laser Facility and the Primate Center at Duke, or the Duke Homestead and Tobacco Museum. Finally, the conference reception and banquet were held on Thursday night at the Dave Thomas (of Wendy's renown) Center on the Duke University campus.

The ICP 1999 meeting provided a clear example that photochemistry is interdisciplinary and international. ICP 1999 attempted to broaden the definition of photochemistry somewhat compared to recent ICPs, and this it did quite successfully. ICP 2001 will be held in Moscow and will be chaired by Professor M. Alfimov.

**International Conferences on Photochemistry  
Durham, NC, 1962 – Durham, NC, 1999**

---

George M. Wyman, 2331 Cranford Road, Durham, NC 27706

PREFACE

With the recently (August 6, 1999) concluded XIX. International Conference on Photochemistry (ICP99) on the campus of Duke University, this series of conferences has completed a full circle since the first meeting in the series was also held on this campus 37 years earlier. The list of these conferences (v. i.) shows that they have been held in alternate (odd) years with just two exceptions. (1) twice during the late seventies the interval was increased to three years (due to an ill-advised suggestion I made to the International Organizing Committee in 1975) and, (2) the 1989 ICP scheduled for Beijing (China) was cancelled by the International Committee due to the tragic events of Tianamen Square that year. My association with this series has also completed nearly a full circle, but with more ups and downs, especially during the past year. In 1962 I was the organizer of the Conference (Symposium on Reversible Photochemical Processes) and in 1969, when the series was officially established (v. i.), I became a member of its International Organizing Committee. I resigned from this Committee in 1995 when Professor David Phillips, Chairman of the Committee, became concerned that over the years the Committee had become so large as to have become unwieldy. All in all I have participated in 10 of the 18 conferences held to date. In the Fall of 1998, when I heard that the XIX. Conference (ICP99) was scheduled to be held in Durham again, I promptly contacted Prof. John D Simon, the chairman of the local organizing committee, and told him about my past association with the ICP's. He added my name to his committee and gave me the job of compiling a list of potential sponsors from the chemical industry. I spent a total of about a week in the University Library and by mid January provided him with a list of ca. 115 companies that would be worth approaching. Shortly after that Prof. Simon dismissed me from the committee in connection with a letter that I had sent to the editor of C&E News. While this letter was critical of an organization (Council for Chemical Research) that has a membership of about 40 chemical companies and most research universities in the U. S. (including Duke), it did not mention Duke or any other university by name and was not going to appear in print. He also informed me that the Duke administration (sic) urged him to do this. (I will let each reader decide how this action can be reconciled with the concept of academic freedom). Of course, under these circumstances I had no intention of participating in ICP99. To my great surprise, about three months later Prof. Simon informed me that he and Prof. Clifford D. Kubiak (UC-San Diego), the co-chairmen of ICP99, wanted me to speak at the opening session about the conference that I organized on the Duke campus in 1962 (which was later to become the first in this series) and about the series in general. They also asked me to chair the first session of ICP99. While I have no idea what caused this complete reversal in his (and his university's, if it was indeed involved) attitude, I accepted the invitation. However, I found it ironic that my presentation directly followed the welcoming remarks of the Provost of Duke University on the program of the conference!

At the end of my presentation I pointed out a surprising bit of trivia: Five of the ICP,s held to date (1962, 1973, 1975, 1987 and 1991) were organized by Hungarian-born photochemists. Does this mean that Hungarian-born scientists are more prone to organize conferences? (I am still waiting for an answer!)



E. Fischer, W. Berends, G. M. Wyman and Th. Foerster at the 1962 conference.

#### INTRODUCTION

Perhaps some readers will remember the brief retrospective article I wrote in 1993 entitled "Reminiscences of an Accidental Photochemist" which appeared in the I-APS and EPA Newsletters where I mentioned that in 1962 I organized a symposium on Reversible Photochemical Processes in Durham, NC, the first truly international conference on Photochemistry . So, when I was asked by the organizers of this year's ICP to talk about that meeting and how it became the first in this long-lived series, all I had to do was to search my long-term memory for some of the details, an exercise that becomes easier as one gets older. I also had help from two documents that I have kept over the intervening 37 years: the 662-page volume of Preprints of Papers (extended abstracts) and the December, 1962 issue of the Journal of Physical Chemistry which contained most of the papers that were presented. My talk to the Conference (and this article) concerned three questions: (1) how did the 1962 meeting come about; (2) what transpired at that symposium and who were some of the key participants and (3) why it is considered to be the first in this series.

The idea to organize the 1962 conference was the direct result of three successive steps in the development of my early professional career: In 1949-1956 I was actively involved in research in photochemistry (mainly cis-trans

isomerization of azo- and indigo dyes). Then, at the end of 1956 I gave up research to join the staff of the Army's new European Research Office (Frankfurt) where much of work involved attending conferences dealing with all aspects of chemistry and visiting researchers (chemists) in universities and research laboratories in Western Europe. This gave me an opportunity to get personally acquainted with many of the photochemists whose work was familiar to me from the literature. The conferences varied a great deal in size and format and I was especially impressed with the format of the Discussions of the Faraday Society (now the Faraday Division of the Royal Society of Chemistry). Then, in the middle of 1960 I returned to the U. S. to become Director of the Chemistry Division of the U. S. Army Research Office, located on the Duke University campus at that time. This was a medium-sized government research-supporting agency at a time when funds were relatively plentiful.

Once I got settled in my new surroundings it was only natural to think about inviting my European colleagues to meet with their American counterparts at a meeting to present their most recent results and explore research ideas. I was fortunate that, when I first tried out this idea on my boss (ARO's Chief Scientist, Dr. John Dawson, also a chemist) and on Professor John Saylor, Chairman of the Chemistry Department at Duke University at the time, they both gave me their enthusiastic support. Dr. Dawson's approval permitted me to use ARO funds for all the expenses of the conference and Professor Saylor made all the arrangements with his university where the conference would be held. He located a suitable meeting room (the auditorium in the Engineering Sciences Building that could accommodate 150) and he arranged to have the university host a banquet where President Hart welcomed the participants. The Chemistry Department of the University of North Carolina in nearby Chapel Hill treated the participants to a dinner on the other evening of the Conference.

As a formal ARO project we had tremendous flexibility in planning the symposium. by then we had a local organizing committee, consisting of Prof. Saylor, Dr. Marvin Silver, another ARO staff member, and myself. We were free to choose the date, the format and the participants. The date we picked was the middle of April when the weather is pleasant and the trees and azaleas are in bloom in our area. The format was to conform to the format of the Faraday Discussions, even though the Faraday Society was unwilling to extend its sponsorship to the meeting. We had funds available to pay the travel expenses of all participants from academic institutions who needed it (the Army even had access to reduced transatlantic air fares!) regardless of whether they had papers on the program or were simply coming to contribute to the discussion. The list of scientists to be invited was put together with the assistance of several external advisors and frequently invitees would suggest names of others to be invited. For example, George Porter (now Lord Porter), who couldn't come due to a conflict with a long-planned ski-trip, suggested that we invite a promising young former student of his in his place: Frank Wilkinson. (Frank became the Chairman of the EPA 25 years later.) Mike Kasha, who was one of our advisors, suggested that we invite two bright young Egyptians who had academic positions in the U. S.: Mostafa El-Sayed and Ashraf El-Bayoumi. (professor El-Sayed was one of the plenary lecturers at ICP99 and is one of America's best-known physical chemists; Dr. El-Bayoumi returned to Egypt later and the last time I saw him, he was carrying picket signs, protesting the attendance of Israeli scientists at an International Photochemistry Conference in Alexandria in 1983!) In general, this turned out to be a tremendous help in identifying promising young scientists who were at the beginning of their careers! Unfortunately Mike Kasha and Wilse Robinson were among the few who had to cancel their planned participation in the 1962 symposium. There were no public announcements or advertising of the conference and attendance was limited to 125 in order to allow for the free entry of faculty and students of the neighboring universities to participate whenever they wished. The subject of the symposium (reversible photochemical processes) was interpreted rather broadly to include photophysical processes and the third (and last) day of the conference was devoted to biochemical and

photobiological systems. We also made arrangements to have the papers published as a package in the December, 1962 issue of the *Journal of Physical Chemistry*.

Invitations, accompanied by a call for extended abstracts were sent out late in 1961 with a warning to the authors that they would have only five minutes to point out the highlights of their research when they spoke at the meeting and this time limitation was strictly enforced. (The only exception was a 15-minute talk by Ernst Fischer of the Weizmann Institute, reviewing the accomplishments of his late mentor, Yehuda Hirshberg, who died in 1960.) Forty papers were submitted and the volume of Preprints of Papers was mailed to each participant late in February. About 15 minutes were available for discussing each presentation and the discussion periods for related papers were combined. While the discussion was always stimulating and sometimes even got heated, there is unfortunately no record of the discussion except for the three papers that appeared in *J. Phys. Chem.* that had not been on the original program of the Symposium.

#### HOW WERE THINGS IN 1961?

The world was sharply divided (East vs. West). This was the height of the cold war, the Berlin Wall was built this year. The State of Israel was only 13 years old, nonetheless it had one of the world's most active research groups in photochemistry at the Weizmann Institute. The U. S. currency was so strong (\$1.00 = DM 4.20) that few foreigners could afford to travel to the U. S.

Our area: The Research Triangle was mostly a dream with just one tenant research laboratory (Chemstrand Division of Monsanto) on site. Now, over 40,000 people work in Research Triangle Park! The chemistry departments of the two universities were still housed in 35-year old buildings!

Techniques (available for research in photochemistry): Flash photolysis, recording spectrometers, chromatography, NMR and ESR {in their infancies!}, double-focusing MS (brand new). Lasers were not invented until a few years later!

Research: Physical photochemistry (mostly gas-phase); organic photochemistry (largely empirical), inorganic photochemistry just getting started; excited state chemistry {well underway}.

Centers: NRC-Ottawa (spectroscopy, physical photochemistry)

Weizmann Institute (photochromism)

Universities of Alberta, Minnesota, Rochester (physical photochem)

AEC National Laboratories (as a sideline to radiation chemistry)

Cambridge, Sheffield, Uppsala (flash photolysis)

Muelheim (beginnings of a new MPI)

T. U. Munich (photochemistry and spectroscopy of dyes)

T. U. Stuttgart (excited state chemistry)

Cal Tech (spectroscopy and mechanistic organic photochemistry)

University of Wisconsin (start of mechanistic organic photochem)

#### SYMPOSIUM ON REVERSIBLE PHOTOCHEMICAL PROCESSES

April 16-18, 1962

One 15-minute oral presentation: Eulogy about Prof. Y. Hirshberg {by E. Fischer} 40 papers (extended abstracts), author has 5 minutes to discuss the highlights! Three more were added to the conference publication (*J. Phys. Chem.*), based on the authors' contributions during the discussion.

---

The symposium received a fair amount of publicity in the local press, including this photo that shows me with Professors Th. Foerster (Stuttgart), E. Fischer (Weizmann Institute) and W. Berends (Delft); the first two became life-long friends.

#### PARTICIPANTS

Unfortunately there is no List of Participants extant, but it was possible to reconstruct a partial list from the preprints and from the publication.

- (1) Elder Statesmen: E. J. Bowen, Glenn H. Brown, Stig Claesson, M. J. S. Dewar\*, Henry Eyring\*, Th. Foerster, G. Kortuem, R. Livingston, C. A. Parker, E. Rabinowitch, G. O. Schenck, George Wald
  - (2) Middle-age group: A. W. Adamson, M. D. Cohen, F. Doerr, E. Fischer, G. S. Hammond, H. Linschitz, E. Lippert, G. Oster, J. N. Pitts, D. Schulte-Frohlinde, G. Weber, A. Weller
  - (3) Youngsters: E. A. Chandross, M. A. EI-Sayed, G. A. Crosby, E. C. Lim, L. Lindquist, J. D. Margerum\*, D. Mauzerall, S. P. McGlynn, H. Stegemeyer\*, Brian Stevens, A. M. Trozzolo, Ed Wasserman\*, G. Wettermark, Frank Wilkinson
- \*Not primarily photochemists, spectroscopists or photobiologists.

#### TOPICS DISCUSSED:

Photochromism ( spiroopyrane., merocyanine tautomerism)  
cis-trans Isomerization  
Quantum yields  
Triplet excitation  
Triplet sensitized reactions  
Photochemistry of complex ions  
Proton transfer in the excited singlet state  
Hydrogen-bonding in the excited singlet state  
Spectroscopy of rare-earth chelates  
Phosphoresence and delayed fluorescence  
Theory of radiationless decay  
Photosynthesis  
Porphyrins  
Chlorophyll  
Retinene - rhodopsin

Some of the participants at ICP99 commented that (1) there was a remarkable collection of exceptionally talented scientists at ICP62 and that (2) the topics discussed on the program were not all that different from what is currently being pursued in research laboratories, except that the tools and techniques have changed a great deal.

#### PHOTOCHEMISTRY CONFERENCES IN THE 60's

Our conference was followed in quick succession by a number of others:

- 1963 Symposium in honor of the retirement of W. Albert Noyes, Jr., University of Rochester
- 1964 First Gordon Conference on Organic Photochemistry, Tilton, NH (USA)\*

- 1965 International Conference on Photochemistry, Tokyo (Japan)  
1966 Symposium in honor of the retirement of Robert Livingston, University of Minnesota  
1967 1st IUPAC Symposium on Photochemistry, Strasbourg (France)\*\*  
1968 International Conference on Photochemistry, Munich(Germany)  
1967 International Conference on Photochromism, Dayton, OH (USA)  
1969 International Conference on Photochemistry, Yorktown Heights, NY (USA)  
\*Conferences held subsequently in alternate years, always in the USA.  
\*\*Conferences held subsequently in alternate years, always in Europe.

(A series of Informal Photochemistry Conferences had been held in even years since the early 50's-these were started by Prof. Francis Blacet at UCLA ---but they were limited to North America and North Americans.)

#### BIRTH OF THE SERIES OF ICP'S (with retroactivity!)

Some time during the International Conference on Photochemistry that was held in the summer of 1969 at IBM's Thomas J. Watson Research Center in Yorktown Heights, NY, Dr. R. Srinivasan, the organizer of the Conference suggested that:

- (1) This Conference would be considered as one of a series of biennial such conferences.
- (2) The series would trace its origin to the conference held in Durham, NC in 1962.
- (3) An international Organizing Committee should be established that will oversee the selection, planning, location, etc. of each future conference. The organizers of previous conferences were asked to serve on this Committee, along with some other prominent photochemists. The chairman was to be the organizer of the previous conference, via Dr. Srinivasan (for the next two years).
- (4) The technical (and social) program and the funding of each conference was to be the responsibility of the organizer of each ICP. (Thus the organizer was free to decide the size and scope of the Conference.) He/she was also encouraged to consult with members of the International Committee periodically.
- (5) Because the Gordon Conferences and the IUPAC Symposia emphasized organic photochemistry, the ICP's were expected to concentrate on the other sub-fields.

#### LIST OF ICP'S

- 1962 Durham, NC (USA)  
1963 Rochester, NY (USA)  
1965 Tokyo (Japan)  
1967 Munich, (Germany)  
1969 Yorktown Heights, NY (USA)  
1971 Bordeaux (France)  
1973 Jerusalem (Israel)  
1975 Edmonton (Canada)  
1978 Cambridge (U.K.)  
1981 Heraklion (Greece)  
1983 College Park. MD (USA)  
1985 Tokyo (Japan)  
1987 Budapest (Hungary)

1989 Beijing (China)--cancelled by the International Committee due to the tragic events at Tianamen Square earlier that summer.  
1991 Paris (France)  
1993 Vancouver (Canada)  
1995 London (U.K.)  
1997 Warsaw (Poland)  
1999 Durham, N.C. (USA)  
2001 planned for Moscow (Russia)

#### ACKNOWLEDGEMENTS

The author wishes to take this opportunity to express his appreciation to Professor M. A. El-Sayed (the only other participant in both ICP62 and ICP99!) for suggesting that this talk be written up for publication and to the editors of the two Newsletters for their interest in publishing it.

The author is also grateful to several Japanese participants at ICP99 who pointed out to him that during his presentation he overlooked the International Photochemistry Conference that was held in Tokyo in 1965.

\*Based on a talk presented at the XIXth International Conference on Photochemistry, Durham, N.C., August 2, 1999.

**Light Compendium – Ultraviolet Principles and Applications**

James R. Bolton, Ph.D.  
**Bolton Photosciences Inc.**

Business Office, 92 Main St., Ayr, ON, Canada N0B 1E0  
Tel: 519-741-6283; Fax: 519-632-8941; email: [jbolton@boltonuv.com](mailto:jbolton@boltonuv.com)  
Web site: [www.boltonuv.com](http://www.boltonuv.com)

Research Laboratory, Siebens Drake Research Institute  
Room 230, 1400 Western Road, London, ON, Canada N6G 2V4  
Tel: 519-663-3112; Fax: 519-663-3067

**Forward**

The following article is a primer on light, particularly ultraviolet light. It has been excerpted from “Ultraviolet Applications Handbook” by James R. Bolton. This book is available free by writing or by email to: Bolton Photosciences Inc., 92 Main St., Ayr, ON Canada N0B 1E0; tel: 519-741-6283; fax: 519-632-8941; email: [jbolton@boltonuv.com](mailto:jbolton@boltonuv.com) or leave a message on his web site ([www.boltonuv.com](http://www.boltonuv.com)).

## Table of Contents

1.	<a href="#">Introduction</a>	6
2.	<a href="#">Units and Physical Constants</a>	6
3.	<a href="#">Light and its Measurement</a>	6
3.1.	<a href="#">Characteristics of light</a>	7
3.1.1.	<a href="#">Planck Law of Radiation</a>	7
3.1.2.	<a href="#">Photochemical wavelength ranges</a>	7
3.1.3.	<a href="#">Coherent and incoherent light</a>	9
3.1.4.	<a href="#">Point sources</a>	9
3.2.	<a href="#">Spherical-polar coordinates and solid angles</a>	9
3.3.	<a href="#">Terms and concepts associated with the emission of light</a>	10
3.3.1.	<a href="#">Radiant energy</a>	10
3.3.2.	<a href="#">Radiant power</a>	10
3.3.3.	<a href="#">Radiant power efficiency</a>	10
3.3.4.	<a href="#">Radiant emittance or excitance</a>	11
3.3.5.	<a href="#">Radiant intensity</a>	11
3.3.6.	<a href="#">Radiance</a>	11
3.4.	<a href="#">Terms and concepts associated with the receipt of light</a>	12
3.4.1.	<a href="#">Fluence Rate</a>	12
3.4.2.	<a href="#">Irradiance</a>	13
3.4.3.	<a href="#">Light dose or fluence</a>	13
3.5.	<a href="#">Spectral units</a>	13
3.6.	<a href="#">Photon based units</a>	14
3.6.1.	<a href="#">Photon emission weighted average</a>	14
3.6.2.	<a href="#">Photon irradiance, photon fluence rate and photon flow</a>	14
3.6.3.	<a href="#">Quantum yield</a>	15
3.7.	<a href="#">Light sources</a>	16
3.7.1.	<a href="#">Blackbody light sources</a>	16
3.7.2.	<a href="#">Line sources</a>	16
3.7.3.	<a href="#">Excimer lamps</a>	17
3.7.4.	<a href="#">Flash lamps</a>	18
3.8.	<a href="#">Measurement of light</a>	18
3.8.1.	<a href="#">Radiometers</a>	19
3.8.2.	<a href="#">UV sensors</a>	19
3.8.3.	<a href="#">Actinometry</a>	19
4.	<a href="#">Light in a Condensed Medium</a>	20
4.1.	<a href="#">Refractive index</a>	20
4.2.	<a href="#">Refraction and Snell's Law</a>	20
4.3.	<a href="#">Reflection and the Fresnel Laws</a>	20
4.4.	<a href="#">Absorption and transmittance – the Beer-Lambert Law</a>	22
4.4.1.	<a href="#">Transmittance</a>	22
4.4.2.	<a href="#">1 cm transmittance (<math>T'</math>)</a>	23
4.4.3.	<a href="#">Absorbance</a>	23

4.5.	<a href="#">Fraction of light absorbed</a> .....	23
4.5.1.	<a href="#">For a monochromatic or narrow band light source</a> .....	23
4.5.2.	<a href="#">For a broad-band light source</a> .....	24
5.	<a href="#">Advanced Oxidation Technologies</a> .....	42
5.1.	<a href="#">Homogeneous AOTs</a> .....	25
5.1.1.	<a href="#">The UV/O<sub>3</sub> process</a> .....	25
5.1.2.	<a href="#">The UV/H<sub>2</sub>O<sub>2</sub> process</a> .....	25
5.1.3.	<a href="#">UV Fentons processes</a> .....	26
5.2.	<a href="#">Heterogeneous AOTs</a> .....	26
6.	<a href="#">Ultraviolet Disinfection</a> .....	26
6.1.	<a href="#">UV irradiance, UV fluence rate, UV dose and their measurement</a> .....	26
6.1.1.	<a href="#">Collimated beam apparatus</a> .....	26
6.1.2.	<a href="#">UV reactors</a> .....	27
6.2.	<a href="#">Mechanism of UV disinfection</a> .....	28
6.3.	<a href="#">Sensitivity of microorganisms to UV</a> .....	28
6.4.	<a href="#">Biodosimetry</a> .....	28
7.	<a href="#">Ultraviolet Curing</a> .....	46
7.1.	<a href="#">The chemistry of UV curing</a> .....	29
7.2.	<a href="#">UV lamp geometry</a> .....	30

## 1. Introduction

This article has been prepared to provide user-friendly information and discussion on light (particularly ultraviolet light) technology and photochemistry. It is intended as not only a first introduction to light and ultraviolet light, but also as an example of the proper use of terms of importance in photochemistry.

Photochemistry encompasses any chemical reaction driven by the absorption of (usually) visible or ultraviolet (UV) light. Photochemical reactions are common in almost all areas of the environment, such as photosynthesis in green plants, sun tanning and sun burning, sun fading of textiles, light sensors, UV curing of coatings, UV photodegradation of pollutants in contaminated waters and UV disinfection.

## 2. Units and Physical Constants

All of the units used in this Handbook conform to the "Système International" (SI). An excellent reference for terms and nomenclature in Physical Chemistry is the International Union of Pure and Applied Chemistry (IUPAC) "Green Book"<sup>1</sup>. Another important reference is the Report of the IUPAC Photochemistry Commission, "Glossary of Terms in Photochemistry".<sup>2</sup>

## 3. Light and its Measurement

---

<sup>1</sup> IUPAC Green Book, "Quantities, Units and Symbols in Physical Chemistry" 2<sup>nd</sup> Ed., I. Mills et al., Blackwell Scientific Publications, London, UK, 1993.

<sup>2</sup> "Glossary of Terms used in Photochemistry", J. W. Verhoeven, *Pure Appl. Chem.* **68**, 2223-2286

Light is important to almost all life forms. We “see” only a very small fraction of the “colors” of light. In this booklet we are interested primarily in the light with wavelengths “beyond the violet” end of the rainbow or the “ultraviolet”. There are several references for information on light and its measurement, but one of the best and most readable is the free “Light Measurement Handbook” available from International Light.<sup>3</sup>

### 3.1. Characteristics of light

#### 3.1.1. Planck Law of Radiation

Light has both particle and wave properties. It is transmitted in discrete packets of energy (photons) and yet has a frequency and wavelength. The connection between these two properties is embodied in the Planck Law of Radiation

$$u = h\nu = hc/\lambda = hc\bar{\nu} \quad (1a)$$

$$U = N_A h\nu = hcN_A/\lambda = hcN_A\bar{\nu} \quad (1b)$$

Where  $u$  is the energy (J) of one photon,  $\nu$  is the frequency ( $s^{-1}$ ),  $\lambda$  is the wavelength (m),  $\bar{\nu}$  is the wavenumber ( $m^{-1}$ ),  $c$  is the speed of light ( $2.9979 \times 10^8 \text{ m s}^{-1}$ ),  $h$  is the Planck constant ( $6.6261 \times 10^{-34} \text{ J s}$ ),  $N_A$  is the Avogadro number ( $6.02214 \times 10^{23} \text{ mol}^{-1}$ ) and  $U$  is the energy per einstein.<sup>4</sup> The units here have been given in the standard SI forms; however, for applications in Ultraviolet light and Photochemistry,  $\lambda$  is usually given in nanometers (nm) and  $\bar{\nu}$  in  $cm^{-1}$ , with appropriate numerical factors to make the left-hand side of equation come out to joules (J).

**Example:** What is the radiant energy of one einstein (one mole) of photons at 325 nm?

Using equation 1b

$$\begin{aligned} U &= \frac{hcN_A}{\lambda} \\ &= \frac{6.6260755 \times 10^{-34} \text{ J s} \times 2.99792458 \times 10^8 \text{ m s}^{-1} \times 6.0221367 \times 10^{23} \text{ mol}^{-1}}{325 \times 10^{-9} \text{ m}} \\ &= 368,082 \text{ J mol}^{-1} = 368,082 \text{ J einstein}^{-1} = 368.1 \text{ kJ einstein}^{-1} \end{aligned}$$

#### 3.1.2. Photochemical wavelength ranges

The usual wavelength range in Photochemistry is 100 – 1000 nm ( $100,000 - 10,000 \text{ cm}^{-1}$ ). Light photons with wavelengths longer than 1000 nm have a photon energy too small to cause chemical change when absorbed, and photons with wavelengths shorter than 100 nm have so much energy that ionization and molecular disruptions characteristic of radiation chemistry prevail. The total photochemical wavelength range is divided up into bands with specific names as given in Table 1.

<sup>3</sup> “Light and its Measurement”, A. Ryer, International Light, 17 Graf Road, Newburyport, MA, 01950, 1997; <http://www.intl-light.com>.

<sup>4</sup> <http://www.intl-light.com>, 6.6260755 x 10<sup>-34</sup> J s, 2.99792458 x 10<sup>8</sup> m s<sup>-1</sup>, 6.0221367 x 10<sup>23</sup> mol<sup>-1</sup>

**Table 1. Spectral ranges of interest in Photochemistry**

Range Name	Wavelength Range / nm	Wavenumber Range / cm <sup>-1</sup>	Energy Range (kJ einstein <sup>-1</sup> )
Near Infrared	700 – 1000	14,286 – 10,000	120 – 171
Visible	400 – 700	25,000 – 14,286	171 – 299
Ultraviolet			
UVA	315 – 400	31,746 – 25,000	299 – 380
UVB	280 – 315	35,714 – 31,746	380 – 427
UVC	200 – 280	50,000 – 35,714	427 – 598
Vacuum Ultraviolet (VUV)	100 – 200	100,000 – 50,000	598 – 1196

Little photochemistry occurs in the *Near Infrared*, except for some photosynthetic bacteria, which are capable of storing solar energy at wavelengths out to 980 nm. The *Visible* range is completely active for photosynthesis in green plants and algae. Also many dyes can undergo photochemical transformations themselves or sensitize reactions in other molecules. Most studies in photochemistry involve the *Ultraviolet* ranges. The division into three sub-ranges is connected with the human skin's sensitivity to ultraviolet light. The UVA range causes changes in the skin that lead to sun tanning. The UVB range can cause sun burning and is known to eventually induce skin cancer. The UVC range is extremely dangerous since it is absorbed by proteins, RNA and DNA and can lead to cell mutations and/or cell death. The UVC range is sometimes called the *germicidal range*, since it is very effective in inactivating bacteria and viruses. The *Vacuum Ultraviolet* range is absorbed by almost all substances (including water and air). Thus it can only be transmitted in a vacuum. The absorption of a VUV photon causes one or more bond breaks. For example, water is dissociated according to



**Example:** The O-O bond energy in the H<sub>2</sub>O<sub>2</sub> (H-O-O-H) molecule is 213 kJ mol<sup>-1</sup>. What is the maximum wavelength of light that would be capable of dissociating a hydrogen peroxide molecule on absorption of one photon?

Rearrange eq. 1b

$$\begin{aligned} &= \frac{hcN_A}{U} \\ &= \frac{6.6260755 \times 10^{-34} \text{ J s} \times 2.99792458 \times 10^8 \text{ ms}^{-1} \times 6.0221367 \times 10^{23} \text{ mol}^{-1}}{213000 \text{ J mol}^{-1}} \\ &= 5.616 \times 10^{-7} \text{ m} = 561.6 \text{ nm} \end{aligned}$$

However, even though photons with wavelengths less than 561.6 nm are capable of splitting the H<sub>2</sub>O<sub>2</sub> molecule, no photolysis occurs in this wavelength region because H<sub>2</sub>O<sub>2</sub> does not begin to absorb ultraviolet light until below 300 nm. This illustrates the *First Law of Photochemistry*, namely that no photochemical reaction can occur unless a photon of light is absorbed.

### 3.1.3. Coherent and incoherent light

Light sources used in photochemistry can either be *coherent* (all emitted photons are *in phase* with each other as they propagate) or *incoherent* (all emitted photons have random phases). All *lasers* emit coherent radiation and usually at one wavelength. The dispersion is very small so that a laser beam remains at or near its original diameter as it propagates. The light emitted by all other light sources is almost always incoherent. Most of these sources are either “hot element” sources (e.g., the incandescent light bulb) or “plasma” sources (e.g., a fluorescent light tube).

### 3.1.4. Point sources

Light sources have finite dimensions (e.g., often a cylindrical shape). Emission from such a source is difficult to treat mathematically. It is convenient to model these sources as a collection of *point sources*, in which all light is emitted from the point equally in all directions. The optics treatment for point sources is especially simple.

## 3.2. Spherical-polar coordinates and solid angles

In the description of light emission and incidence it is useful to employ spherical-polar coordinates and solid angles. These are illustrated in Figure 1. The *polar angle*  $\theta$  is measured from the polar axis  $z$  of a sphere; the *azimuthal angle*  $\phi$  is measured from the  $x$ -axis to the projection of the  $\mathbf{r}$  vector onto the  $xy$  plane.

The solid angle ( $\Omega$ ) is defined as the surface area of a section of a sphere divided by  $r^2$ , where  $r$  is the radius of the sphere. The maximum solid angle (corresponding to a complete sphere) is  $4\pi$  steradians (sr). An element of solid angle  $d\Omega$  is given by  $dA/r^2$ , where  $dA$  is the area on the sphere subtended by the solid angle  $d\Omega$ .  $d\Omega$  is related to the angles  $\theta$  and  $\phi$  by

$$d\Omega = \sin\theta \, d\theta \, d\phi \quad (3)$$

### 3.3. Terms and concepts associated with the emission of light

The light emitted from a source can be viewed in many different ways. In this Section, the various terms that may be used to describe this emission are defined and explained.

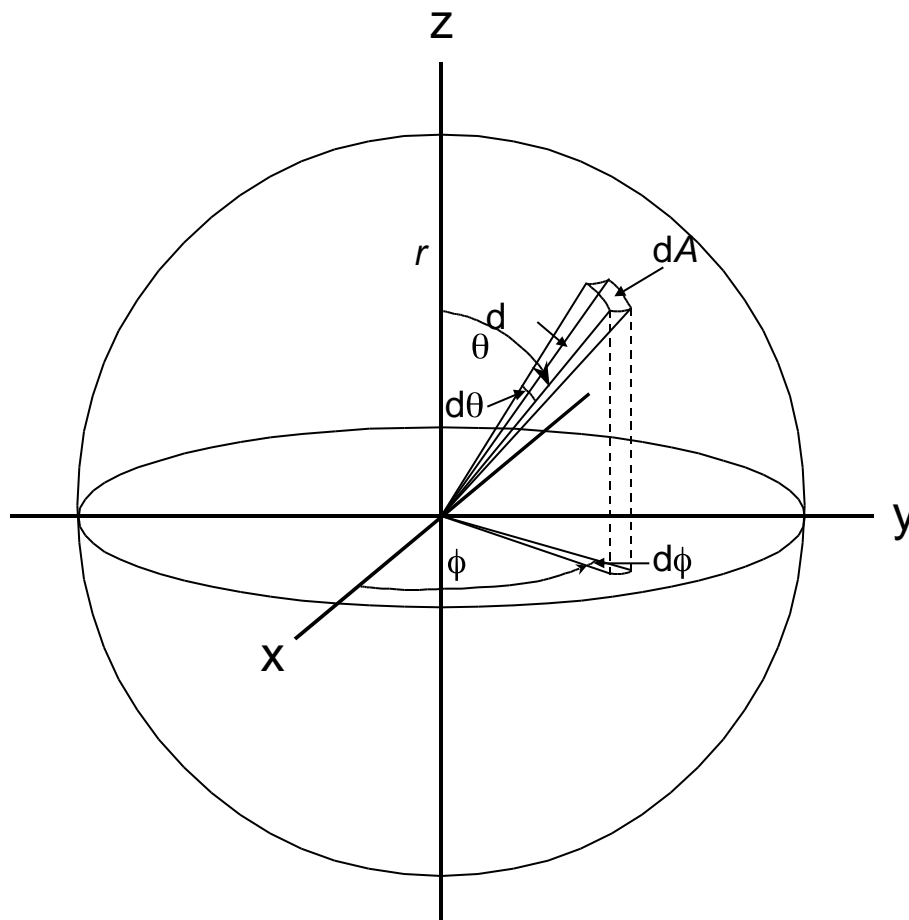


Figure 1. Spherical-polar coordinate system.

#### 3.3.1. Radiant energy

*Radiant energy* ( $Q$ ) is a total amount of radiant emission (J) from a source over a given period of time.

#### 3.3.2. Radiant power

The *radiant power* ( $P$ ) of a source is the rate of radiant energy or total radiant power (W) emitted in all directions by a light source.

$$P = \frac{dQ}{dt} \quad (4)$$

For example, the radiant power of the Sun is  $3.842 \times 10^{26}$  W. In theory,  $P$  should include all wavelengths emitted by the source; however,  $P$  is usually restricted to the wavelength range of interest to photochemistry. For example, if a light source is being used for ultraviolet photochemistry,  $P$  would be specified for emission in the 200 – 400 nm ultraviolet range.

#### 3.3.3. Radiant power efficiency

The *radiant power efficiency* ( $\eta$ ) is defined as

$$\eta = \frac{P}{P_E} \quad (5)$$

where  $P_E$  is the input electrical power (W) from the wall to run the lamp and its power supply.

### 3.3.4. Radiant emittance or excitance

The *radiant emittance or excitance* ( $M$ ) ( $\text{W m}^{-2}$ ) of a source is the radiant power emitted from an infinitesimal area  $dA$  on the surface of the source (Figure 2a).

**Example:** The average radius of the Sun  $r_s$  is  $6.9585 \times 10^8$  m; calculate the average emittance  $M_s$  of the Sun

$$M_s = \frac{P}{4 r_s^2} = \frac{3.842 \times 10^{26} \text{W}}{4 (6.9585 \times 10^8 \text{m})^2} = 6.314 \times 10^7 \text{W m}^{-2}$$

### 3.3.5. Radiant intensity

The *radiant intensity* ( $I$ ) ( $\text{W sr}^{-1}$ ) is the total radiant power  $P$  emitted by a source in a given direction about an infinitesimal solid angle  $d$  (Figure 2b). Note that in a non-absorbing medium the radiant intensity does not fall off with distance. Since a total sphere corresponds to a solid angle of  $4\pi$  steradians

$$I = \frac{P}{4\pi} \quad (6)$$

### 3.3.6. Radiance

*Radiance* ( $L$ ) is defined as the radiant power  $d^2P$  emitted from an infinitesimal area  $dA$  of the source surface in a given direction about the solid angle  $d\Omega$ , divided both by the solid angle  $d\Omega$  and the orthogonally projected area  $dA \cos\theta$ .

$$L = \frac{d^2P}{d\Omega dA} = \frac{d^2P}{d\Omega dA \cos\theta} \quad (7)$$

The emittance  $M$  from an infinitesimal surface element  $dA$  is obtained by integrating  $L$  in spherical polar coordinates over the hemisphere of all outward-bound directions above  $dA$ , that is

$$M = \int_0^{2\pi} \int_0^{\pi/2} L \cos\theta \sin\theta d\theta d\phi \quad (8)$$

An *isotropic* light source is defined as one in which the radiance  $L$  is uniform over all outward directions; for such a source  $M = \pi L$ .

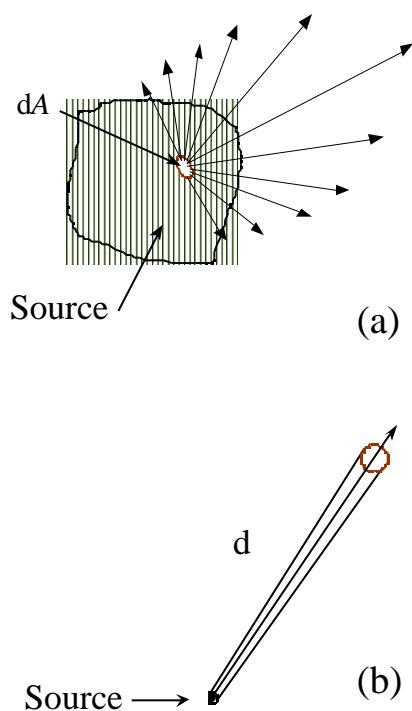


Figure 2. (a) *Emittance* of light from an infinitesimal area  $dA$  on the surface of a light source; (b) Concept of *radiant intensity* in a given direction about  $d$ .

### 3.4. Terms and concepts associated with the receipt of light

When light is emitted from a source, it radiates outward at the speed of light ( $c = 2.99792458 \times 10^8 \text{ m s}^{-1}$ ) (slower in a condensed medium). When it impinges on an object, it may be reflected, transmitted or absorbed. There are several terms that relate to the receipt of light.

#### 3.4.1. Fluence Rate

*Fluence Rate* ( $E_o$ ) ( $\text{W m}^{-2}$ ) is the radiant power of all wavelengths passing from *all* directions through an infinitesimally small sphere of cross-sectional area  $dA$ , divided by  $dA$  (see Figure 3).

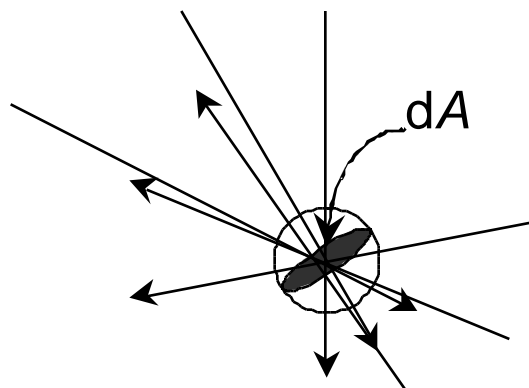


Figure 3. Illustration of the concept of fluence rate through an infinitesimally small sphere of cross-sectional area  $dA$ .

### 3.4.2. Irradiance

*Irradiance* (symbol  $E$ ; units  $\text{W m}^{-2}$ ) is defined as the total radiant power of wavelengths incident on an infinitesimal element of surface of area  $dS$  containing the point under consideration divided by  $dS$ . Note that  $E = \int E_\lambda d\lambda$ , where  $E_\lambda$  is the *spectral irradiance* (units  $\text{W m}^{-2} \text{nm}^{-1}$ ) at wavelength  $\lambda$ . Note that for the receipt of light, “irradiance” is the counterpart to “emittance” for the emission of light (see Fig. 2a).

The following are some important points regarding characteristics and differences between “irradiance” and “fluence rate”:

1. For a parallel and perpendicularly incident beam, not scattered or reflected, irradiance and fluence rate become identical.
2. For any UV source within a three-dimensional volume, the integration of UV irradiance over the interior surface of the volume yields the UV power of the lamp. This is not true for UV fluence rate.
3. The appropriate term for UV disinfection is “UV fluence rate” because a microorganism can receive UV power from any direction, especially when there is more than one UV lamp in the vicinity.

For a position at  $r$  cm from a point source, the irradiance is given by

$$E = \frac{P}{4\pi r^2} \quad (9)$$

**Example:** The average Earth-Sun distance is  $1.4957 \times 10^{11}$  m; calculate the average solar irradiance just outside the Earth’s atmosphere.

$$E_{\text{Earth}} = \frac{3.843 \times 10^{26} \text{ W}}{4\pi (1.4957 \times 10^{11} \text{ m})^2} = 1,367 \text{ W m}^{-2}$$

(Note that part of this irradiance is absorbed in the Earth’s atmosphere, so that at the surface of the Earth on a cloudless day, the irradiance is about  $1,000 \text{ W m}^{-2}$ .)

In general usage, the irradiance or fluence rate may be expressed as  $\mu\text{W cm}^{-2}$  or  $\text{mW cm}^{-2}$  ( $= 10 \text{ W m}^{-2}$ ). The irradiance is often termed “light intensity” – this is incorrect – see the proper definition of “radiant intensity” above.

### 3.4.3. Light dose or fluence

The *light dose* or *fluence* (symbol  $H$ , units  $\text{J m}^{-2}$ ) is the total radiant energy of all wavelengths passing from *all* directions through an infinitesimally small sphere of cross-sectional area  $dA$ , divided by  $dA$  (see Figure 3). It is given by the *average fluence rate* times the *exposure time* in seconds. The term *UV dose* is often used in UV disinfection literature. It represents the UV exposure of a given organism in the germicidal range. Many authors have used the units  $\text{mW.s cm}^{-2}$ , but the equivalent  $\text{mJ cm}^{-2}$  is preferred.

### 3.5. Spectral units

All of the terms for light emission or incidence refer to all relevant wavelengths. One can define *spectral derivatives* for each of these terms. For example, the light power emission of a UV lamp is often expressed as the *spectral power* ( $\text{W nm}^{-1}$ ), defined as the power output in a narrow wavelength band divided by the width of the band. The solar spectrum received at the Earth’s surface is described in terms of the *solar spectral irradiance* ( $\text{W m}^{-2} \text{nm}^{-1}$ ). Also the spectral distribution of a lamp emission is often given as a plot of spectral power versus wavelength.

### 3.6. Photon based units

Photochemistry involves the interaction of photons of light with molecules. Hence it is important to define some units that are based on photons.

#### 3.6.1. Photon emission weighted average

In several places throughout this Handbook, for polychromatic UV light sources, a *weighted average* of some quantity is required. This is because the average must be taken accounting for the different relative photon emission from the UV lamp. If the wavelength range of interest ( $\lambda_1$  to  $\lambda_2$ ) is divided into infinitesimal bands  $d\lambda$  and  $z_\lambda$  is the average value of some physical quantity in that band, then the *photon emission weighted average*  $\bar{z}$  is given by

$$\bar{z} = \frac{\int_{\lambda_1}^{\lambda_2} N_\lambda z_\lambda d\lambda}{\int_{\lambda_1}^{\lambda_2} N_\lambda d\lambda} \quad (10a)$$

where  $N_\lambda$  is the spectral photon flow emission (einstein  $s^{-1} nm^{-1}$ ) from the UV lamp (with appropriate corrections for transmission through any medium (e.g., quartz) between the lamp and the irradiated suspension) in the wavelength band  $\lambda$  to  $\lambda + d\lambda$ , and  $z_\lambda$  is the average value of some physical quantity in that band. In practice, the  $N_\lambda$  values can be relative numbers.

Usually,  $\bar{z}$  can be adequately approximated by using finite intervals. If the wavelength range of choice (e.g., 200-300 nm) is divided into small bands  $\Delta\lambda$  (e.g., 5 nm), then the *photon emission weighted average*  $\bar{z}$  is approximated by

$$\bar{z} = \frac{\sum_{\lambda=200}^{300} N_\lambda z_\lambda \Delta\lambda}{\sum_{\lambda=200}^{300} N_\lambda \Delta\lambda} \quad (10b)$$

where now  $N_\lambda$  is the spectral photon flow averaged over the wavelength band  $\Delta\lambda$ .

#### 3.6.2. Photon irradiance, photon fluence rate and photon flow

Each of the spectral terms can be converted to a corresponding equivalent *photon flow* by dividing the term by the average photon energy in the narrow wavelength band. For example, the *spectral irradiance* ( $W m^{-2} nm^{-1}$ ) can be converted to the *photon irradiance* ( $E_p$ ) (photons  $s^{-1} m^{-2}$ ) by dividing it by the photon energy

$$E_p = \frac{E}{hc/\lambda} \quad (11)$$

$E_p$  can also be expressed in molar terms on dividing by the Avogadro number, in which case the units are einstein  $s^{-1} m^{-2}$ . When the photon irradiance is multiplied by the incident area ( $m^2$ ) one obtains the *photon flow*  $N_p$  (photons  $s^{-1}$ ).

**Example:** A Petri dish 6.0 cm in diameter is irradiated with a low-pressure Hg lamp at 253.7 nm, such that the average irradiance is 1.05 mW cm<sup>-2</sup>. What is the incident photon flow (einstein s<sup>-1</sup>) on the Petri dish?

The energy of one einstein of light at 253.7 nm is

$$\begin{aligned}
 U &= \frac{hcN_A}{\lambda} \\
 &= \frac{6.6260755 \times 10^{-34} \text{ J s} \times 2.99792458 \times 10^8 \text{ ms}^{-1} \times 6.0221367 \times 10^{23} \text{ einstein}^{-1}}{253.7 \times 10^{-9} \text{ m}} \\
 &= 471,528 \text{ J einstein}^{-1}
 \end{aligned}$$

Thus the photon flow is

$$\begin{aligned}
 N_p &= \frac{EA}{U} = \frac{1.05 \times 10^{-3} \text{ Wcm}^{-2} \times (3.0 \text{ cm})^2}{471,528 \text{ J einstein}^{-1}} \\
 &= 6.296 \times 10^{-8} \text{ einstein s}^{-1}
 \end{aligned}$$

The total *photon flow* over a broad wavelength band is obtained by integrating over that band

$$N_p(\text{total}) = \int_1^2 N_p d\lambda \quad (12a)$$

where  $N_p$  is the spectral photon flow in the wavelength band from  $\lambda$  to  $\lambda + d\lambda$ . In practice, this integral is approximated by finite differences, that is

$$N_p(\text{total}) = \sum_1^2 N_p \quad (12b)$$

where now  $N_p^\lambda$  is the average spectral photon flow (einstein s<sup>-1</sup> nm<sup>-1</sup>) over the wavelength range from  $\lambda$  to  $\lambda + \Delta\lambda$ , and  $\Delta\lambda$  is a finite wavelength range (e.g., 5 nm).

For a polychromatic light source, the *photon fluence rate* ( $E_{op}$ ) (units einstein s<sup>-1</sup> m<sup>-2</sup>) is defined as the total number of einsteins (moles of photons) of all wavelengths passing from *all* directions through a small sphere of cross-sectional area  $dA$ , divided by  $dA$ . The photon fluence rate can be determined by actinometry (see Section 3.8.3). In this case, the conversion of photon fluence rate to fluence rate requires knowledge of the spectral distribution of the light source.

$$E_o = E_{op} \times \bar{U} \quad (13)$$

where  $\bar{U}$  is the photon emission weighted average (see Section 3.6.1) photon energy per einstein (see eq. 1b) over the emission spectrum of the lamp.

### 3.6.3. Quantum yield

The *quantum yield* (unitless) is a measure of the photon efficiency of a photochemical reaction. It is defined as the number of moles of product formed or reactant removed ( $P$ ) per einstein of photons absorbed. If steady-state is achieved, it can also be defined in terms of rates as

$$\phi_P = \frac{\text{rate of generation of } P}{N_a} \quad (14)$$

where the “rate of generation” of  $P$  is in mol s<sup>-1</sup> and  $N_a$  is the absorbed photon flow (einstein s<sup>-1</sup>). Note that  $\phi_P$  is based on the *absorbed* and not the *incident* photon flow. This is an error often made in the literature.

### 3.7. Light sources

#### 3.7.1. Blackbody light sources

Any object at a temperature above absolute zero emits light, called *blackbody radiation*. The wavelength distribution of the spectral emittance  $M$  ( $\text{W m}^{-2} \text{nm}^{-1}$ ) of a blackbody is governed by the Planck Blackbody Law

$$M = \frac{2 \times 10^{-9} hc^2}{n^2 \lambda^5} \frac{1}{\exp(hc/k_B T) - 1} \quad (15)$$

where  $n$  is the refractive index of the medium ( $n = 1.00$  for air),  $\lambda$  is the wavelength (m),  $T$  is the absolute temperature in degrees Kelvin (K),  $h$  is the Planck constant,  $c$  is the speed of light and  $k_B$  is the Boltzmann constant. Figure 4 shows the blackbody emission spectra for three different temperatures. It is readily apparent that the *blackbody* must be extremely hot to have a significant output in the ultraviolet.

#### 3.7.2. Line sources

When atoms are raised to an excited state, they emit only in very narrow lines with virtually no emission between the lines. The low-pressure mercury lamp is a very common lamp of this type. Table 2 gives the wavelengths and relative emittances for the emission lines of a low-pressure mercury vapor lamp.

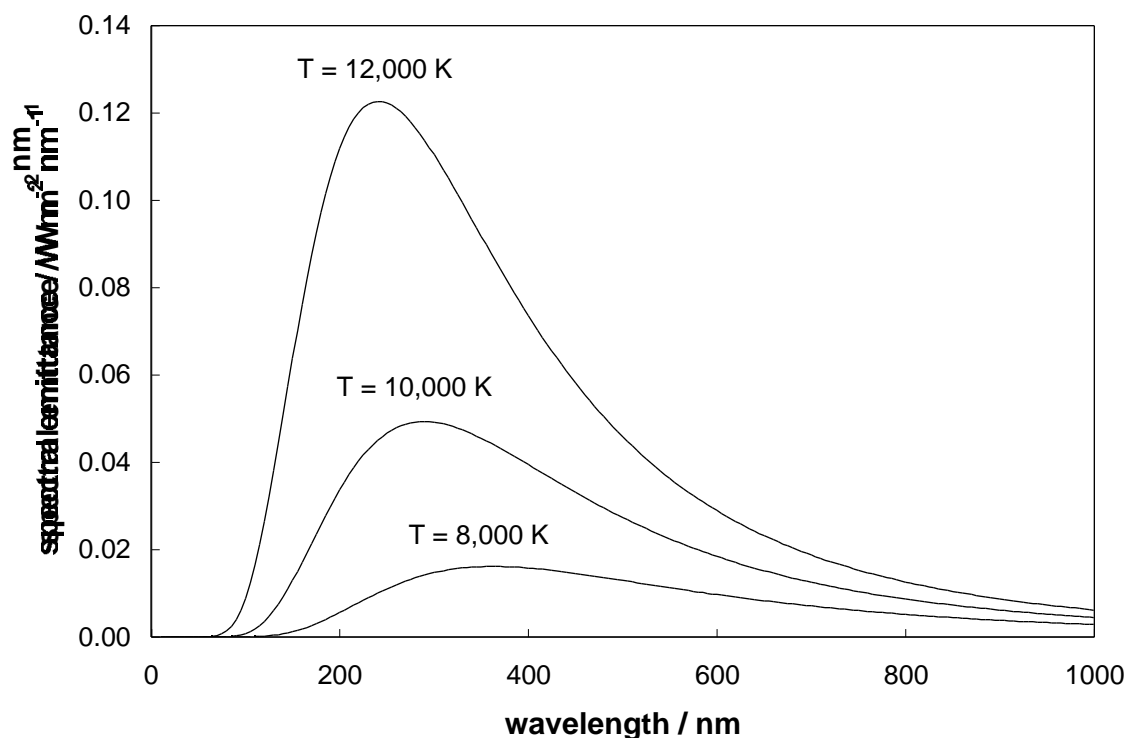


Figure 4. Wavelength distribution of the spectral emittance of a blackbody source.

**Table 2. Wavelengths and relative emittances of a low pressure mercury lamp<sup>5</sup>**

Wavelength / nm	Emittance (rel)	Wavelength / nm	Emittance (rel)
184.9	8	302.2-302.8	0.06
248.2	0.01	312.6-313.2	0.6
253.7	100	334.1	0.03
265.2-265.5	0.05	365.0-366.3	0.54
275.3	0.03	404.5-407.8	0.39
280.4	0.02	435.8	1.0
289.4	0.04	546.1	0.88
296.7	0.2	577.7-579.0	10.1

The low-pressure mercury lamp is very common. With a quartz sleeve, the principal emission is at 253.7 nm, which is effective in inactivating bacteria and viruses; such a lamp is thus called a *germicidal lamp*. Hence, the output power is rather low; for example, a 4 foot (122 cm) lamp would be rated at 40 W. The inner surface of the lamp envelope can be coated with various types of *phosphors*, which absorb the 253.7 nm radiation and emit at longer wavelengths. This is the basis of the very popular *fluorescent lamp*.

The emission lines of a mercury lamp are only sharp when the pressure of the gas is low (<10 torr). If the pressure is increased, the lamp can carry much more power, but the emission lines broaden. For the same length of lamp (about 120 cm), a *medium pressure lamp* (pressure about 1000 torr) can carry up to 30,000 W. These lamps are very common in commercial systems utilizing ultraviolet light. Figure 5 shows a comparison of the emission of low pressure and medium pressure lamps in the ultraviolet region.

### 3.7.3. Excimer lamps

Excimer lamps are unique in that they emit in a narrow band of wavelengths. An excimer is an atomic dimer that is stable only in the excited state and dissociates on decaying to the ground state. Table 3 gives the wavelengths of some of the common excimer lamps.

<sup>5</sup> Largely taken from "Photochemistry", J. G. Calvert and J. N. Pitts, Jr., Wiley, New York, 1966, p. 696.

**Table 3. Emission wavelengths for some common excimer lamps<sup>6</sup>**

Excimer	Wavelength / nm	Excimer	Wavelength / nm
Xe <sub>2</sub> *	172	XeCl*	308
KrCl*	222	I <sub>2</sub> *	342
Cl <sub>2</sub> *	259		

### 3.7.4. Flash lamps

Flash lamps are similar to continuous wave (CW) arc lamps in that they consist of a cylindrical quartz tube with electrodes at each end and filled with a gas (e.g., xenon). A power supply “fires” the lamps by discharging a large amount of electrical energy in a very short period of time (several  $\mu$ s) by applying a very high voltage (10 – 30 kV). The resulting plasma reaches temperatures of 10,000 – 13,000 K and the emission is essentially that of a blackbody (see Fig. 4). In commercial flash lamp systems the lamp is “flashed” about 30 times per s.

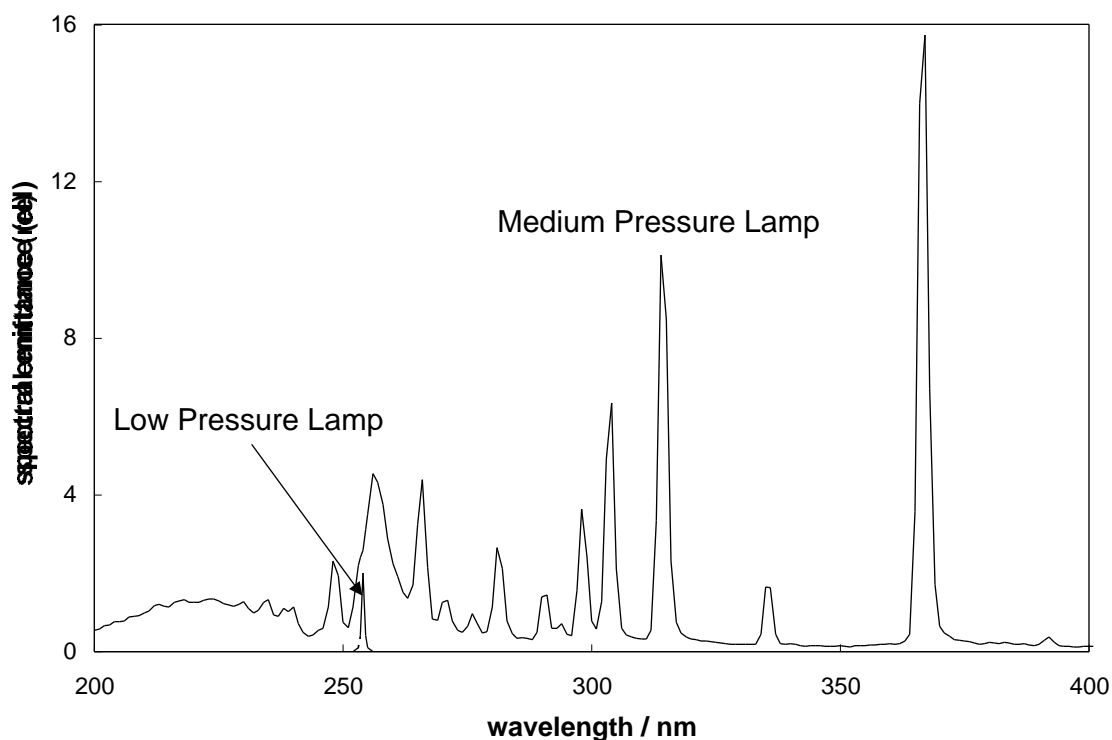


Figure 5. Relative spectral emittance from low pressure (···) and medium pressure (—) lamps.

### 3.8. Measurement of light

The measurement of light irradiance or fluence rate requires that the light be converted into a form that causes a change in a measuring device. There are two types of light detectors: *thermal*, where the light is converted to heat, and *photonic*, where the absorption of single photons drive electrons through an electronic circuit.

<sup>6</sup> “Novel incoherent excimer UV irradiation units for the application in photochemistry, photobiology/medicine and for waste water treatment”, T. Oppenländer, EPA Newsletter, March 1994,

### 3.8.1. Radiometers

A *radiometer* is a device that senses the total *irradiance* incident on a sensor element.

A *thermal radiometer detector* consists of a black surface where all the incident light is converted to heat. A *thermistor* is placed in thermal contact behind the black element. This, along with a similar black element kept in the dark, form a Wheatstone bridge producing a current proportional to the incident irradiance. *Thermal radiometer detectors* can be calibrated in an absolute sense, but they are not very sensitive.

A *photonic radiometer detector* usually involves a photocell with a UV-sensitive cathode that converts the incident *photon flow* into a current. These detectors are highly sensitive, but their sensitivity varies with wavelength. If the incident light is monochromatic, a conversion to irradiance is easily made. However, for a broadband light source, one must know the spectral distribution of the source and the spectral sensitivity of the UV detector to convert the radiometer reading into a true irradiance. The true irradiance is given by

$$E = \bar{C} \times (\text{meter reading}) \quad (16a)$$

where  $\bar{C}$  is a weighted average sensor correction factor given by

$$\bar{C} = \frac{S_{254}}{\bar{S}} \quad (16b)$$

where  $\bar{S}$  is the photon emission weighted average (see Section 3.6.1) detector sensitivity over the wavelength range of interest, and  $S_{254}$  is the detector sensitivity at 254 nm where the radiometer is usually calibrated.

### 3.8.2. UV sensors

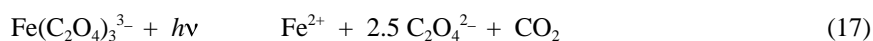
Certain semiconductors absorb only in the UV region (e.g., diamond, 190-230 nm; SiC, 210-380 nm and GaN, 250-370 nm) and are insensitive to visible light. These semiconductors can be incorporated into an electronic circuit and thus serve as convenient online UV sensors in UV reactors. However, UV sensor circuits based on these semiconductors tend to drift with age; hence, they must be calibrated periodically with a radiometer.

### 3.8.3. Actinometry

An *actinometer* is a photochemical reaction for which the quantum yield is very well known. Thus the measurement of the chemical yield after exposure to light allows the determination of the photon flow.

There are three common actinometers that are important for ultraviolet applications:

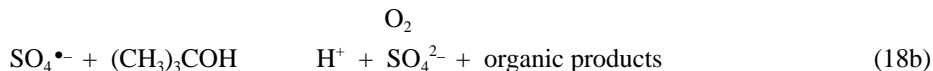
- a. The *ferrioxalate actinometer* is based on the photochemical reaction



The concentration of  $\text{Fe}^{2+}$  is easily assayed by the formation of a colored complex with *o*-phenanthroline. The quantum yield for the generation of  $\text{Fe}^{2+}$  depends slightly on wavelength, but in the 200-300 nm region, it is about 1.25.<sup>7</sup> Reaction 17 is sensitive to light in the range 200-500 nm, thus one must work in subdued or red light. In addition, one must know the fraction of the 200-500 nm emission that is in the 200-300 nm band.

<sup>7</sup> S. L. Murov, I. Carmichael and G. L. Hug, *Handbook of Photochemistry*, 2<sup>nd</sup> Ed., Marcel Dekker, New York, 1988, pp. 200-207.

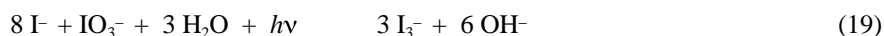
b. The *persulfate actinometer* is based on the photochemical reaction



The quantum yield for the production of  $\text{H}^+$  is 1.8. This actinometer is very easy to use, and the reaction is sensitive only to UV below 300 nm, hence one can work in normal light.<sup>8</sup>

c. The *iodide/iodate actinometer* is based on the photolysis of iodide in the presence of iodate, which acts as an electron acceptor.<sup>9</sup>

The overall photolysis reaction is



The quantum yield for generation of the triiodide ion ( $\text{I}_3^-$ ) is 0.75; a 0.6 M KI/0.01 M  $\text{KIO}_3$  solution absorbs UV only from 200 to 300 nm, and the triiodide ion absorbs strongly ( $\epsilon = 26,450 \text{ M}^{-1} \text{ cm}^{-1}$ ) at 352 nm. Hence the analysis is very easy, and one does not need to worry about absorption of room light.

## 4. Light in a Condensed Medium

### 4.1. Refractive index

The refractive index  $n$  for a medium is the ratio of the speed of light in a vacuum to that in the medium.

### 4.2. Refraction and Snell's Law

Snell's Law governs the refraction properties of light transmitted through a surface (see Fig. 6).

$$n_1 \sin \theta_1 = n_2 \sin \theta_2 \quad (20)$$

where  $n_1$  and  $n_2$  are the refractive indices of the two media. Note that if  $n_2 > n_1$ , the angle of refraction ( $\theta_2$ ) is less than the angle of incidence ( $\theta_1$ ).

### 4.3. Reflection and the Fresnel Laws

Whenever light passes through an interface between two media of different refractive index, a certain fraction of the light is reflected at the angle  $\theta_r = \theta_1$  (see Fig. 6), and the rest passes through the interface into the second medium and undergoes refraction. The optics involving the description of this process are complicated, since the amount reflected depends on the polarization of the light. If  $r$  is the *amplitude* of light *perpendicular* to the plane of incidence and  $r_{\parallel}$  is the *amplitude* of the light *parallel* to the plane of incidence, then the Fresnel Laws define these two amplitudes as:

<sup>8</sup> "A chemical actinometer for use in connection with UV treatment in drinking-water processing", G. Mark, M. N. Schuchmann, H.-P. Schuchmann and C. von Sonntag, *J. Water SRT-Aqua*, **39**, 309-313 (1990).

<sup>9</sup> "Potassium iodide as a chemical actinometer for 254 nm radiation: use of iodate as an electron

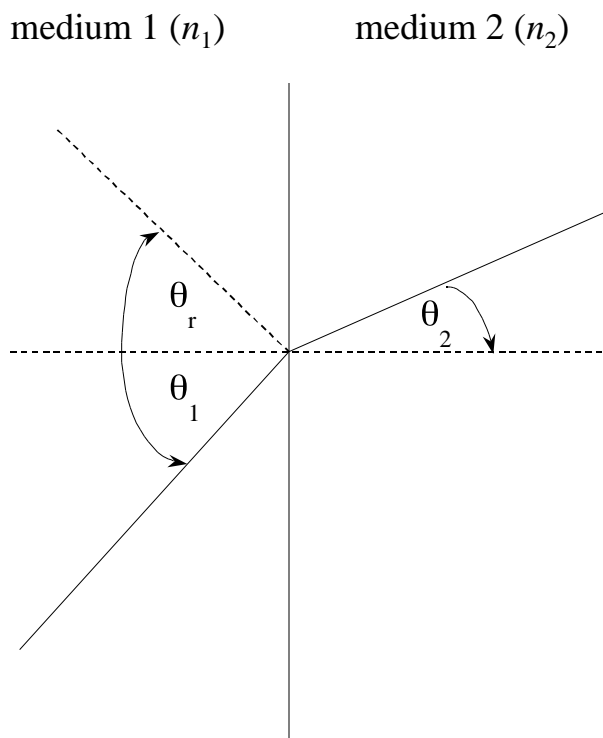


Figure 6. Reflection and refraction as a light beam passes from one medium to another.

$$r = \frac{n_1 \cos \theta_1 - n_2 \cos \theta_2}{n_1 \cos \theta_1 + n_2 \cos \theta_2} \quad (21a)$$

$$r_{\perp} = \frac{n_2 \cos \theta_1 - n_1 \cos \theta_2}{n_1 \cos \theta_2 + n_2 \cos \theta_1} \quad (21b)$$

The *Reflectance*  $R$  for unpolarized light is given by:

$$R = \frac{1}{2} [r_{\perp}^2 + r^2] \quad (21c)$$

Figure 7 illustrates how  $R$  varies with angle for an air/quartz interface. It is interesting that  $R$  remains fairly independent of angle (at about 4-5%) up to about  $40^\circ$  and then increases rapidly.

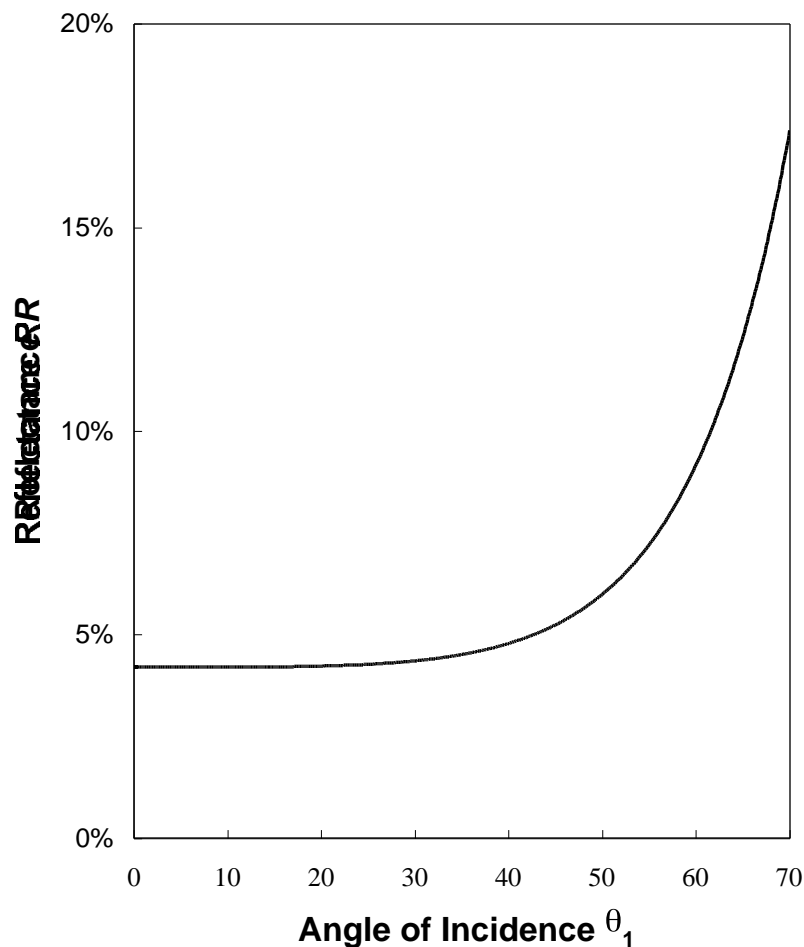


Figure 7. Percent Reflectance  $R$  versus angle of incidence.

The *transmittance*  $T$  refracted and transmitted into the second medium is given by

$$T = 1 - R \quad (22)$$

Thus the incident beam is split into two parts (see Fig. 6): a reflected part of fraction  $R$  and a refracted and transmitted part of fraction  $T$ .

#### 4.4. Absorption and transmittance – the Beer-Lambert Law

The Beer-Lambert Law describes how light is attenuated as a result of any material absorbing light in the medium.

##### 4.4.1. Transmittance

As a given light beam passes through a solution, the light will get attenuated by absorbing substances in the solution and by reflection from particles and the walls of the cell. (The *internal transmittance* refers to energy loss only by absorption, whereas the *total transmittance* is that due to absorption,

reflection, scatter, etc.) The attenuation factor or *transmittance*  $T_\lambda$  (unitless) for a given beam of wavelength  $\lambda$  is

$$T_\lambda = \frac{E_\lambda^t}{E_\lambda^o} \quad (23a)$$

where  $E_\lambda^t$  and  $E_\lambda^o$  are the transmitted (over a pathlength  $l$ ) and incident irradiances, respectively, at a fixed wavelength  $\lambda$ . If the attenuation in transmittance is due primarily to absorption (internal transmittance), this attenuation can also be described by the expression

$$T = 10^{-a_\lambda l} \quad (23b)$$

where  $a_\lambda$  is the *absorption coefficient* ( $\text{cm}^{-1}$ ) at wavelength  $\lambda$ , and  $l$  is the path length (cm). Often the subscript  $\lambda$  is dropped, so that the symbol  $T$  for transmittance *implies* monochromatic radiation.

#### 4.4.2. 1 cm transmittance ( $T'$ )

Often the absorption characteristics of the solvent are described by the “% transmittance” at a fixed wavelength. The “1 cm *transmittance* ( $T'$ )” is given by eq. 23b where  $l = 1$  cm. The “percent transmittance” is then  $100 \times T'$ .

#### 4.4.3. Absorbance

The *absorbance* (unitless) is defined as the logarithm to the base 10 of the ratio of the incident spectral irradiance ( $E_\lambda^o$ ), essentially monochromatic, to the spectral irradiance of transmitted radiation ( $E_\lambda^t$ ):

$$A = \log \frac{E_\lambda^o}{E_\lambda^t} \quad (24a)$$

Since a small fraction (4%) of the beam is reflected from each quartz surface, in practice  $E_\lambda^o$  and  $E_\lambda^t$  are the spectrophotometer responses for monochromatic UV light at wavelength  $\lambda$  transmitted through a quartz cell containing pure solvent (e.g., water) and the same cell containing the sample of interest, respectively. Often the subscript  $\lambda$  is dropped, so that the symbol  $A$  for absorbance *implies* monochromatic radiation.

The absorbance is related to the concentrations of absorbing components by

$$A = \sum_i \epsilon_{\lambda_i} c_i l \quad (24b)$$

where  $\epsilon_{\lambda_i}$  and  $c_i$  are the molar absorption coefficient ( $\text{M}^{-1} \text{cm}^{-1}$ ) at wavelength  $\lambda$  and concentration (M) of component  $i$  in the solution and  $l$  is the pathlength (cm).

Absorbance and transmittance are related by

$$T = 10^{-A} \quad (25a)$$

or

$$A = -\log T \quad (25b)$$

### 4.5. Fraction of light absorbed

Since photochemistry is initiated only by the photons that are absorbed by the medium, it is important to determine the fraction of light absorbed from an incident beam.

#### 4.5.1. For a monochromatic or narrow band light source

Note that all of the equations related to the Beer-Lambert Law apply only for monochromatic light or in a narrow band of wavelengths where the absorption coefficient does not change significantly with wavelength. For monochromatic or narrow band light, the fraction of light absorbed  $f_\lambda$  in the medium is given by

$$f_\lambda = 1 - T_\lambda = 1 - 10^{-A_\lambda} \quad (26)$$

**Table 4. Spreadsheet for the calculation of the fraction of light absorbed.**

$[\text{H}_2\text{O}_2] = 25 \text{ ppm}$ $[\text{H}_2\text{O}_2] = 0.734 \text{ mM}$ pathlength = 14 cm $F(\text{H}_2\text{O}_2) = 0.2189$							
wavelength band (nm)	H <sub>2</sub> O <sub>2</sub> absorption coefficient M <sup>-1</sup> cm <sup>-1</sup>	A(water) (1 cm)	Total A due to H <sub>2</sub> O <sub>2</sub>	Total A due to water	lamp photon flow (rel)	total photon flow absorbed	photon flow absorbed by H <sub>2</sub> O <sub>2</sub>
200-204	179.21	0.300	1.843	4.200	30	30.3	9.2
205-209	155.84	0.250	1.602	3.500	74	73.8	23.2
210-214	132.23	0.210	1.360	2.940	177	177.2	56.0
215-219	110.12	0.170	1.132	2.380	364	364.2	117.4
220-224	89.97	0.140	0.925	1.960	552	551.6	176.9
225-229	72.07	0.110	0.741	1.540	578	575.2	186.9
230-234	55.83	0.080	0.574	1.120	485	475.5	161.1
235-239	43.28	0.060	0.445	0.840	421	399.2	138.2
240-244	33.45	0.040	0.344	0.560	202	176.9	67.3
245-249	25.31	0.020	0.260	0.280	636	453.0	218.2
250-254	19.02	0.010	0.196	0.140	658	354.3	206.5
255-259	14.13	0.000	0.145	0.000	1154	328.1	328.1
260-264	10.47	0.000	0.108	0.000	1091	239.7	239.7
265-269	7.68	0.000	0.079	0.000	543	90.2	90.2
270-274	5.57	0.000	0.057	0.000	344	42.5	42.5
275-279	3.99	0.000	0.041	0.000	674	60.7	60.7
280-284	2.83	0.000	0.029	0.000	246	15.9	15.9
285-289	1.94	0.000	0.020	0.000	402	18.0	18.0
290-294	1.32	0.000	0.014	0.000	473	14.5	14.5
295-299	0.88	0.000	0.009	0.000	893	18.5	18.5
Totals					10000	4459	2189
% total flow absorbed =						44.6 %	
% flow absorbed by H <sub>2</sub> O <sub>2</sub> =						21.9 %	
% flow absorbed by background =						22.7 %	

**4.5.2. For a broad-band light source**

When the light source spans over a broad band of wavelengths, one can calculate an overall fraction of light absorbed  $F$  by breaking the spectral band into a number of narrow bands (e.g., 5 nm).  $F$  is then calculated as a photon emission weighted average (see Section 3.6.1) over the spectral wavelength range of interest. Table 4 illustrates how  $F$  for hydrogen peroxide can be calculated in a water with a background absorbance using a spreadsheet.

## 5. Advanced Oxidation Technologies

Advanced Oxidation Technologies (AOTs) are those that utilize powerful oxidizing intermediates (e.g., the hydroxyl radical  $\bullet\text{OH}$ ) to remove primarily organic pollutants from contaminated air and water. Most of the commercially viable AOTs use ultraviolet and visible light to generate  $\bullet\text{OH}$  radicals. These can be subdivided into homogeneous and heterogeneous technologies. A very useful Handbook on Advanced Oxidation Technologies is available for free. Two other reviews may be consulted for further coverage. The second last column is obtained by multiplying the *lamp photon flow (rel)* by  $f$  from eq. 26. The last column is obtained by multiplying the total *photon flow absorbed* by the ratio  $A \cdot (\text{H}_2\text{O}_2) / [A (\text{H}_2\text{O}_2) + A (\text{water})]$ .

AOTs have proven to be very effective in treating a wide variety of organic contaminants, such as trichloroethylene, perchloroethylene, 1,4-dioxane, methyl-*tert*-butyl ether, acetone, phenols, BTEX (benzene, toluene, ethylbenzene and xylenes found in waters contaminated ground waters and industrial effluents).

### 5.1. Homogeneous AOTs

Homogeneous AOTs are those that involve absorption of UV and/or visible light in a homogeneous aqueous solution. Photochemical processes in solution lead to the generation of  $\bullet\text{OH}$  radicals, which initiate the oxidation and degradation of the organic pollutants.

#### 5.1. The UV/O<sub>3</sub> process

The photolysis of ozone (O<sub>3</sub>) in the 200-280 nm region (UVC) can lead to the generation of  $\bullet\text{OH}$  radicals through the reactions:



where the square brackets in reaction 27b represent a solvent cage in which almost all the hydroxyl radical pairs combine to form H<sub>2</sub>O<sub>2</sub> within the cage.

The UV/O<sub>3</sub> process has been used commercially, particularly in the treatment of clear ground waters containing contaminants such as trichloroethylene (TCE) and perchloroethylene (PCE); however, now it is not considered economic compared to the UV/H<sub>2</sub>O<sub>2</sub> process.

#### 5.1.2. The UV/H<sub>2</sub>O<sub>2</sub> process

This is by far the most important commercial AOT. It is based on the direct photolysis of added hydrogen peroxide.



The quantum yield for generation of  $\bullet\text{OH}$  radicals is 1.0, and most organic pollutants can be degraded rapidly. Enough H<sub>2</sub>O<sub>2</sub> must be added so that about 30% of the UV between 200 and 300 nm is absorbed. However, if the water absorbs UV strongly in the 200-300 nm region and/or the alkalinity is very high, this process may not be effective.

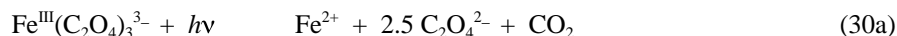
### 5.1.3. UV Fentons processes

When the contaminated water absorbs strongly in the 200-300 nm region and contaminant concentrations are high, one of the UV Fentons processes may be effective. The UV Fentons processes are based on the photoreduction of ferric ion and ferric complexes. The resulting  $\text{Fe}^{2+}$  then reacts with  $\text{H}_2\text{O}_2$  in a Fentons reaction to generate  $\bullet\text{OH}$  radicals. These processes require a pH of about 3, so there are added costs of acidifying the water. The simplest process is the photolysis of  $\text{Fe}^{\text{III}}(\text{OH})^{2+}$ .



The quantum yield of reaction 29a is about 0.15 and the  $\text{Fe}^{\text{III}}(\text{OH})^{2+}$  ion absorbs UV out to about 400 nm.

$\text{Fe}(\text{III})$  forms complexes with many organic acids. One of the most effective is the trioxalato complex with oxalic acid. The overall reactions are



The quantum yield of reaction 30a is 1.2, and ferrioxalate absorbs out to 500 nm. This makes this a very efficient form of the UV Fentons process. However, the need for addition of oxalate adds to the chemical costs.

## 5.2. Heterogeneous AOTs

Certain metal oxides (particularly the anatase form of  $\text{TiO}_2$ ) absorb UV and generate  $\bullet\text{OH}$  radicals on the surface of the particles. The relevant reactions are



The organic pollutant adsorbs to the surface of the  $\text{TiO}_2$  particle and is then attacked by the adsorbed  $\bullet\text{OH}_{\text{TiO}_2}$  radical. Unfortunately, the quantum yield for reaction 31b is only about 0.04-0.05; hence, this AOT is unlikely to be important commercially.

## 6. Ultraviolet Disinfection

Ultraviolet light has been used to disinfect both drinking water and secondary effluent from sewage treatment plants over a good part of the 20<sup>th</sup> century. Before discussing the details and mechanism of UV disinfection, some basic concepts need to be introduced.

### 6.1. UV irradiance, UV fluence rate, UV dose and their measurement

*UV Dose* is defined in Section 3.4.3. Note that the UV dose is the *UV fluence rate* times the irradiation time in seconds. Often the units of UV dose are given as  $\text{mW}\cdot\text{s}/\text{cm}^2$ , but  $\text{mJ}/\text{cm}^2$  is preferred. UV fluence rate is usually estimated (measured as UV irradiance) with a calibrated radiometer (see Section 3.8.1).

#### 6.1.1. Collimated beam apparatus

Figure 8 illustrates a collimated beam apparatus. The UV lamp is housed in the upper cabinet and is separated from a long collimator by a pneumatically driven shutter. The inner walls of the collimator are painted a flat black, so that any UV light that hits the wall is absorbed. The result is that at the end of the collimator, a reasonably uniform *collimated beam* of UV can be used to irradiate suspensions of microorganisms.

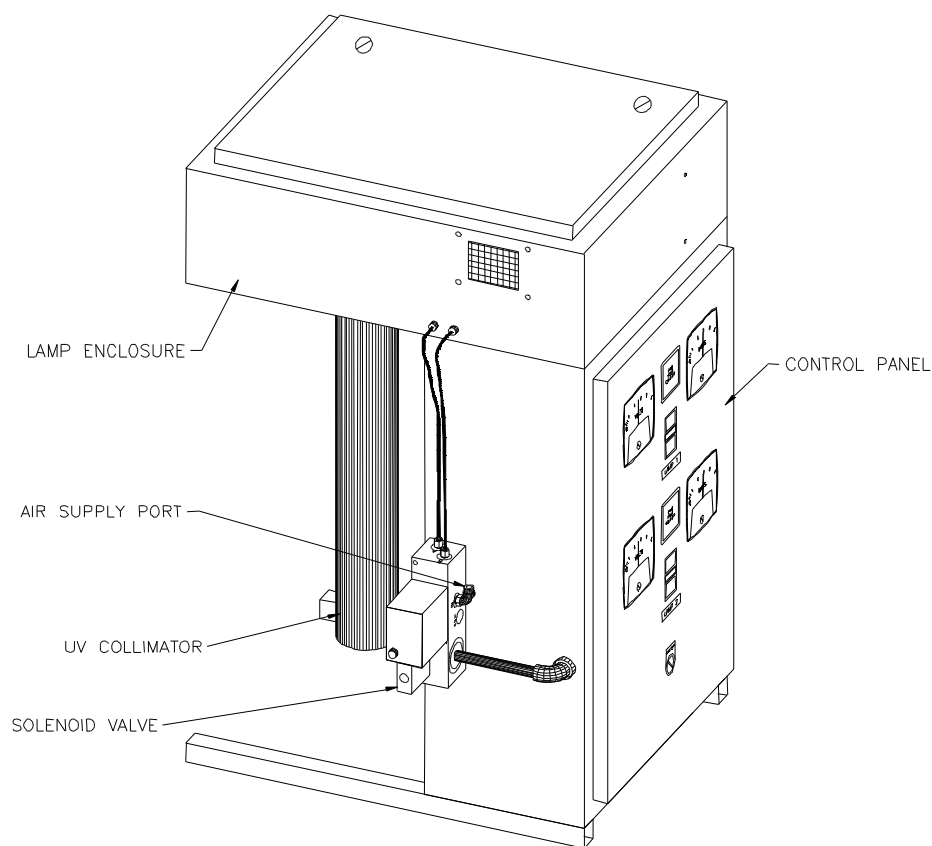


Figure 8. Collimated beam apparatus (courtesy Calgon Carbon Corporation, Markham, ON, Canada).

If the light source is a low-pressure mercury lamp, the incident irradiance can be measured directly by a radiometer calibrated at 254 nm. One must make a correction for the variation of the irradiance across the Petri dish containing the stirred suspension of microorganisms. Also if the water absorbs UV, corrections must be made for this absorption. If the light source is a medium pressure lamp, then a *sensor correction* must be made (eqs. 16).

The UV dose ( $\text{mJ cm}^{-2}$ ) is then obtained by multiplying the average fluence rate in the water ( $\text{mW cm}^{-2}$ ) by the exposure time (s).

### 6.1.2. UV reactors

The determination of the UV dose in a UV reactor through which water is flowing at a given flow rate is very complex. The reason is that the UV fluence rate varies considerably throughout the reactor, being very high near the quartz sleeve around the UV lamp and very low near the walls. If one makes the assumption that the flow through the reactor exhibits perfect *plug flow* behavior and perfect *radial mixing*, then it is possible to calculate an *average UV fluence rate* in the reactor. The *UV dose* is then the average UV fluence rate times the residence time given by  $V/F$ , where  $V$  is the volume (L) of the

reactor and  $F$  is the flow rate ( $L s^{-1}$ ). The calculation is quite sophisticated and involves the *Multiple Point Source Summation* approximation, in which the linear lamp is replaced by a string of  $n$  point sources. The fluence rate in any small element of volume in the reactor is then the sum of the fluence rates from all  $n$  point sources.

## 6.2. Mechanism of UV disinfection

Ultraviolet light is absorbed by proteins, RNA and DNA in a given microorganism. Absorption of UV by proteins in membranes at high doses ultimately leads to the disruption of the cell membranes and hence death of the cell. However, at much lower UV doses, absorption of UV by DNA can disrupt the ability of the microorganism to replicate. A cell that cannot replicate cannot infect.

DNA is a nucleic acid polymer in a double-stranded helix linked together by a sequence of four constituent bases (adenine, cytosine, guanine and thymine), which constitute the genetic code. These form "base pairs" (adenine with thymine and cytosine with guanine) held together by hydrogen bonds. This is the "glue" that holds the two "strands" of DNA together. Of these four bases, thymine undergoes a unique photochemical reaction (see Fig. 9). If two thymine bases are located adjacent to each other, absorption of a UV photon by one of the thymines leads to formation of a chemical bond between the two thymines (called a thymine dimer). This disrupts the structure of the DNA, so that if enough thymine dimers are formed, the DNA cannot replicate in cell mitosis. This then is the fundamental mechanism of UV disinfection.

Some microorganisms (particularly bacteria) have a repair mechanism that dissociates the thymine dimers. This process is triggered by the absorption of UVA light and is thus called *photoreactivation*. The repair mechanism can be inhibited, but this requires a higher UV dose.

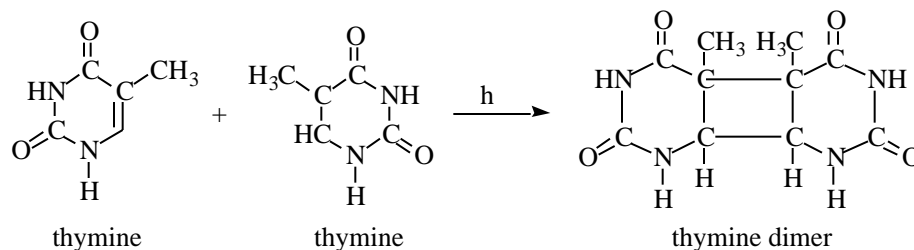


Figure 9. Photochemical dimerization of two thymine bases.

## 6.3. Sensitivity of microorganisms to UV

Various microorganisms respond differently to UV radiation. Figure 10 gives the UV dose necessary for 4 logs inactivation (99.99%) with and without photoreactivation.

## 6.4. Biodosimetry

Biodosimetry is the most reliable method available at present for the measurement of UV dose in a UV reactor. This method consists of seeding a harmless microorganism into the water upstream of a UV reactor. Samples are taken of the influent and effluent and from this a log inactivation can be calculated. At the same time, a dose-response curve is determined using a collimated beam apparatus using the same water. One can then obtain an estimate of the UV dose by reading off the dose-response curve the dose corresponding to the log inactivation found in the UV reactor.

## **7. Ultraviolet Curing**

Ultraviolet curing involves the use of ultraviolet light to “cross-link” inks and coatings (e.g., wood varnishes) so that after UV exposure the surface is “dry” or “cured”. This is a major advantage in production, since very little time is required for “drying” of the ink or coating.

### **7.1. The chemistry of UV curing**

The ink or coating to be irradiated usually consists of a base polymer (e.g., polyisoprene) and a UV absorbing “tackifier” (e.g., 1,6-hexanediol diacrylate). Under the action of the absorption of UV photons, the “tackifier” forms bonds with polyisoprene chains, which results in “cross-linking” of the chains. This markedly increases the viscosity of the polymer to the point that becomes “hard” and thus “dry”.

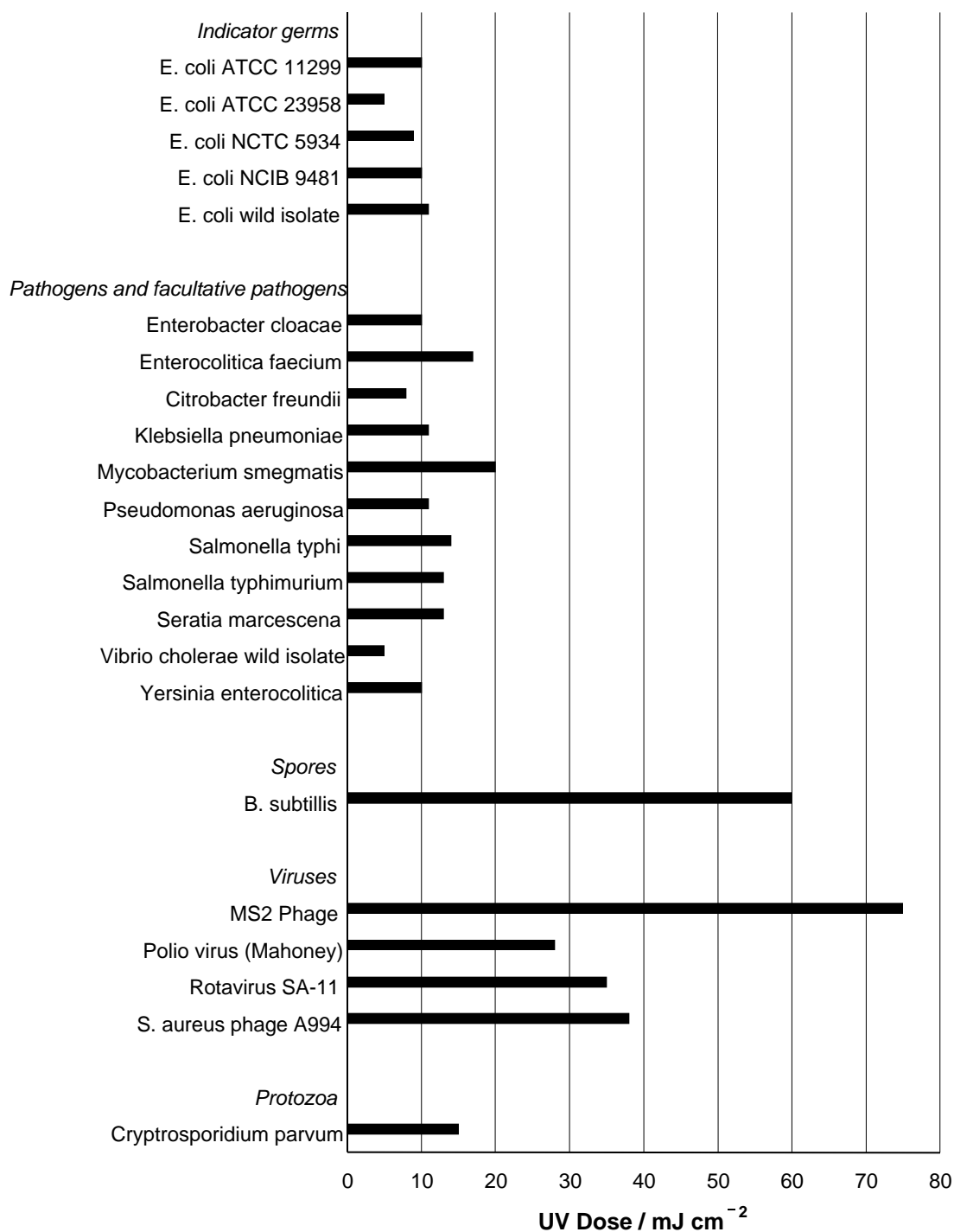


Figure 10. UV dose required for 4 logs (99.99%) inactivation of bacteria, spores, viruses and protozoa. The solid and open bars represent with (open) and without (solid) photoreactivation.<sup>10</sup>

## 7.2. UV lamp geometry

The UV lamps used are usually medium-pressure mercury lamps mounted above the surface to be irradiated. A reflector is placed above the UV lamps to direct all the light onto the surface. This

<sup>10</sup> Partially taken from Fig. 3 of "Testing performance and monitoring of UV systems for..."

reflector can be elliptical or parabolic (see Figure 11). In the former case, the UV rays are focussed to a line parallel to the lamp, whereas in the latter case, the rays are spread out uniformly across a wide area.

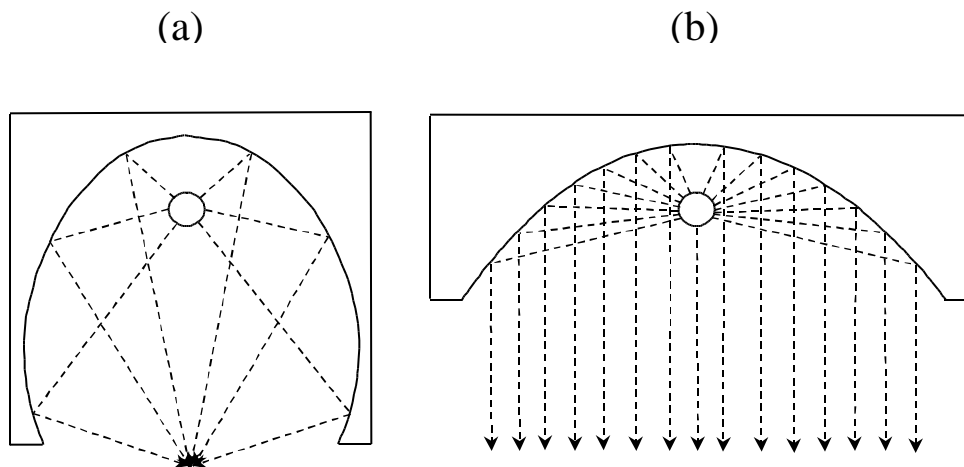


Figure 11. Reflector configurations for UV curing lamps: (a) elliptical reflector; (b) parabolic reflector.

#### Acknowledgements

The author very much appreciates the comments he has received for improvements and particularly would like to thank Dr. Mihaela I. Stefan and Dr. R. D. Samuel Stevens for their comments and professional expertise in preparing this Handbook.

## Using Stark Spectroscopy to Probe Polymer and Organic Glass Matrices

Linda A. Peteanu\*, Arindam Chowdhury, Sarah A. Locknar, Lavanya Premvardhan,  
Department of Chemistry, Carnegie Mellon University, Pittsburgh, PA 15213,  
[peteanu@andrew.cmu.edu](mailto:peteanu@andrew.cmu.edu)

### **Abstract**

The science of photochemistry has greatly benefited by the constant expansion in the number of techniques suitable for probing the electronic and structural properties of molecules as well as their dynamics. The purpose of this article is to (re-)acquaint the photochemistry community with spectroscopic methods based on the Stark effect in the hope of stimulating others to consider applications of this method to problems under study in their own laboratories. The organization is as follows: we will first present a short (and by no means exhaustive) survey of work in this area, followed by a brief description of how we perform the experiment and analyze the data. Finally, we will outline one of the several applications that we have been pursuing over the last several years in the areas of photochemistry, biological systems, and materials science.

### **Introduction and Overview**

The Stark effect refers to the perturbation in the energies of states of a molecule due to the application of an external electric field that is typically  $\sim 10^5$ - $10^6$  V/cm in magnitude. Electroabsorption or Stark spectroscopy is somewhat analogous to solvatochromism with the important distinction that the magnitude of the externally applied electric fields is used as a variable rather than the solvent polarity. Using Stark spectroscopy, one may obtain the magnitude of the change in dipole moment ( $|\underline{\mu}|$ ) and the change in polarizability ( $\overline{\alpha}$ ) between two rotational, vibrational, or, most commonly, two electronic states of a molecule. We refer to these quantities as the dipolar properties of the molecule and they represent some of the most fundamental parameters that characterize the electronic structure of the system. In general, the change in molecular polarizability is *not* obtained from a solvatochromic analysis, particularly if the molecules of interest are polar. Nonetheless, the polarizability of a molecule is an extremely important quantity for understanding the most basic characteristics of its electronic states and how they are perturbed by the large ( $10^7$ - $10^8$  V/cm) electric fields that are present in all condensed-phase environments. To appreciate the role of electronic polarizability one should realize that, in its absence, the dipole moment of a molecule would be the same in the gas phase as in the condensed phase. In contrast, the dipole moment sometimes increases by as much as a factor of two. It is therefore easy to see why accurate measurements of polarizability are critical to achieving agreement between experimental and calculated properties of molecules

particularly for those that undergo considerable charge-transfer in the excited state. This class of molecules forms an important part of our work.

Historically, the first applications of Stark spectroscopy were to study rotational transitions in small gas-phase molecules.<sup>1</sup> From this work, highly accurate molecular dipole moments for isolated molecules are available that provide critical checks to the results of high-level quantum calculations. Comparison of measurements for the same molecule in the gas phase with those in solution can provide an important confirmation of the accuracy of reaction field methods. These methods model how the parameters  $|\underline{\mu}|$  and  $\overline{\underline{\alpha}}$  are altered by interactions of a solute with the large fields present in a typical condensed phase environment.

One of the best known and most prolific researchers in this field, Wolfgang Liptay, was among the first to extend the Stark technique to measurements both to molecules in solution phase and in organic glasses. The formalism that he developed to analyze Stark data, described qualitatively below, is the most commonly used one today. Baumann and coworkers<sup>2</sup> have continued to work extensively in the area of organic molecules and to further develop the methodologies.

One of the attributes that makes Stark spectroscopy powerful is the ability to study optical chromophores in a wide range of environments including glasses, proteins, membranes, and polymers. The application of Stark spectroscopy to proteins and to biological chromophores was advanced by Richard Mathies<sup>3,4</sup> and by Steven Boxer, whose work on the Stark spectroscopy of the photosynthetic reaction center and associated chromophores is very widely known.<sup>5</sup> The biological applications of Stark spectroscopy are quite numerous, particularly for the study of proteins involved in electron transfer processes. In this realm, we have been pursuing a series of studies on the charge-transfer electronic states of the blue copper protein azurin, in collaboration with Prof. Glen Loppnow.

The study of charge-transfer reactions in inorganic complexes is another area that has received a great deal of attention in the past few years.<sup>6-8</sup> In the area of materials science, Stark spectroscopy has seen a resurgence of interest for the study of large conjugated polymer systems,<sup>9-11</sup> molecular crystals<sup>12,13</sup>, molecular aggregates<sup>14</sup> and smaller organic systems with interesting non-linear optical properties.<sup>15-17</sup> Our group has extended this method to the study of the conducting polymeric system polyaniline in collaboration with Prof. Alan MacDiarmid.

An emerging area is the application of Stark spectroscopy to study the characteristics of polymeric environments by monitoring the effect of the applied field on chromophores doped within the polymer.<sup>18</sup> An example of this type of experiment is discussed in this review. Such work has applications for the development of polymeric non-linear optical devices based on electrical poling of dopant molecules. Poling refers to the use of an electric field to create a macroscopic alignment of polar chromophores within a matrix. This technique generates a non-centrosymmetric environment that can support the generation of second harmonic radiation if the chromophores have large hyperpolarizabilities ( $\beta$ ). In favorable cases, Stark spectroscopy combined with a high resolution optical technique such as hole burning, fluorescence line narrowing, or single molecule spectroscopy, can give very detailed pictures of the molecular environments of glasses and films.<sup>19-21</sup>



### Experimental Methods

**Apparatus:** The instrument that we have constructed to perform the measurements reported here is described in detail in Ref. 22. A diagram, labeling the most important elements is shown in Fig. 1 below.

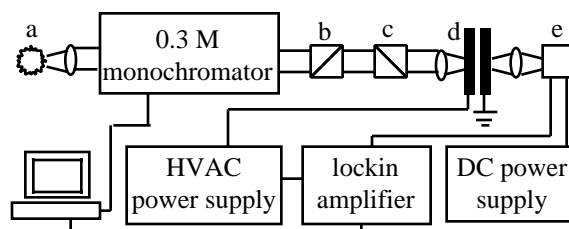


**Figure 1:** Structural diagram of electroabsorption instrument. The light source (a), depolarizer (b), polarizer (c), sample (d) and photodiode detector (e) are shown.

Below, an expanded view of the sample is shown (Fig. 2).

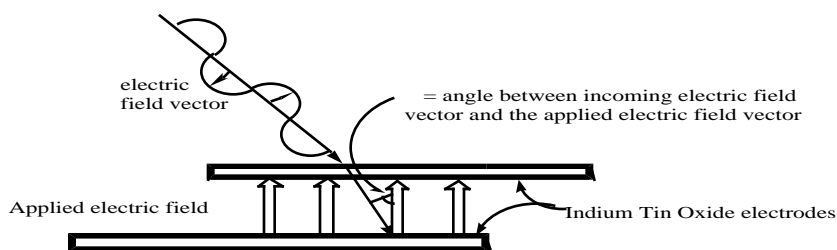


**Figure 2:** Bird's Eye view of Sample Configuration. The light is horizontally polarized and the sample is mounted on a rotating rod so that the angle can be easily changed. For all experiments reported here, is set at 54.7 degrees (magic angle). For UV absorbing samples, the electrode material is inconel deposited on quartz substrate.

**Computational Methods:** One of our primary interests is in establishing whether or not good correspondence exists between the results of electronic structure calculations, which are usually gas phase, and the measured properties of molecular systems in the condensed phase. Thus far we have primarily used generally available *ab initio* (Gaussian)<sup>23</sup> and semi-empirical (MOPAC and INDO/s)<sup>24,25</sup> codes for our electronic structure calculations.

For the studies described here we required a method for the calculation of ground- and excited-state polarizabilities. We perform these calculations using a finite-field method with either INDO1/s or *ab initio* hamiltonians, Hartree-Fock for the ground state and singles configuration interaction for the excited state. Prior to this work, the validity of this approach to obtain the polarizabilities of *excited* states had not been extensively established in the literature, especially for polyenes which are molecules that have a complex electronic state structure. Therefore, we performed<sup>26</sup> an extensive comparison of the finite-field results for the polarizabilities of both polar and non-polar short chain polyenes to those obtained using a higher level method. The latter calculations

were performed by our collaborator, Dr. Zhigang Shuai. The method that he used incorporates correlation at a higher level (doubles, triples, and quadruples) by using a multireference determinant coupled to INDO hamiltonian and the sum-over-states formalism is used to calculate the polarizabilities.<sup>27</sup> Excellent agreement for a wide variety of molecules has been found between the results of the finite-field method that we use and both the higher-level calculations and published experiments.

To correct these calculated results for the effect of the dielectric environment of our matrices, we have used a modified Onsager reaction field formalism.<sup>28</sup> The modification produces a more realistic solvation correction by more accurately accounting for the true volume of the cavity occupied by the molecule in the dielectric medium. The calculated values in Table 1 have been corrected for both the cavity field and the reaction field. More will be said regarding this correction later.

**Data Analysis:** A detailed description of the data analysis procedure is available in a number of references.<sup>1,29,30</sup> Here we offer a qualitative description of how the electric field perturbs the ground and excited (Franck-Condon) states of a molecule and therefore its absorption spectrum. Our starting assumption is that the sample consists of an ensemble of randomly oriented dipoles within a matrix that give rises to an absorption spectrum that is a single inhomogeneously broadened gaussian. This treatment can be extended to absorption spectra that are better modeled as sums of gaussians as well. The Stark spectrum is essentially a *difference* spectrum between the absorption with the field "off" and the absorption with the field "on". As described below, the resulting lineshape of the Stark spectrum will therefore resemble the zeroth, first, or second derivative of the absorption spectrum or some linear combination of all three, depending on the properties of the molecule.

If the field acts to change the transition moment (extinction coefficient) of the transition, the intensity of the absorption band will change in the field, giving rise to what is termed a zeroth-derivative contribution to the Stark spectrum. This may occur due to field-induced intensity borrowing or symmetry breaking causing a forbidden transition in the isolated molecule to acquire some "allowed" character. Rotation of the transition moment through orientation of the molecule in the applied field may also occur, generating a zeroth-derivative component to the Stark spectrum. This is also common in electrofluorescence measurements if the molecules can rotate prior to emitting.

A first-derivative lineshape will result from the change in electronic polarizability between the ground and excited states ( $\overline{\alpha}$ ). The absorption band will red shift if  $\overline{\alpha}$  is positive. While this is most common, examples of molecules with negative  $\overline{\alpha}$ 's are sometimes found and their Stark spectrum shows the expected blue shift.<sup>31,32</sup> The Stark spectrum will reveal the sign of the *average value* of  $\overline{\alpha}$ . In Liptay's formalism, the electronic  $\overline{\alpha}$  is but *one* of the effects that can cause the absorption band of a molecule to shift in the applied field. As will be described below, we have found

that, if the matrix containing the molecules is not fully rigid, field-induced orientation of the ground state dipoles can lead to a shift in the absorption spectrum as well. This shift may, in some cases, dominate that due to the electronic  $\overline{\alpha}$ . Because this effect causes the distribution of dipoles in the sample to become slightly anisotropic, it therefore also affects the measurement of  $|\underline{\mu}|$  as described below. As will be demonstrated later, one can normally minimize the contribution of this orientation effect by lowering the sample temperature or otherwise making the matrix highly rigid.

A second derivative lineshape arises through the interaction of the applied field with the permanent dipole moments of the ground and excited states. For a molecule with a non-zero  $|\underline{\mu}|$  on excitation, the field interacts with the dipole to stabilize the energies of the ground and excited states by an amount proportional to their respective dipole moments. If the dipoles are isotropically oriented, there will be an equal number of molecules that are stabilized versus those that are destabilized depending on the specific orientation of the ground-state dipole of each molecule relative to the direction of the field. The applied field will cause those molecules that are stabilized to have their absorption frequencies shifted to lower energies while those that are destabilized will absorb at a higher frequency. The net effect of the field on the absorption spectrum will be to broaden it. As a consequence, the *magnitude* ( $|\underline{\mu}|$ ) but not the *sign* of  $\Delta\underline{\mu}$  may be determined by Stark spectroscopy on an isotropic sample.

**Local Field Effects:** An important point to emphasize here is that, when an electric field is applied to a sample in the condensed phase, there is an enhancement of that field that is referred to as the cavity field effect. This effect is independent of the  $\Delta\underline{\mu}$  and the  $\overline{\alpha}$  of the molecule itself but rather depends only on the dielectric constant of the medium and the size of the cavity in which the molecule is considered to reside. If a simple approximation of a spherical cavity is used, the cavity field factor ( $f$ ) is given by the expression  $f = 3 / (\epsilon + 2)$  where  $\epsilon$  is the dielectric constant of the medium. The experimental  $|\underline{\mu}|$  should be divided by  $f$  and the experimental  $\overline{\alpha}$  by  $f^2$  in order to account for this enhancement of the applied field.

There are two important assumptions that one can make to compute the cavity field. The first is that the cavity shape is spherical. This can be improved by using published formulas<sup>28</sup> for ellipsoidal cavities that presumably model the true molecular shape more accurately. The use of these corrections is described in Ref. 31. However, these models require some estimate of the cavity size. Because the prescription for accurately determining the cavity size of a molecule in condensed phase is not universally agreed upon, this can introduce some error into the correction term as well. The second assumption is that the effective dielectric constant of the medium next to the molecule in the glassy matrix is that which would characterize the bulk. That issue is addressed again later in this paper. However, it is important to recognize that  $f$  varies only from  $\sim 1.2$  to  $\sim 1.46$  for  $\epsilon$  ranging from 2 to 20. This demonstrates that the measured  $|\underline{\mu}|$ 's and  $\overline{\alpha}$ 's should not be strongly sensitive to the magnitude of the local field.

As noted earlier, the experimental values of  $|\underline{\mu}|$  and  $\overline{\underline{\alpha}}$  are also enhanced relative to the corresponding values for the isolated molecule by the reaction-field effect. This reflects the response of the dielectric environment to the charge distribution of the probe molecule. It therefore depends on the ground and excited state dipole moments, polarizabilities, *and* the molecular size and shape.

Because of the numerous approximations involved in both the cavity field and reaction field corrections, we have chosen to report the experimental  $|\underline{\mu}|$ 's and  $\overline{\underline{\alpha}}$ 's *without* including any corrections. We apply the corrections to the calculated values to facilitate comparison to experiment.

**Measurements of Polarizabilities:** In this section, we will describe some of our group's work on the measurement of  $\overline{\underline{\alpha}}$ 's for molecules in polymer films and in glasses. For these measurements, we used two classes of molecules: the solvatochromic probe coumarin 153 and the biological conjugated chromophore all-*trans* retinal.<sup>33</sup> The results for coumarin 153 will be discussed in detail here. A full account of this work will appear in Journal of Physical Chemistry A.<sup>34</sup>

Coumarin 153 (Fig. 3) is a frequently used fluorescent probe for the static and dynamic aspects of solvation. It is a polar molecule with a large ground state dipole moment and a substantial increase in dipole moment on excitation. Interest in accurate measurements and calculations of the change in dipole moment and in polarizability on excitation of coumarin 153 and other coumarins stems from the importance of this quantity to modeling the solvation dynamics of these molecules and to predicting their values of  $\beta$ . The extent to which the polarity of the environment can be used to tune the value of  $\beta$  depends on the magnitude of  $\overline{\underline{\alpha}}$  for the molecule.

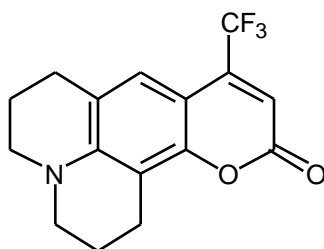


**Figure 3:** Coumarin 153

There are a number of simplifications afforded by the choice of coumarin 153 as a probe of how matrix polarity affects the values of  $|\underline{\mu}|$ ,  $\overline{\underline{\alpha}}$ , and consequently the value of  $\beta$  for a molecule. The first is that coumarin 153 is structurally rigid, minimizing the possibility of polarity-induced changes in conformation. The second is that no significant changes in ground state electronic structure, bond lengths, or conjugation with solvent polarity are expected for coumarin 153. For these reasons, coumarin 153 is thought to behave as a simple dipole and is therefore a good probe of the properties of its environment.

**Matrix Properties:** We have performed a series of measurements on coumarin 153 in number of organic glasses and polymers (Table 1). The polarity of the matrices was varied over a fairly wide

range (Table 1) in order to explore the effect of this parameter on the measured dipolar properties of this molecule. The phase of the matrix also proved to be an important parameter. Among the polymer films, we examined one, polyethylene (PE) that is above its glass-transition temperature ( $T_g$ ) at room temperature and two others, polymethyl methacrylate (PMMA) and polyvinyl chloride (PVC) that are below their respective  $T_g$ 's at 298 K. Molecules doped into PE are believed to reside in the amorphous phase of the polymer or at the interface between the amorphous and crystalline phases.<sup>35</sup> The polymers were examined both at 298 K and at 77 K, the latter temperature being below the  $T_g$  of PE.

As matrix characteristics and sample preparation techniques proved to be critical factors in the results obtained, our methods are detailed here. To prepare the organic glasses, the solvents (2-methyl THF (Me-THF), methylcyclohexane (MCH), and toluene) were dried by refluxing under an Argon atmosphere over  $CaH_2$  in order to remove water. Otherwise, at least in Pittsburgh, these solvents may contain enough water to interfere with the formation of good glasses. The PE films were prepared by soaking commercially available films (~ 50 micron thick) in solutions that are  $\sim 1 \times 10^{-3}$  M in the molecule of interest, washing the films with methanol, and allowing them to air dry. The PMMA and PVC films were made by casting from a solution of the polymer and the molecule of interest in dichloroethane and allowing the solvent to evaporate. Aggregation of the coumarin 153 molecules in the polymer films and organic glasses was apparently minimal judging from a comparison of the absorption and emission spectra of the molecules in the matrices with the corresponding spectra in the solution phase.

In order to adhere the PMMA films to the electrodes, which are a metal coated quartz substrate, two methods were employed. The first was to "glue" the film to the electrodes using a viscous solution of PMMA and dichloroethane, and allow the sample to dry for about a week. This produced what we called "glued PMMA samples" which are likely to contain residual dichloroethane. The second method is to heat the film between the two electrodes in a drying oven at  $\sim 150^\circ$  C for  $\sim 5$  minutes. This produces what we refer to as "heated PMMA" samples that we expect to contain much less residual dichloroethane. This heating process did not appear to harm even fairly thermally labile compounds such as retinal polyenes. The heating method exclusively was used to prepare the PE and PVC samples.

### **Results and Summary of Data**

Figures 4 and 5 contain some representative electroabsorption data for coumarin 153. Figure 4 shows coumarin 153 in PE at 298 K (a-c) and 77 K (d-f). Figure 5 shows coumarin 153 in the solvent glasses toluene (a-c) and MeTHF, both at 77 K.

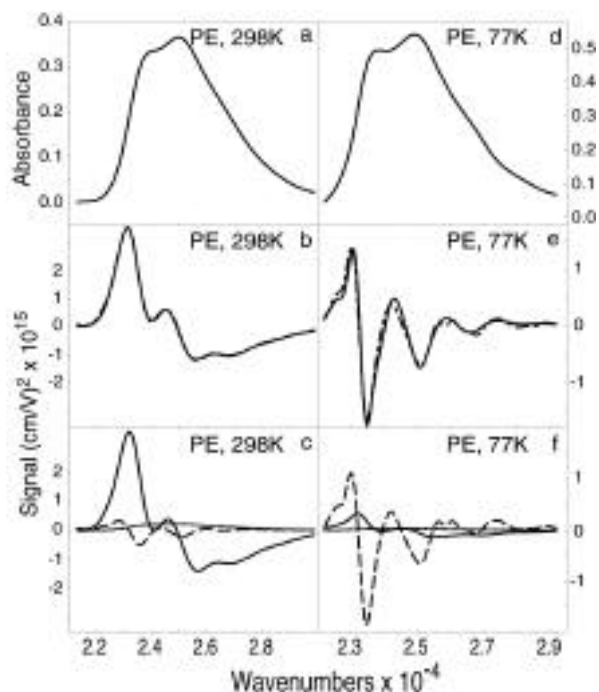


**Figure 4:** C153 in PE matrix at 298K (a-c) and 77K (d-f). The top panels show the absorption spectrum. The middle panels show the electroabsorption (solid) and fit (dashed-dot). The bottom panels show the individual components of the fit to the electroabsorption signal. The zeroth derivative (dotted), first derivative (solid) and the second derivative (dashed) of the absorption spectrum, all normalized to the applied field, are shown.

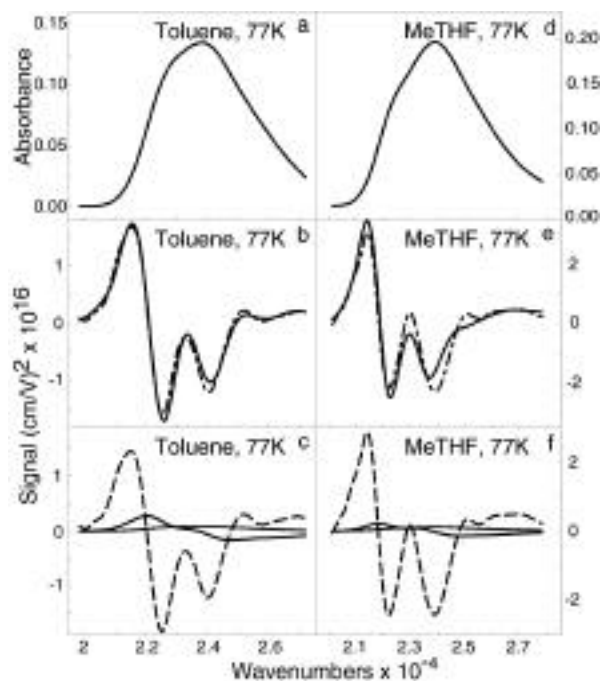


**Figure 5:** C153 at 77K in toluene (a-c) and MeTHF (d-f) organic glasses. The top panels show the absorption spectrum. The middle panels show the electroabsorption (solid) and fit (dashed-dot). The bottom panels show the individual components of the fit to the electroabsorption signal. The zeroth

derivative (dotted), first derivative (solid) and the second derivative (dashed) of the absorption spectrum, all normalized to the applied field, are shown.

Note that the second derivative component (related to  $\overline{\underline{\alpha}}$ ) contributes most strongly to the PE electroabsorption spectrum at 298 K and much less so to the electroabsorption spectra in all of the other environments. The molecular parameters derived for coumarin 153 in all of the matrices used is summarized in Table 1 below.

**Table 1. Electroabsorption results for C153 in various matrices and different temperatures<sup>a</sup>**

Matrix	T <sub>g</sub> <sup>b</sup>	ε	n <sub>2</sub>	max <sup>c</sup>	$\overline{\underline{\alpha}}$	$f^2 \cdot \overline{\underline{\alpha}}_{\text{calc}}^{\#\#}$		$\underline{\mu}$	$f \cdot \Delta \underline{\mu}_{\text{calc}}^{\#\#}$	
						3-21G	6-21G*		3-21G	6-21G*
PE(298K)	148	2.3	1.51	396	374 (3)	6.62	6.87	4.4 (0.3)	6.23	5.01
PE(77K)	148	2.3	1.58	397	26 (7)	6.62	6.87	5.3 (0.2)	6.23	5.01
PMMA <sup>d</sup>	---	10.7	1.44	418	564 (80)	----	----	5.7 (0.6)	---	---
PMMA <sup>e</sup>	378	3.6	1.49	418	60 (3)	7.54	7.88	5.6 (0.1)	6.70	5.42
PVC <sup>f</sup>	354	3.5	1.55	426	46 (3)	7.50	7.83	5.3 (0.1)	6.68	5.40
Toluene <sup>g</sup>	119	2.6 <sup>†</sup>	1.5 <sup>†</sup>	418	6 (1)	6.89	7.70	5.8 (0.4)	6.37	5.13
MeTHF <sup>g</sup>	91	5.4 <sup>†</sup>	1.41 <sup>†</sup>	418	4 (2)	8.15	8.57	7.0 (0.4)	7.00	5.68
		19 <sup>‡</sup>	1.73 <sup>‡</sup>			9.27	9.82		7.56	6.16

<sup>a</sup>Polarizabilities in Å<sup>3</sup> and dipole moments in Debye. <sup>b</sup>In Kelvin. <sup>c</sup>In nanometers. <sup>#</sup>Calculated values have been scaled by both cavity and reaction fields for an oblate spheroid.

**\*The first column shows results of 3-21G calculations on a 6-31G optimized structure. The second column shows results of 6-21G\* calculations.**

<sup>d</sup>Glued PMMA. <sup>e</sup>Heated PMMA. <sup>f</sup>Measurements at 298 K. <sup>g</sup>Measurements at 77 K. <sup>†</sup>298K parameters. <sup>‡</sup>94 K parameters.

The important results from Stark spectroscopy on coumarin 153, as shown in Table 1 and the figures, can be summarized as follows: (1) The measured values of | $\underline{\mu}$ | and  $\overline{\underline{\alpha}}$  do *not* vary substantially with polarity (as measured by dielectric constant). This is consistent with the trend observed in the calculated values which are solvent corrected. (2) The measured  $\overline{\underline{\alpha}}$ 's agree with the calculated values (both being ~10 Å<sup>3</sup> or less) only at low temperatures while a number of the measured values are an order of magnitude or more larger than calculation. The variation of the calculated values with polarity is due to the effect of increasing ε<sub>0</sub> on the magnitudes of the cavity and applied fields.

In order to rationalize the trends we observe, we note that the largest  $\overline{\underline{\alpha}}$ 's were measured in matrices that we have reason to believe are also the least *rigid*. This is most obviously the case for coumarin 153 in room temperature PE, for which the largest values of  $\overline{\underline{\alpha}}$  are seen. At 298 K, PE is in the amorphous phase in which considerable motion of the polymer chains, and presumably the embedded chromophore, is possible. When the sample temperature is lowered to below the T<sub>g</sub> of the

matrix, such motion is effectively diminished. The comparison between heated and glued PMMA is less obvious. Presumably trapped solvent molecules can plasticize the matrix, particularly in the region surrounding the polar coumarin 153 molecules, leading to a less rigid environment. In addition, heating glassy polymers above their  $T_g$  and then cooling them is known to cause annealing. This could minimize the size of the voids containing the coumarin 153 dopants. In all cases, lowering the temperature of the matrix lowers the value of  $\overline{\alpha}$  obtained. Particularly in the case of PE, the effect is quite dramatic owing to the change in the phase of the polymer that is produced on cooling. Note that there is an increase of  $\sim 20$  percent in the value of  $|\underline{\mu}|$  for coumarin 153 in PE as the matrix is cooled. As described below, this effect can also arise due to increasing the matrix rigidity.

In contrast, we note that the polarities of the polymer matrices are *not* significantly altered by cooling or by the presence of residual chlorinated solvents. This can be seen by comparison of the absorption maximum of coumarin 153 in each environment. However, as described above, both cooling of the matrix and removal of residual solvent appears to alter the rigidity of the matrix to a measurable extent. *To summarize, we believe that rigidity rather than polarity of the matrix is the dominant parameter determining the value of the  $\overline{\alpha}$  measured in these systems.*

In order to understand the role that matrix rigidity would play in the measurement of  $\overline{\alpha}$  by Stark spectroscopy, we postulate that, in a non-rigid environment, the applied field can act to partially align the dipoles of the coumarin 153 molecule and/or the dipoles of the surrounding matrix. As a result, there would be a non-isotropic distribution of molecules and environments, with more of the ground state dipoles aligned with the field than against it. In a very simple picture, if  $\underline{\mu}$  is positive, this would cause the absorption band to shift to lower energy. Such a shift would be interpreted as a positive  $\overline{\alpha}$  in the analysis of the Stark spectrum. We can estimate that a value for  $\overline{\alpha}$  of a few hundred of  $\text{\AA}^3$  can result from aligning coumarin 153 by  $\sim 20$  degrees at the field strengths used in this experiment. In reality, there is likely to be a distribution of mobilities within a given sample. It is interesting to note that Liptay partially accounted for this effect by including a term proportional to the ground-state dipole moment of the molecule in his expression for  $\overline{\alpha}$ .<sup>1</sup>

We expect that an anisotropic distribution of ground-state dipoles that may be present in the non-rigid matrices would also affect the measured value of  $|\underline{\mu}|$ . This is indeed found to be the case, as can be seen by comparing the value of  $|\underline{\mu}|$  for coumarin 153 in room-temperature PE versus low-temperature PE (Table 1). However, we find that the increase in  $|\underline{\mu}|$  observed in the more rigid matrix is only  $\sim 20$  percent, while the decrease in  $\overline{\alpha}$  is nearly two orders of magnitude. Interestingly, a comparison of the electro-optical properties of a dye doped in a polymer film above and below the  $T_g$  of the polymer also reveals a dramatic change in the magnitude of the *zeroth* derivative component.<sup>36</sup> This component also contains terms that depend on molecular alignment in the field.<sup>29</sup>

In summary, we believe that the  $\overline{\alpha}$  obtained in a non-rigid matrix represents an *orientational* polarizability that is over and above the intrinsic *electronic* polarizability of the molecule. As the temperature is lowered and the matrix is made more rigid, the polarizability measured by Stark spectroscopy approaches the electronic  $\overline{\alpha}$  of the molecule. Because the electronic polarizability is

the quantity that is calculated by the electronic structure methods we have used, the agreement between experiment and calculation improves as the temperature of the matrix is lowered.

**Matrix Polarity:** An issue that often arises in studies of glassy or solid matrices is whether the polarity of the environment local to the dopant molecule is well described by the bulk dielectric constant of the matrix. This issue is of critical importance in interpreting the results from solvatochromic measurements and from Stark spectroscopy as well as for attaining good agreement between these results and calculation. For example, it has been demonstrated that the local polarity of the glass of a dissolved chromophore is higher than that of the bulk glass and that it depends on the ground state dipole moment of the chromophore itself.<sup>37</sup> A useful feature of coumarin 153 is that the wavelength of its absorption maximum provides a measure of the local polarity of its environment. Here, we find evidence of a similar polarity enhancement, this time for coumarin 153 in polymers that form glasses at room temperature. This may be seen by comparing absorption maxima of coumarin in PMMA and PVC (Table 1) with those in solutions of comparable dielectric constants.<sup>38</sup> In both cases, the polymer absorption maxima are shifted to lower energies, indicating a more polar local environment.

The important consequences of this internal field enhancement for measurements of molecular hyperpolarizabilities, at least for molecules in organic solvents and their glasses, has been previously demonstrated.<sup>37</sup> As PMMA is frequently used for fabricating non-linear optical devices, the observation that the local polarity of the environment of dopant molecules is *also* enhanced in some polymeric media is of significance from the standpoint of applications.

In order to estimate the predicted effect of an increase in local polarity on  $|\underline{\mu}|$  and  $\overline{\underline{\alpha}}$ , we can compare the calculated values ( $\overline{\underline{\alpha}}_{\text{calc}}$  and  $\underline{\mu}_{\text{calc}}$ ) which have been corrected for both cavity and reaction field effects using dielectric constants of between 2 and 20 (Table 1). The value of 20 for the  $\epsilon_0$  of MeTHF at 77K was chosen based on a published low-temperature determination.<sup>39</sup> One can see, once again that the predicted variation in  $|\underline{\mu}|$  and  $\overline{\underline{\alpha}}$  is fairly small over this fairly substantial polarity range. Therefore, we conclude that an increase in local polarity *alone* does *not* explain the trends in  $\overline{\underline{\alpha}}$  that we observe. This again supports our proposal that matrix rigidity makes the most substantial contribution to the size of the measured  $\overline{\underline{\alpha}}$  in the systems studied here.

## **Conclusions and Future Directions**

The calculated values of  $\overline{\underline{\alpha}}$  for C153 and the measured values  $\overline{\underline{\alpha}}$  agree, both being less than  $10 \text{ \AA}^3$ , when the matrix containing the probe molecule is rigid. In non-rigid matrices, the orientational contribution to  $\overline{\underline{\alpha}}$  can be several hundreds of  $\text{\AA}^3$ . Therefore, Stark spectroscopy is a sensitive probe of molecular motion, even in polymers that are below their glass-transition temperatures. We have also performed experiments of the type described here on polar conjugated systems (retinals) for which similar trends were observed.<sup>33</sup> Studies are currently under way in which we are examining the effects of varying the frequency of the applied field, the temperature of the matrix, and the polarity of the solvent used to cast the films. These should enable us to make a more

systematic study of the correlation between the properties of the matrix used and both  $\overline{\alpha}$  and other parameters obtained from the Stark spectrum.

### **Acknowledgments**

We would like to thank Dr. David Yaron and Dr. Hyung Kim for useful discussions, Dr. Zhigang Shuai for INDO/SCI/SOS calculations on C153, and Dr. Marshall Newton for *ab initio* (6-21G\*) results on C153. We acknowledge our sources of funding. The NSF-CAREER and POWRE programs, and the Center for Molecular Analysis at Carnegie Mellon University for the use of the absorption spectrometer.

### **References Cited**

- (1) Liptay, W. In *Excited States*; E. C. Lim, Ed.; Academic Press: New York, 1974; Vol. 1; pp 128.
- (2) Baumann, W.; Bischof, H. *Journal of Molecular Structure* **1982**, *84*, 181.
- (3) Ponder, M. C. Ph.D. Thesis, Univ. of California, Berkeley, 1983.
- (4) Mathies, R.; Stryer, L. *Proceedings of the National Academy of Sciences USA* **1976**, *73*, 2169-2173.
- (5) Lockhart, D. J.; Boxer, S. G. *Biochemistry* **1987**, *26*, 664-668.
- (6) Vance, F. W.; Karki, L.; Reigle, J. K.; Hupp, J. T.; Ratner, M. *Journal of Physical Chemistry A* **1998**, *102*, 8320-8324.
- (7) Oh, D. H.; Sano, M.; Boxer, S. G. *Journal of American Chemical Society* **1991**, *113*, 6880-6890.
- (8) Shin, Y.-G.; Brunschwig, B. C.; Creutz, C.; Sutin, N. *Journal of Physical Chemistry* **1996**, *100*, 8157.
- (9) Phillips, S. D.; Worland, R.; Yu, G.; Hagler, T.; Freedman, R.; Cao, Y.; Yoon, V.; Chiang, J.; Walker, W. C.; Heeger, A. J. *Physical Review B* **1989**, *40*.
- (10) Hovarth, A.; Bassler, H.; Weiser, G. *Physics Status Solidi* **1992**, *173 B*, 755.
- (11) Hagler, T. W.; Pakbaz, K.; Heeger, A. J. *Physical Review B* **1994**, *49*, 10968.
- (12) Hochstrasser, R. M. *Accounts of Chemical Research* **1973**, *6*, 263.
- (13) Sebastian, L.; Weiser, G.; Bassler, H. *Chemical Physics* **1981**, *61*, 125.
- (14) (a) Somsen, O. J. G.; Chernyak, V.; Frese, R. N.; von Grondelle, R.; Mukamel, S. *Journal of Physical Chemistry, B* **1998**, *102*, 8893. (b) Popovic, Z. D.; Khan, M. I.; Atherton, S. J.; Hor, A.-M.; Goodman, J. L. *Journal of Physical Chemistry B* **1998**, *102*, 657.
- (15) Bublitz, G. U.; Ortiz, R.; Runser, C.; Fort, A.; Barzoukas, M.; Marder, S. R.; Boxer, S. G. *Journal of the American Chemical Society* **1997**, *119*, 2311.
- (16) Rohlfing, F.; Bradley, D. D. C. *Chemical Physics Letters* **1997**, *277*, 406.
- (17) Blanchard-Desce, M.; Wortmann, R.; Lebus, S.; Lehn, J.-M.; Kramer, P. *Chemical Physics Letters* **1995**, *243*, 526.
- (18) Ohta, N.; Koizumi, M.; Umeuchi, S.; Nishimura, Y.; Yamazaki, I. *Journal of Physical Chemistry* **1996**, *100*, 16466.
- (19) Orrit, M.; Bernard, J.; Zumbusch, A. *Chemical Physics Letters* **1992**, *196*, 595.
- (20) Gradl, G.; Kohler, B. E.; Westerfield, C. *Journal of Chemical Physics* **1992**, *97*, 6064.
- (21) Cavus, A.; Lombardi, J. R. *Journal of Physical Chemistry* **1993**, *97*, 9977.
- (22) Locknar, S. A.; Peteanu, L. A. *Journal of Physical Chemistry B* **1997**, *102*, 4240.
- (23) Frisch, M. J.; Head-Gordon, M.; Trucks, G. W.; Gill, P. M.; Wong, M. W.; Foresman, J. B.; Johnson, B. F.; Schlegel, H. B.; Robles, J. E.; Cinkovský, R.; Anderson, J. L.; Replogle, J. S.; Pople, J. A.

- Robb, M. A.; Binkley, J. S.; Gonzales, C.; Defrees, D. J.; Fox, D. J.; Baker, J.; Martin, R. L.; Pople, J. A., Gaussian 94, Revision E.2, Gaussian, Inc., Pittsburgh PA 1995
- (24) (a) Dewar, M. J. S.; Zoebisch, E. G.; Healy, E. F.; Stewart, J. P. P.; *Journal of the American Chemical Society* **1985**, *107*, 3902. (b) Coolidge, M. B.; Stewart, J. P. P.; Technical Report, Seiler Research Laboratory, United States Air Force Academy, Colorado Springs, CO, 1990.
- (25) Thompson, M. A., Argus<sup>TM</sup> v. 1.2
- (26) Locknar, S. A.; Peteanu, L. A.; Shuai, Z. *The Journal of Physical Chemistry A* **1999**, *103*, 2197.
- (27) Shuai, Z.; Beljonne, D.; Bredas, J.-L. *Journal of Chemical Physics* **1992**, *97*, 1132.
- (28) Bottcher, C. J. F. *Theory of Electric Polarisation*; Elsevier Publishing Co.: Amsterdam, **1952**, p. 492.
- (29) Liptay, W. In *Modern Quantum Chemistry Part III: Action of Light and Organic Crystals*; O. Sinanoglu, Ed.; Academic Press: **1965**; p. 45.
- (30) Labhart, H. In *Advances in Chemical Physics* **1967**; Vol. 13; p. 179.
- (31) Premvardhan, L.; Peteanu, L. *Chemical Physics Letters* **1998**, *296*, 521.
- (32) Mathies, R.; Albrecht, A. C. *The Journal of Chemical Physics* **1974**, *60*, 1420 .
- (33) Locknar, S. A.; Chowdhury, A.; Peteanu, L. A. *Journal of Physical Chemistry* (*submitted*)
- (34) Chowdhury, A.; Locknar, S. A.; Premvardhan, L. L.; Peteanu, L. A. *Journal of Physical Chemistry A* (*in press*).
- (35) Zimmerman, O. E.; Weiss, R. G. *Journal of Physical Chemistry A* **1998**, *102*, 5364.
- (36) Saal, S.; Haase, W. *Chemical Physics Letters* **1997**, *278*, 127.
- (37) Bublitz, G. U.; Boxer, S. G. *Journal of American Chemical Society* **1998**, *120*, 3988.
- (38) Maroncelli, M.; Fleming, G. *Journal of Chemical Physics* **1987**, *86*, 6221.
- (39) Richert, R. *Chemical Physics Letters* **1993**, *216*, 223.

## Recent Noteworthy Articles in the Area of Photochemistry and Photophysics

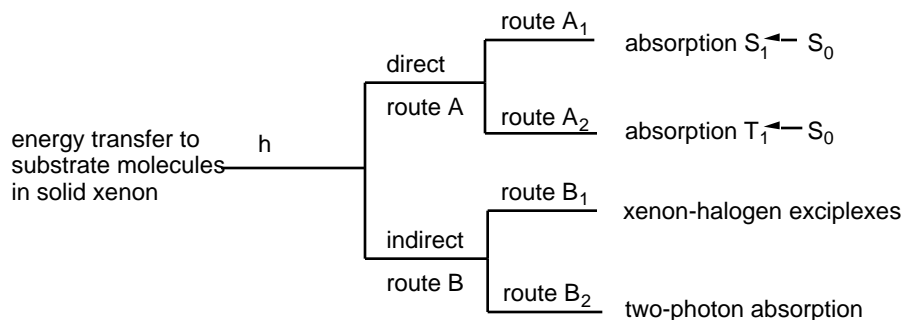
**Editor's note: We are always looking for people to abstract recent exciting articles in photochemistry for the newsletter. Categories include, but are in no way limited to biochemical, organic, inorganic, and physical photochemistry. Please drop a note to William Jenks if you would like to participate.**

### Organic Photochemistry

Selected and abstracted by John Toscano, Department of Chemistry, 3400 North Charles Street, Johns Hopkins University, Baltimore, Maryland 21218

1. "Solid Xenon: A Medium for Unusual Photoreactions" Maier, G.; Lautz, C. *Angew. Chem. Int. Ed.* **1999**, 38, 2038-2041.

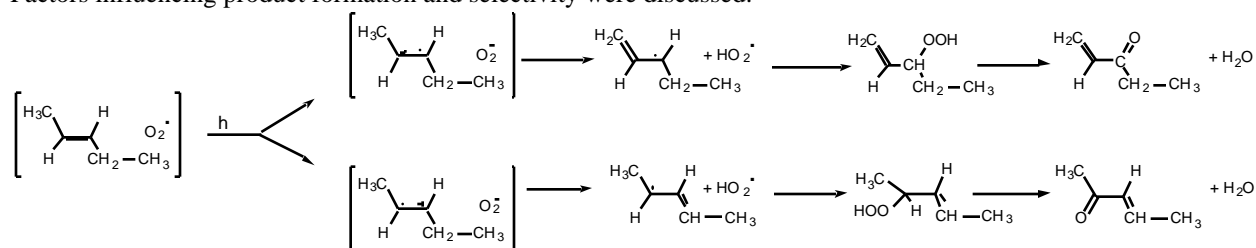
This communication describes photochemical reactions that take place in xenon matrices at 10 K by the four different mechanisms shown below. Even for strain-free open chain hydrocarbons, experiments show that bond cleavage takes place when irradiations are carried out in a halogen-doped xenon matrix. Propane, which is photostable in doped argon, undergoes reaction in bromine atom-doped xenon when irradiated at 254 nm. The products from irradiation were identified as propene, allyl radical, propyne, allene, ethene, methane, and acetylene.



Surprisingly, propane fragmentation was observed following 185 nm photolysis in an *undoped* xenon matrix, although propane is photostable in an argon matrix under the same conditions. A two-photon process was ruled out and the results were interpreted in terms of the heavy-atom effect of xenon that

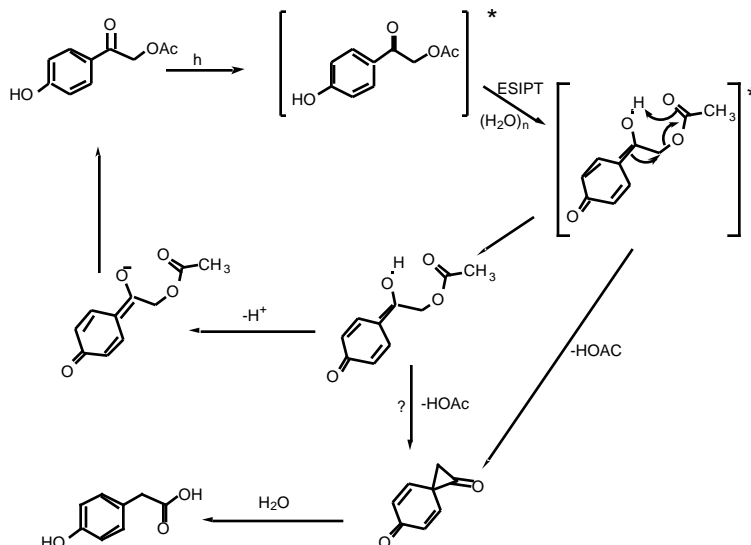
2. "Photooxidation of 1-Alkenes in Zeolites: A Study of the Factors that Influence Product Selectivity and Formation" Xiang, Y.; Larsen, S. C.; Grassian, V. H. *J. Am. Chem. Soc.* **1999**, *121*, 5063-5072.

Factors that influence product formation and selectivity in the room temperature photooxidation of 1-alkenes with broadband visible light in zeolites was investigated. In the zeolites BaX and BaY, aldehydes and ketones, as well as thermal ring opening products of epoxides, were detected. Aldehydes and ketones were proposed to be formed via a mechanism involving hydroperoxide intermediates. These intermediates also reacted with the alkenes to form alcohols and epoxides. Additionally, secondary photooxidation involving intermediate dioxetanes was suggested to take place. When the irradiations were carried out with shorter wavelengths and at higher temperature, an increase in the yields of aldehydes and ketones was observed. In cation exchanged BaZSM-5 and BaBeta zeolites, the alkenes polymerized and then underwent oxidation to yield oxygenated polymers. Factors influencing product formation and selectivity were discussed.



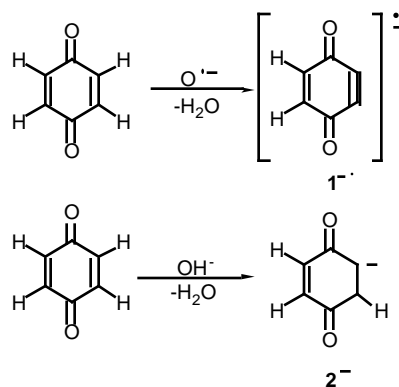
3. "Mechanism of Photosolvolytic Rearrangement of *p*-Hydroxyphenacyl Esters: Evidence for Excited-State Intramolecular Proton Transfer as the Primary Photochemical Step" Zhang, K.; Corrie, J. E. T.; Munasinghe, V. R. N.; Wan, P. *J. Am. Chem. Soc.* **1999**, *121*, 5625-5632.

The mechanism of photosolvolytic rearrangement of various *p*-hydroxyphenacyl esters, potentially useful photoprotecting groups, was the subject of this study. A novel mechanism was suggested from photolysis studies involving product analyses, triplet quenchers, and nanosecond laser flash photolysis. Photolyses were done in solutions with up to 50% aqueous content. An intramolecular proton transfer of the phenolic proton to the carbonyl oxygen was proposed as the primary step. This transfer takes place on the singlet excited surface at a rate  $> 10^8 \text{ s}^{-1}$  and is mediated by solvent water generating the corresponding *p*-quinone methide phototautomer. The removal of a carboxylic acid in a concerted step results in the formation of a spiroketone intermediate. The proposed involvement of an excited-state intramolecular proton transfer (ESIPT) was supported by the observation of a change in the absorption intensity of the phenacyl ester excited singlet state at 330 nm as a function of pH. An alternative mechanism suggested is deprotonation of the phenolic proton, loss of the acetate, and rearrangement to a spiroketone intermediate all in one concerted primary photochemical step from  $S_1$ .



4. "Photoelectron Spectroscopy of Benzoquinonide and Dehydrobenzoquinone Anions" Davico, G. E.; Schwartz, R. L.; Ramond, T. M.; Lineberger, W. C. *J. Am. Chem. Soc.* **1999**, *121*, 6047-6054.

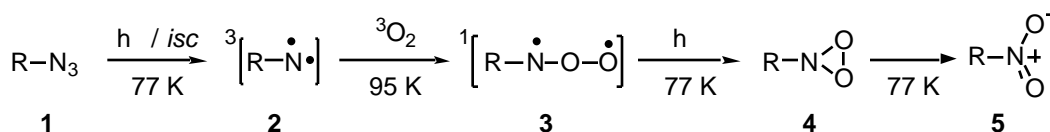
The photoelectron spectrum of the dehydrobenzoquinone radical anion (**1**<sup>•-</sup>) and the benzoquinonide anion (**2**<sup>-</sup>) were reported. The electron affinity for **1** was determined to be 1.859 ± 0.005 eV. From the very rich vibrational structure observed in the spectrum of **1**<sup>•-</sup>, several fundamental frequencies were identified. This study represents the first experimental report on the structure of dehydrobenzoquinone, the benzyne analogue of *p*-benzoquinone. The photoelectron spectrum of **2**<sup>-</sup> showed numerous vibrational bands attributed to the low molecular symmetry of the species. An upper value of 2.18 eV is estimated for the electron affinity of **2** although it was not possible to resolve its origin peak.



5. "Photochemical Reactions of Nitroso Oxides at Low Temperature: The First Experimental Evidence of Dioxaziridines" Harder, T.; Wessing, P.; Bendig, J.; Stosser, R. *J. Am. Chem.* **1999**, *121*, 6580-6588.

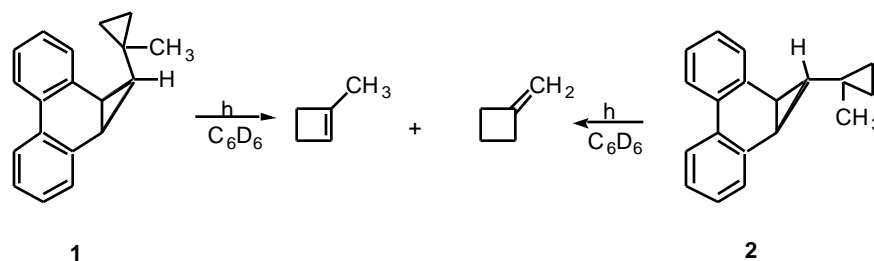
The thermal reaction of triplet nitrenes (**2**) with triplet oxygen at 95 K in 2-methyltetrahydrofuran is reported to produce nitroso oxides (**3**) in quantitative yields. These oxides are

reported to be thermally stable at temperatures below 100 K. Photolysis of the nitroso oxides at 77 K using strong intensity light resulted in the formation of intermediates which, based on spectroscopic, kinetic, and chemical arguments, are postulated to be the highly reactive dioxaziridines (**4**). At 77 K, these intermediates underwent thermal ring opening to form the corresponding nitro compounds (**5**). The rate of the ring opening reaction of the dioxaziridines (**4** → **5**),  $k = 0.0030 \pm 0.0005 \text{ s}^{-1}$  at 77 K, was found to be insensitive to substitution effects. The transients were characterized by stationary UV/vis and/or ESR spectroscopy. *Ab initio* calculations suggest that dioxaziridines are experimentally observable species because they are separated from **5** by a symmetry-forbidden energy barrier.



6. "Experimental and Theoretical Investigations of Ring-Expansion in 1-Methylcyclopropylcarbene" Thamattoor, D. M.; Snoonian, J. R.; Sulzbach, H. M.; Hadad, C. M. *J. Org. Chem.* **1999**, *64*, 5886-5895.

1-Methylcyclopropylcarbene, generated by the photolysis of two isomeric phenanthrene derivatives **1** and **2**, is reported to undergo ring-expansion readily to give 1-methylcyclobutene. No evidence was found that indicated intramolecular carbon-hydrogen insertions. Trapping studies with tetramethylethylene and independent synthesis of the cyclopropanated product confirmed the formation of the expected cyclopropane adduct. The lifetime of 1-methylcyclopropylcarbene in 1,1,2-trichlorotrifluoroethane was determined to be 12 ns. Computational studies showed that the barrier to ring-expansion is significantly smaller in 1-methylcyclopropylcarbene than in cyclopropylcarbene. Suggestion is made that the origin of the increased rate of ring-expansion is due to stabilization of the positive charge at the tertiary carbon that is attached to the migrating carbon center.



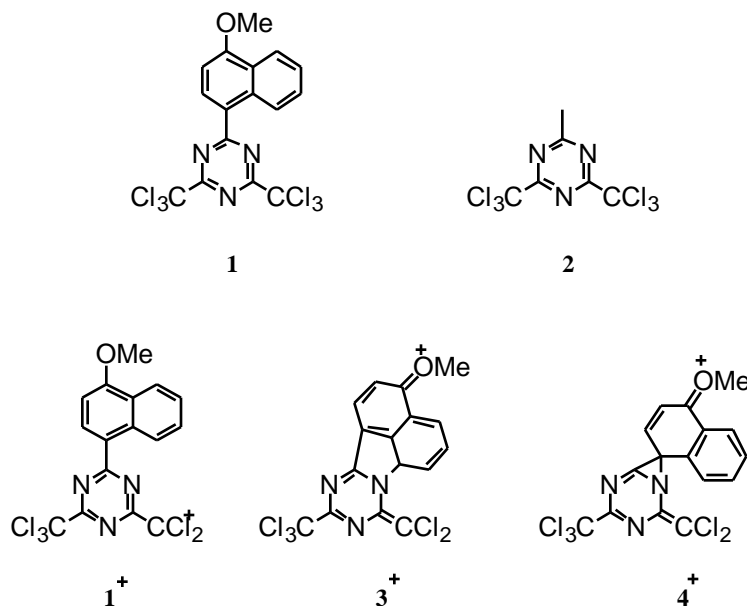
**Selected and abstracted by Jerry Cubbage, Woojae Lee, and Brian Vos, Department of Chemistry, Iowa State University**

1. "Mechanism of Photosolvolytic Rearrangement of *p*-Hydroxyphenacyl Esters: Evidence for Excited-State Intramolecular Proton Transfer as the Primary Photochemical Step" Zhang, K.; Corrie, J. E. T.; Munasinghe, V. R. N.; Wan, P. *J. Am. Chem. Soc.* **1999**, *121*, 5625-5632.

In recent years, homolytic and heterolytic cleavage of the C-OCOR bond have been proposed to explain the mechanism for photorelease of *p*-hydroxyphenacyl moiety, which is a photoprotecting



In this paper, the photochemistry and the photophysics of the compound **1** have been investigated by laser flash photolysis, emission spectroscopy and evaluation of acid generation. No fluorescence at room temperature was shown but both fluorescence and phosphorescence were obtained at 77 K. Strong absorption at 377 nm, which was very different from both methoxynaphthalene (MN) and bis(trichloromethyl)-1,3,5-triazine (TT) moieties, indicated an intramolecular charge transfer from the electron rich MN to the good electron acceptor (TT). This was supported by the fact that laser photolysis of equimolar mixture of 1-methoxynaphthalene and **2** in acetonitrile gave 1-methoxynaphthalene radical cation whereas without **2** only the triplet state transient of 1-methoxynaphthalene was obtained. Laser flash photolysis in acetonitrile strongly supports  $1^+$  formation by heterolysis of C-Cl bond because the transient of the generated radical cation of **1** by photosensitized electron transfer was different from that of  $1^+$ . The possible  $1^+$  structures were suggested ( $1^+$ ,  $3^+$ ,  $4^+$ ). Triplet sensitizers enhance the quantum yield of heterolytic cleavage by at least one order of magnitude. Acid generation occurs via addition of  $1^+$  to a nucleophile with an acidic hydrogen and followed by release of proton. In nonpolar solvent, only homolysis of C-Cl bond was observed. Unlike the ionic pathway, the triplet sensitizer has little influence on the amount of photogenerated acid.



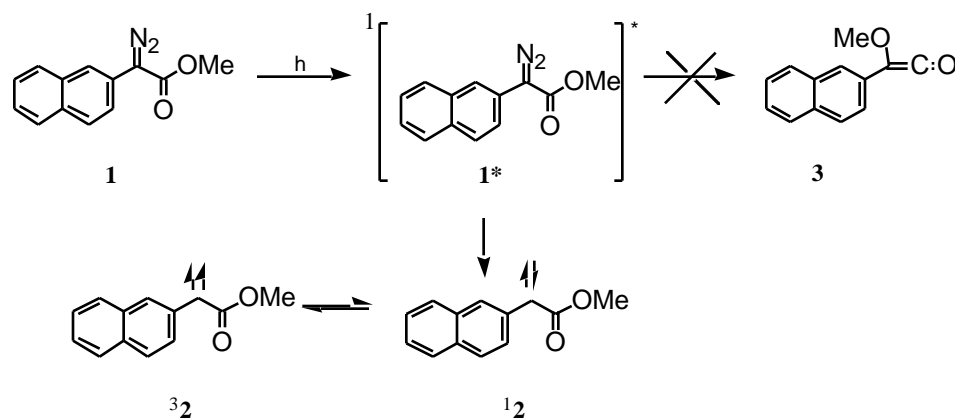
3. "Time-Resolved IR Studies of 2-Naphthyl(carbomethoxy)carbene: Reactivity and Direct Experimental Estimate of the Singlet/Triplet Energy Gap" Wang, Y.; Yuzawa, T.; Hamaguchi, H.; Toscano, J.P. *J. Am. Chem. Soc.* **1999**, *121*, 2875-2882.

Time-resolved IR (TRIR) was utilized to aid in clarification the role of the excited state diazo-precursor in the Wolff rearrangement. Methyl 2-diazo-(2-naphthyl) acetate (**1**) was selected to be investigated. Irradiation of **1** led to production of 2-naphthyl-(carbomethoxy)carbene (**2**) and **2** was found to produce the Wolff rearrangement product (ketene **3**). No evidence was found for  $1^*$  leading directly to the ketene without intervention of the carbene. The rate of decay of **2** equaled the rate of growth of **3**. This rate study proved that **3** arises from **2** and not from  $1^*$ . The high equilibrium concentration of **1** in its anti-conformation of the diazo and carbonyl groups, as determined from calculations<sup>1</sup>, was also used to rationalize this result. Detection of IR bands for both spin-equilibrated

states in **2** ( $^1\mathbf{2}$  and  $^3\mathbf{2}$ ) allowed experimental estimate for the singlet/triplet energy gap of **2**. The free energy difference was found to be  $0.2 \pm 0.1$  kcal/mol with  $^3\mathbf{2}$  being the ground-state carbene. This was the first identification of a singlet/triplet energy gap by TRIR in solution at ambient temperature. Two other papers accompanied this paper which utilized matrix-isolation<sup>1</sup> and laser flash photolysis<sup>2</sup> which provided Toscano and co-workers with valuable information on **1** and **2**. These papers are also must reads.

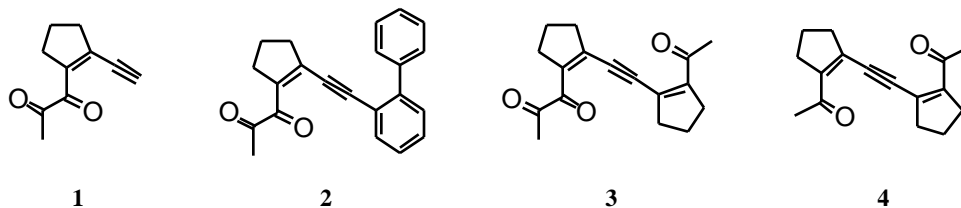
(1) Zhu, Z.; Bally, T.; Stracener, L.L.; McMahon, R.J. *J. Am. Chem. Soc.* **1999**, *121*, 2863-2874.

(2) Wang, J.-L.; Likhovtorik, I.; Platz, M.S. *J. Am. Chem. Soc.* **1999**, *121*, 2883-2890.

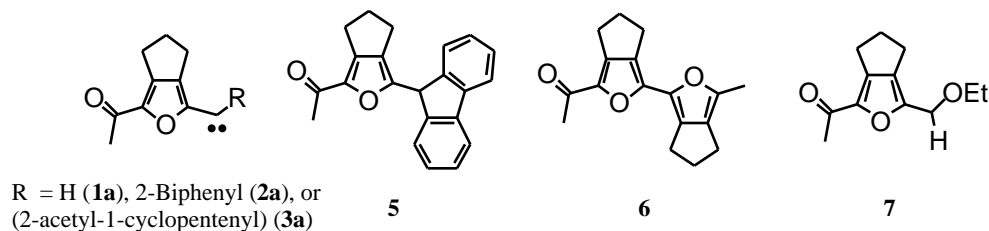


4. "Tandem Cyclization Involving Carbene as an Intermediate: Photochemical Reactions of Substituted 1,2-Diketones Conjugated with Ene-Yne" Nakatani, K.; Adachi, K.; Tanabe, K.; Saito, I. *J. Am. Chem. Soc.* **1999**, *121*, 8221-8228.

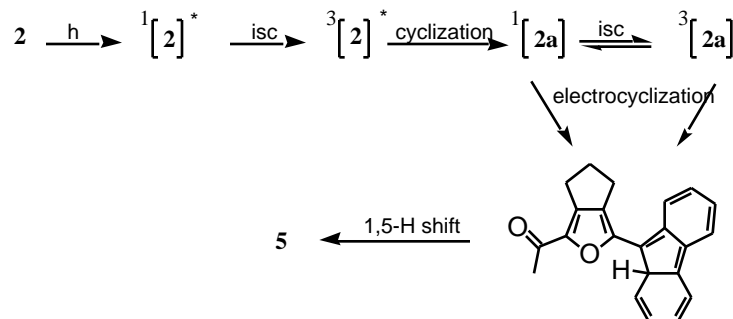
Tandem cyclizations with cations, anions, and radicals are well known. This paper described a novel photoinduced tandem cyclization of 1,2-diketones conjugated to ene-yne involving carbene intermediates. 1,2-Diketones **1**, **2**, **3**, and a reference ketone **4** were synthesized.



Compounds **1**, **2**, **3**, and **4** were irradiated at 365 nm and solvent effects were probed. It was found that **2** and **3** in aprotic solvent were found to cyclize to fluorenylfuran **5** and bifuran **6**, respectively. In aprotic solvent, **1** was discovered to be photostable because of no available carbene trap. However, in protic solvent, (2-furyl)carbene **1a** was trapped with solvent to give **7**. Photolysis of **2** in protic solvent led to trapping of (2-furyl)carbene **2a** whereas (2-furyl)carbene **3a** could not be trapped from irradiation of **3**. Irradiation of **4** produced no cyclized product and therefore it was deduced that the 1,2-diketone is a necessary feature for this carbene-producing cyclization. The proposed first step of the photoreaction produced a triplet biradical intermediate as concluded from triplet quenching experiments (scheme 1). The triplet biradical then cyclizes to the carbene, and the carbene (either  $^1\mathbf{2a}$  or  $^3\mathbf{2a}$ ) then undergoes electrocyclicization to produce **5** via 1,5-H shift. These results look promising for investigation of long-range carbene transfer through an extended ene-yne system that contains a carbene trap such as a biphenyl

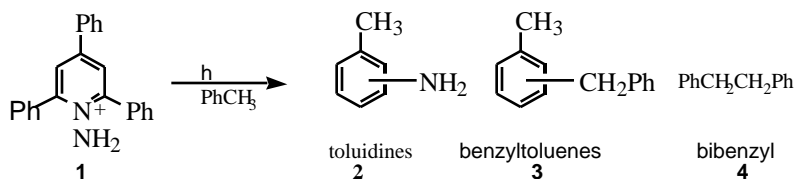


### Scheme 1



5. "On the Solution Chemistry of Parent Nitrenium Ion  $\text{NH}_2^+$ : The Role of the Singlet and Triplet States in Its Reactions with Water, Methanol, and Hydrocarbons" Srivastava, S.; Kercher, M.; Falvey, D.E.; *J. Org. Chem.* **1999**, *64*, 5853-5857.

Many studies have been reported recently regarding aromatic nitrenium ion chemistry. This paper concerns the parent,  $\text{NH}_2^+$ , which has the ground state triplet lying 30 kcal below the singlet. Photolysis of 1-amino-2,4,6-triphenylpyridinium perchlorate (**1**), either directly to the singlet, or sensitization by Xanthone to triplet, will give the dissociated nitrenium parent ion in the respective energy state. The chemical behavior of nitrenium ion with toluene was observed to result in products via two different mechanisms. Bibenzyl (**4**) is formed by dimerization of benzyl radicals formed by H atom abstraction by triplet nitrenium, whereas toluidines (**2**) and benzyltoluenes (**3**) are produced from benzyl cations formed by hydride transfer from toluene to singlet nitrenium. Addition of benzene trapped the benzyl cation resulting in a higher ratio of triplet to singlet products, and evidence for a benzyl radical pathway was found by photolysing triphenylmethane and observing the resulting radical in an EPR experiment, where the spectrum grew in as a function of irradiation time. In a separate experiment, the triplet to singlet product ratio was increased by diluting the toluene with  $\text{C}_6\text{F}_6$ . The reduced molarity of traps allows a greater fraction of  $\text{NH}_2^+$  to reach ground state before reaction. The insertion of singlet  $\text{NH}_2^+$  into O-H bonds was also observed in methanol and water, reactions which are analogous to carbenes.



### Photobiology

**Selected and abstracted by Joe Spicha, Photobiology Laboratory, Department of Chemistry, University of Nebraska-Lincoln**

1. "Antagonistic actions of *Arabidopsis* cryptochromes and phytochrome B in the regulation of floral induction."

Mockler, T. C.; Guo, H.; Yang, H.; Duong, H.; Lin, C. *Development* **126**, 2073-2082 (1999).

Cryptochromes are blue-light photoreceptors that sense blue (450 nm) and UV-A (320-400 nm) light and in turn mediate a variety of light-regulated responses like control of flowering time and the biological clock in plants. Recently, cryptochromes (CRY gene family) have also been discovered in mammals to be involved in the entrainment of circadian rhythms. Based on amino acid sequence identity, the animal cryptochromes are much more recently evolved from photolyases (a family of proteins that correct UV-damaged DNA) than the plant cryptochromes. All cryptochromes and their presumptive evolutionary predecessors the photolyases contain two chromophores: one light harvesting and one catalytic. Cryptochromes and photolyases are flavoproteins; they share flavin-adenine dinucleotide (FAD) as the catalytic chromophore, whilst the cryptochromes differ from the type I photolyases in that they may only contain methenyltetrahydrofolate (MTHF) as the light harvesting chromophore (Fig. 1). Through a molecular mechanism that remains unclear, this light-energy that MTHF perceives is transferred to the catalytic FAD chromophore and used by cryptochromes to initiate signal transduction. Recent physiological evidence presented by Mockler *et al.* (1999) points towards a convergence in the cryptochrome and phytochrome (a red/far-red light photoreceptor) signal transduction pathways in plants.

Although substrates of the cryptochromes are unknown, cryptochromes are believed to function just like photolyases, mediating light-dependent redox reactions. *Arabidopsis* cryptochrome1 binds to and is phosphorylated by phytochromeA (currently thought to be a serine/threonine kinase) *in vitro* and undergoes phosphorylation *in vivo* in a red-light dependent manner. Human cryptochrome2 binds to and modulates the activity of a nuclear Ser/Thr phosphatase *in vitro*. Mockler *et al.* studied the effects of blue and red (658 nm) light on the start of flowering of *CRY1*, *CRY2*, and *PHYB* mutants, *CRY2/CRY1* double mutants compared to wild-type *Arabidopsis* plants (1999). The *CRY2/CRY1* double mutants displayed delayed flowering under blue light, while neither of the single *CRY1* or *CRY2* mutants showed this same phenotype. A very interesting finding was that the light-quality that the plant perceives between days one and seven after seed germination determines the flowering time, as mutations in either *PHYB* or both *CRY1* and *CRY2* resulted in the loss of this 'light-quality sensitive' phase. Results indicate that cryptochrome1, cryptochrome2 and phytochromeB function antagonistically in the regulation of flowering time. That is, cryptochrome2 mediates a blue light inhibition of phytochromeB function, the red light inhibition of floral initiation (Fig. 2). All of the photoreceptors influence photoperiodic flowering by the regulation of the biological clock, although the *Arabidopsis* *CRY2* mutant had no significant defect in circadian clock period length control. Clearly, signal transduction cascades initiated by these different photoreceptors converge at the same downstream factors (Fig. 2).

Figure 1.

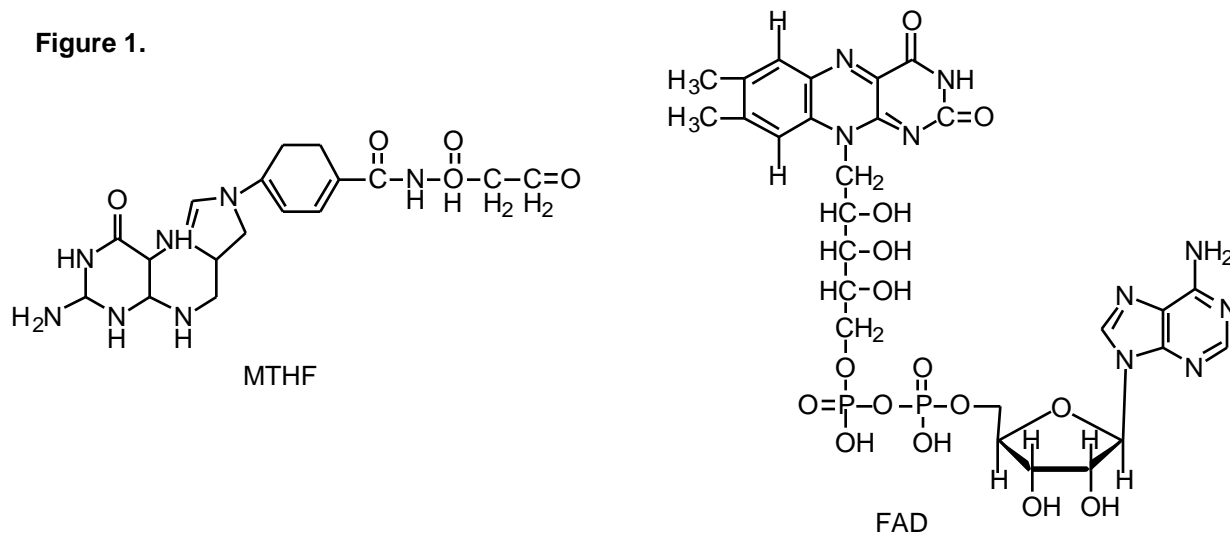
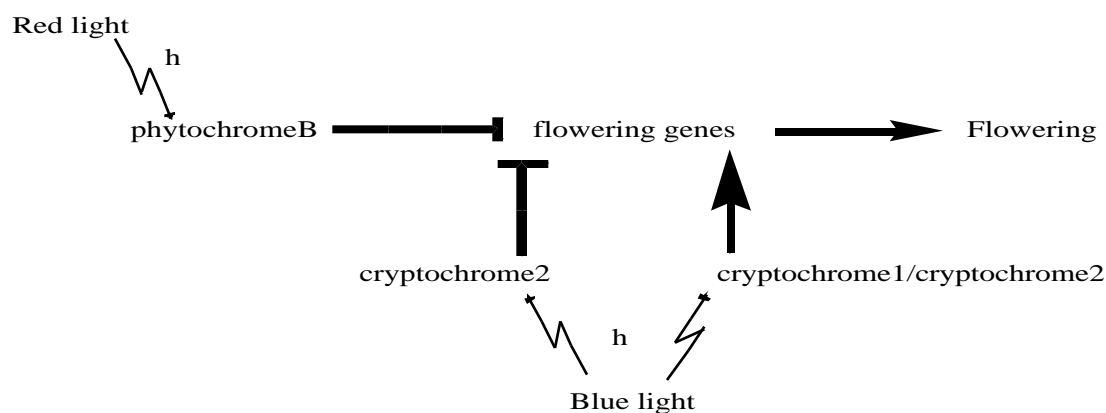


Figure 2.



Selected by Steven Woo Il Park, Photobiology Laboratory (Dr. Pill-Soon Song), Department of Chemistry, University of Nebraska-Lincoln

1. "LOV (light, oxygen or voltage) Domains of the Blue-Light Photoreceptor Phototropin (nph1): Binding Sites for the Chromophore Flavin Mononucleotide" Christie, J. M.; Salomon, M. Nozue, K.; Wada, M.; Briggs, W. R. *Proc. Natl. Acad. Sci.* **96** 8779-8783 (1999)

Phototropism, a phenomenon of plant growing towards unilateral blue light, is mediated by protein called NPH1. The NPH1 protein is heavily phosphorylated when irradiated with blue light both *in vivo* and *in vitro* with evidence suggesting that this protein is plasma membrane associated. The 120kDa NPH1 protein has a serine-threonine kinase domain in the C-terminus analogous to phytochrome and LOV1 and LOV2 domains in the N-terminus. The LOV domains are known to function as sensor for environmental factors that could change the redox status of the cell like light, oxygen or voltage thus LOV. The mechanism for function in all known LOV containing proteins is based on a flavin prosthetic group that can be used to sense the redox state (Figure 1).

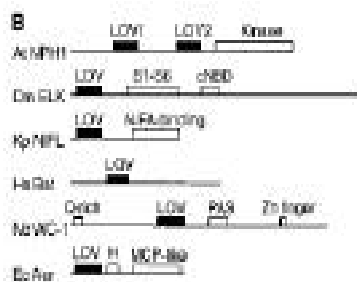


Figure 1. Structural features of several LOV containing proteins

The LOV domain has been found in a variety of proteins with no apparent functional relationship with NPH1 protein like Bat, a regulator of bacterio-opsin in response to oxygen or light, NIFL, a regulator of nitrogenase transcription in response to oxygen, White Collar-1, a regulator of blue light response. Aer, a flavoprotein required for aerotaxis signaling, and Eag, a family of K<sup>+</sup> channel proteins from mammals.

2. From E. Huala *et al. Science* **278**, 2120-2123

Recently a photoreceptor phy3 from fern (*Adiantum capillus-veneris*) was discovered to have similar LOV domains, in addition to a phytochrome like chromophore binding domain. Of the above mentioned LOV domain containing proteins Aer and NIFL are known to non-covalently bind FAD for sensing environmental stimuli like light, oxygen or voltage. Christie *et al*, have shown that both phy3 and NPH1 protein expressed in *E. coli* bind FMN (Figure 2) in stoichiometric amount.

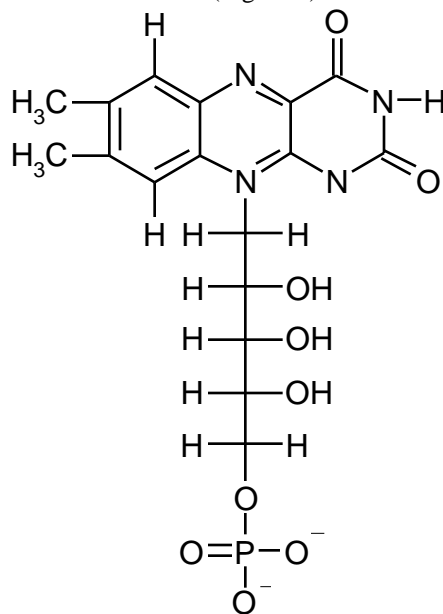


Figure 2. Structure of Oxidized Flavin Mononucleotide (FMN)

The finding further suggests that kinase activity of the NPH1 protein is regulated by the FMN binding LOV domain that can sense the redox changes due to blue-light and relay that message to the kinase domain. Similarities of the action spectrum for the assembled holo-protein NPH1 with the

action spectra for phototropism suggest that FMN is the chromophore of light dependent autophosphorylation and it functions as a photosensor in phototropism.

**Selected by Jeong-II Kim, Photobiology Laboratory , Department of Chemistry, University of Nebraska-Lincoln, 602 Hamilton Hall, Lincoln, NE, 68588-0304**

1. "Binding of phytochrome B to its nuclear signaling partner PIF3 is reversibly induced by light", Min Ni, M.; Tepperman, J. M.; Quail, P. H. *Nature* (1999) **400**, 781-784.

Plants use light signals to regulate various developmental processes such as seed germination, de-etiolation, and floral induction, and phytochrome is the best-characterized photoreceptor controlling light-dependent development in plants. Phytochrome, with gene family members of phytochrome A to E, is a soluble chromoprotein that exists as dimers consisting of an apoprotein of 120kD and a covalently attached linear tetrapyrrole chromophore. Phytochrome is photochemically converted from inactive Pr form to the active Pfr form by absorbing red photons. Conversely, Pfr can be converted back to Pr by absorbing far-red photons. The phytochrome monitors the light environment and enables the plant to optimize growth and development in accordance with prevailing conditions, which includes germination, flowering, chloroplast development and so on (Pill-Soon Song, 1999, *J. Biochem. Molec. Biol.*, **32**, 215-225).

Although the mechanism of phytochrome action is important and has been studied for a long time, the mechanism is not fully understood. The breakthroughs for elucidating the action mechanism of phytochrome will be from two aspects; the structure determination of phytochrome to study structure-function relationship, and the phytochrome interacting proteins for determining the signaling pathways. Recently, there are several reports relating to phytochrome interacting proteins including phytochrome interacting factor-3 (PIF3) (Min Ni *et.al.*, 1999, *Nature*, **400**, 781-784; Min Ni *et.al.*, 1998, *Cell*, **95**, 657-667), nucleotide diphosphate kinase (NDPK2) (Gil-tsu Choi *et.al.*, 1999, *Nature*, in press), and phytochrome kinase substrate-1 (PKS1) (Christian Fankhauser *et.al.*, 1999, *Science*, **284**, 1549-1541). These can give us clues for the action mechanism of phytochrome including direct regulation of gene expression, and kinase activity. Of the phytochrome interacting proteins, PIF3 and NDPK2 are the best-characterized protein so far.

PIF3, fished out by yeast two-hybrid system using C-terminus of phytochrome A and B as baits, binds specifically only to the Pfr of phytochrome *in vitro*. Furthermore, overexpression of PIF3 in transgenic *Arabidopsis* increased light sensitivity, but anti-sense expression decreased it. PIF3 contains helix-loop-helix motif and can be localized to the nucleus suggesting a role in controlling gene expression (Min Ni *et.al.*, 1998, *Cell*, **95**, 657-667). Recently, the localization of phytochrome into nucleus in light dependent manner has also been reported (Rumi Yamaguchi, *et.al.*, 1999, *J. Cell Biol.*, 437-445; Stefan Kircher *et.al.*, 1999, *The Plant Cell*, **11**, 1445-1456). These suggest that the action mechanism of phytochrome includes a direct regulation of photoregulated gene expression via the photoreceptor and a transcriptional regulator. Recent report of Quail's group also showed that PIF3 could bind to *in vitro* synthesized full-length phytochrome B in a light dependent manner; the active form (Pfr) of phytochrome B can bind to PIF3, but inactive form (Pr) of phytochrome B cannot bind to PIF3. They used an immunoprecipitation method using monoclonal antibodies against GAD (Gal4 activation domain) to prove the interaction between *in vitro* synthesized phytochrome B and recombinant GAD-PIF3. They also showed that both N- and C-terminal domains of phytochrome B were needed for the interaction and synergism. This means that the conformational change induced in

phytochrome by red light makes the interaction between full-length phytochrome and PIF3 in a synergistic manner. Their results suggest that there are at least three steps in the signal transduction process between phytochrome B and PIF3; translocation of Pfr of phytochrome B (Pfr-PHYB) to nucleus, binding of Pfr-PHYB to PIF3, and interaction of Pfr-PHYB-PIF3 complex with target genes either directly or indirectly.

**Selected by Shen Yu, Photobiology Laboratory (Dr. Pill-Soon Song), Department of Chemistry, University of Nebraska-Lincoln**

1. "PKS1, a Substrate Phosphorylated by Phytochrome That Modulates Light Signaling in *Arabidopsis*." Frankhauser, C.; Yeh, K. C.; Lagarias, J. C.; Zhang, H.; Elich, T. D.; Chory, J. *Science* **284**, 1539-1541 (1999).

Phytochromes are red/far-red photoreceptors for gene regulation in developmental and morphogenic processes in plants. Recent studies show that phytochromes might belong to the family of eukaryotic serine-threonine kinases with histidine ancestry. The identification of PKS1 protein (phytochrome kinase substrate 1) strongly suggests this mechanism.

The PKS1 protein is a basic soluble protein of 439 amino acids. It is able to bind both Pr and Pfr forms of phytochrome via the interaction with the COOH-termini of phytochromes. Experiments also showed that PKS1 is a substrate of phytochrome's kinase activity in vitro. However, mutant [Ser599Lys] phytochrome was no longer active as a protein kinase for PKS1, suggesting that Ser/Thr residue is critical in kinase activity of phytochrome. Immunoprecipitate analysis indicated that PKS1 along with phytochrome is a phosphoprotein in vivo (Fig. 1). Protein immunoblot analysis on dark-grown versus red light-grown seedlings was also conducted to confirm that PKS1 is phosphorylated in vivo in a phytochrome-dependent manner. Thus PKS1 is a substrate of phytochrome's kinase activity in vivo.

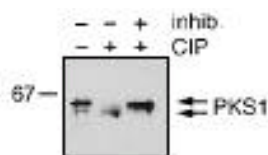


Fig. 1. PKS1 is phosphorylated in vivo. Immunoprecipitated PKS1 treated with or without CIP (calf intestine phosphatase) in the presence or absence of phosphatase inhibitors was subjected to protein immunoblotting and detected with antibodies to PKS1. (From *Science* **284**, 1539-1541, Fig. 3B)

## Upcoming Meetings

An up-to-date version of this list is posted on the I-APS website (<http://www.chemistry.mcmaster.ca/~iaps/index.html>). Please send new meeting announcements to: [wsjenks@iastate.edu](mailto:wsjenks@iastate.edu) and [iaps@mcmaster.ca](mailto:iaps@mcmaster.ca).

### ◆ 11<sup>TH</sup> INTER-AMERICAN PHOTOCHEMICAL SOCIETY WINTER CONFERENCE

January 2-6, 2000

Clearwater Beach, FL U.S.A.

Information: Dr. Edwin F. Hilinski, Florida State University, fax: 850-644-8281; email: [hilinski@chem.fsu.edu](mailto:hilinski@chem.fsu.edu) or Dr. Joseph T. Hupp, Northwestern University, fax: 847-492-7713; email: [jthupp@chem.nwu.edu](mailto:jthupp@chem.nwu.edu) or information may be obtained from the Inter-American Photochemical Society web site at <http://www.chemistry.mcmaster.ca/~iaps>

### ◆ CHIMIE, SOLEIL, ENERGIE ET ENVIRONNEMENT (JCSEE 1)

February 3 - 4, 2000

St. Avold, France

Information: Dr. Didier Robert, Lab. de Chimie Industrielle (LCI), Rue Victor Demange, F-57500 St. Avold, France, Tel: +33 03 87 93 91 00, Fax: +33 03 87 93 91 01, email: [drobot@iut.univ-metz.fr](mailto:drobot@iut.univ-metz.fr)

### ◆ PITTCON 2000, 50TH PITTSBURGH CONFERENCE ON ANALYTICAL CHEMISTRY AND APPLIED SPECTROSCOPY "SCIENCE FOR THE 21ST CENTURY"

March 12 - 17, 2000

New Orleans, LA, USA

Information: Hy Schultz, <http://www.pittcon.org/index.html>

### ◆ IXTH INTERNATIONAL SYMPOSIUM ON LUMINESCENCE SPECTROMETRY IN BIOMEDICAL AND ENVIRONMENTAL ANALYSIS. SPECTROSCOPIC AND IMAGING DETECTION TECHNIQUES

May 15 - 17, 2000

Montpellier, France

Information: Prof. Dan A. Lerner, Univ. of Montpellier, ENSC, 8 Rue de l'Ecole Normale, F-34296 Montpellier cedex 5, tel: x33/04 6714 4323, fax: x33/04 6714 4349, email: [lerner@enscm.fr](mailto:lerner@enscm.fr)

◆ **PHOTOBIOLOGY 2000: JOINT CONGRESS (AIP), ASP AND ESP MEETING**

May 31 – June 4, 2000

San Francisco, CA U.S.A.

Information: Nancy L. Oleinick, Biomedical Res Bldg 3, Case Western Reserve University, 10900 Euclid Avenue, Cleveland, OH 44106-4942, tel: +1 216/368 1117, fax: +1 216/368 1142, email: nlo@po.cwru.edu

◆ **XTH INTERNATIONAL SYMPOSIUM ON LUMINESCENCE SPECTROMETRY-DETECTION TECHNIQUES IN FLOWING STREAMS – QUALITY ASSURANCE AND APPLIED ANALYSIS**

June 4 - 7, 2000

Granada, Spain

Information: Dr. Ana M. Garcia-Campana, Department of Analytical Chemistry, University of Granada, Avenue Fuertenueva s/n, E-18071 Granada, Spain, Tel: +34 9 58 24 85 94, Fax: +34 9 58 24 33 28, email: amgarcia@goliat.ugr.es

◆ **XVIII IUPAC SYMPOSIUM ON PHOTOCHEMISTRY**

July 22 – 27, 2000

Dresden, Germany

Information: Prof. Silvia Braslavsky, Mülheim, fax: +49 208/306 39 51, email: [braslavskys@mpi-muelheim.mpg.de](mailto:braslavskys@mpi-muelheim.mpg.de) (chairperson); Prof. Thomas Wolff, Dresden, fax: +49 351/463 33 91, email: [wolff@cech01.chm.tu-dresden.de](mailto:wolff@cech01.chm.tu-dresden.de) (chairman local committee).

◆ **25TH EUROPEAN CONGRESS ON MOLECULAR SPECTROSCOPY (EUCMOS XXV)**

August 27 – September 1, 2000

Coimbra, Portugal

Information: Dr. Rui Fausto, Department of Chemistry, University of Coimbra, P-3049 Coimbra, Portugal, Tel: +351 39 85 20 80, Fax: +351 39 82 77 03, email: [braslavskys@mpi-muelheim.mpg.de](mailto:braslavskys@mpi-muelheim.mpg.de)

◆ **11TH INTERNATIONAL SYMPOSIUM ON BIOLUMINESCENCE & CHEMILUMINESCENCE**

September 6 – 10, 2000

Pacific Grove, California, USA

Information: Prof. James F. Case, Department of Ecology, Evolution and Marine Biology, University of California Santa Barbara, Santa Barbara, CA 93106, U.S.A., email: case@lifesci.ucsb.edu

# INTER-AMERICAN PHOTOCHEMICAL SOCIETY MEMBERSHIP FORM



Name \_\_\_\_\_

\_\_\_\_\_ First Initial Last

Address \_\_\_\_\_

\_\_\_\_\_

\_\_\_\_\_

\_\_\_\_\_

Position \_\_\_\_\_ Telephone \_\_\_\_\_

\_\_\_\_\_

FAX \_\_\_\_\_ email \_\_\_\_\_

\_\_\_\_\_

**Membership Fees in U.S.\$:** (Canadian \$ prices in parentheses)

	1 Year	2 Years	3 Years	Amount
Full Membership	US\$22 (Cd\$29)	US\$40 (Cd\$53)	US\$56 (Cd\$74)	_____
Postdoctoral Fellow*	\$15 (22)	\$27 (36)	—	_____
Student*	\$8 (11)	\$8 (11)	—	_____
Voluntary Contribution to support student travel				_____
			TOTAL	_____

\*Name of current advisor \_\_\_\_\_

For our information, are you currently a member of the American Society for Photobiology? Yes

No

Signature \_\_\_\_\_

Date \_\_\_\_\_

Return this form with check, payable to the Inter-American Photochemical Society to: Professor Russell H. Schmehl, Tulane University, Department of Chemistry, New Orleans, LA 70118.

Please also fill out the reverse side.

Please indicate your general area of Photochemistry interest below:

Physical	_____	Inorganic	_____	Physical Organic
Organic	_____	Analytical	_____	Photophysics
Theoretical	_____	Photobiology	_____	

Please check specific Photochemistry interests:

<input type="checkbox"/> Air Pollution (AP)	<input type="checkbox"/> Photochemical Kinetics (PK)
<input type="checkbox"/> Atmospheric (AT)	<input type="checkbox"/> Spectroscopy (SP)
<input type="checkbox"/> Chemiluminescence (CL)	<input type="checkbox"/> Photoemission (PE)
<input type="checkbox"/> Dyes (CD)	<input type="checkbox"/> Isotope Separation (IS)
<input type="checkbox"/> Environmental (CE)	<input type="checkbox"/> Photobiochemistry (BC)
<input type="checkbox"/> Extraterrestrial (ET)	<input type="checkbox"/> Photobiophysics (BP)
<input type="checkbox"/> Far UV (UV)	<input type="checkbox"/> Photochromism (PC)
<input type="checkbox"/> Imaging Systems (Silver) (PG)	<input type="checkbox"/> Photoconductivity (PN)
<input type="checkbox"/> Imaging Systems (Nonsilver) (RG)	<input type="checkbox"/> Photoelectrochemistry (PL)
<input type="checkbox"/> Lasers (LS)	<input type="checkbox"/> Photoionization (PI)
<input type="checkbox"/> Macromolecular (CC)	<input type="checkbox"/> Photolithography (PT)
<input type="checkbox"/> Mechanistic (MP)	<input type="checkbox"/> Photomedicine (PM)
<input type="checkbox"/> Ordered Media (OM)	<input type="checkbox"/> Photosynthesis (PS)
<input type="checkbox"/> Organometallic (CM)	<input type="checkbox"/> Radiation Chemistry (RC)
<input type="checkbox"/> Preparative/Synthetic (CR)	<input type="checkbox"/> Solar Energy Utilization (SE)
<input type="checkbox"/> Polymer (CY)	<input type="checkbox"/> Vision (VS)

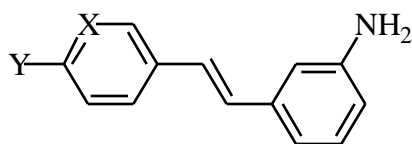
## Tinkering with Stilbene

Frederick D. Lewis and Rajdeep S. Kalgutkar, Department of Chemistry,  
Northwestern University, 2145 Sheridan Road, Evanston, IL 60208

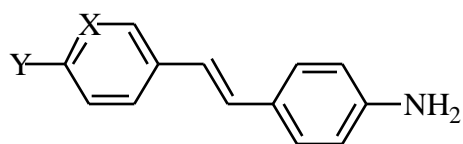
### Introduction

The photophysics of *trans*-stilbene has been studied in considerable detail.<sup>i</sup> Roughly 4% of the excited state population of *trans*-stilbene decays by fluorescence whereas the remaining 96% decays by non-radiative decay.<sup>i</sup> Intersystem crossing does not play a significant role in the photophysics of *trans*-stilbene. The non-radiative decay channel is an activated process where *trans*-stilbene twists about the central double bond leading to photoisomerization.<sup>i</sup> Numerous substituted *trans*-stilbene derivatives have also been studied too, but for the most part only the *para* isomers have been studied in any detail.<sup>ii</sup> Mono-substituted stilbenes with the substituent in the *para* position have photophysical properties that are similar to those of *trans*-stilbene, one exception being bromostilbene.<sup>ii</sup> In that case, a substantially enhanced intersystem crossing rate is observed. *Meta* substituted stilbenes have received less attention. Güsten and Klasinc studied a series of *meta* substituted stilbenes and found no large difference in the photoisomerization quantum yield between the *meta* and *para* isomers.<sup>iii</sup> However, among the *meta* isomers, the amino functional group was not studied even though *para*-aminostilbene was included in their investigation.<sup>iii</sup> They concluded based on this study that *meta* and *para* substituted stilbenes have similar properties.

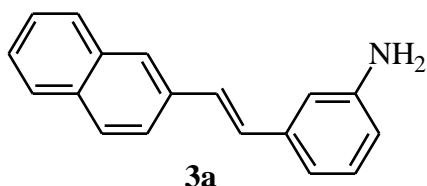
A large number of *para-para'*-disubstituted stilbenes have also been studied but, once again, disubstituted stilbenes where one or both of the substituents is in the *meta* position have received scant attention. Lapouyade and co-workers studied *trans*-4-dimethylamino-3-nitrostilbene and its 4,4'-disubstituted isomer and observed some interesting differences in their electronic spectra.<sup>iv</sup> The splitting of the long wavelength absorption band of 4,3'-isomer into a long-wavelength tail on a higher energy band was attributed, on the basis of CNDO calculations, to configuration interaction in the 4,3'-isomer which is not present in the 4,4'-isomer.<sup>iv</sup>



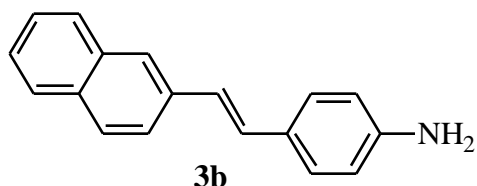
**1a:** X = CH, Y = COOMe  
**2a:** X = N, Y = H



**1b:** X = CH, Y = COOMe  
**2b:** X = N, Y = H



**3a**

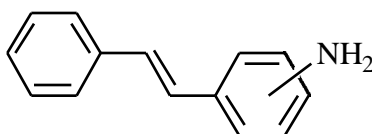


**3b**

Several years ago, J.-S. Yang made the serendipitous discovery that the photophysical behavior of the 3-aminostilbene derivatives **1a-3a** was markedly different from that of their 4'-amino

isomers **1b-3b**.<sup>v</sup> The quantum yields of fluorescence for the meta isomers were found to be significantly larger and the singlet lifetimes were increased by as much as two orders of magnitude relative to the corresponding para isomers.<sup>v</sup> Based on chemical evidence, we suggested that the difference in photophysical properties might result from different geometries, the para isomers having a planar geometry and the meta isomers a nonplanar geometry with twisting about the anilino-styrene bond.<sup>v</sup> This suggestion was greeted with the anticipated response from the two camps in the debate over TICT state geometries. As in the case of the aminonitrostilbenes studied by Lapouyade et al.<sup>iv</sup>, the absorption bands of the meta isomers are more complex than those of the para isomers.<sup>v</sup> Unpublished ZINDO calculations suggested that differences in configuration interaction might be responsible for the differences in electronic spectra.

In a weakly veiled attempt to attract the attention of at least one segment of the photochemical community, we termed these results a new example of the “meta effect”. We should, of course, have termed our results an “inverse meta effect” since the photochemical meta effect, as originally applied to the photosolvolysis of benzenoid compounds, refers to the enhanced reactivity of meta- vs. para-substituted isomers. Our interest in this general area was further stimulated by a recent analysis of substituent effects by Zimmerman who suggested, on the basis of CASSCF calculations, that ortho substituents should be like meta substituents in their ability to enhance the reactivity of benzenoid compounds.<sup>vi</sup> Thus we decided to undertake an investigation of the spectroscopy and photochemistry of the three positional isomers of the simplest of aminostilbenes. Our investigation has led us to “rediscover” some of the fundamentals of molecular orbital theory and spectroscopy that are sadly neglected in most introductory photochemistry courses. We have found these fundamentals to be highly instructive and trust that many of our photochemical colleagues will view them in the same light. As our title suggests, a simple change in substituent position can have a profound effect of the excited state behavior of *trans*-stilbene.



***o*-4:** *trans*-2-aminostilbene

***m*-4:** *trans*-3-aminostilbene

***p*-4:** *trans*-4-aminostilbene

## **Results and Discussion**

### **Absorption and Fluorescence Spectroscopy of Aminostilbenes *o*-4, *m*-4 and *p*-4**

The absorption spectra of the three aminostilbenes in acetonitrile solution are shown below (Figure 1) and their absorption and fluorescence parameters are summarized in Table 1. The absorption spectrum of *para*-aminostilbene<sup>vii</sup> is similar in band shape and integrated intensity to that of *trans*-stilbene<sup>viii</sup> except that it is red shifted due to the presence of the amino group in the para position. However, the absorption spectra of *ortho*- and *meta*-aminostilbene are considerably more complex and have lower integrated intensities.

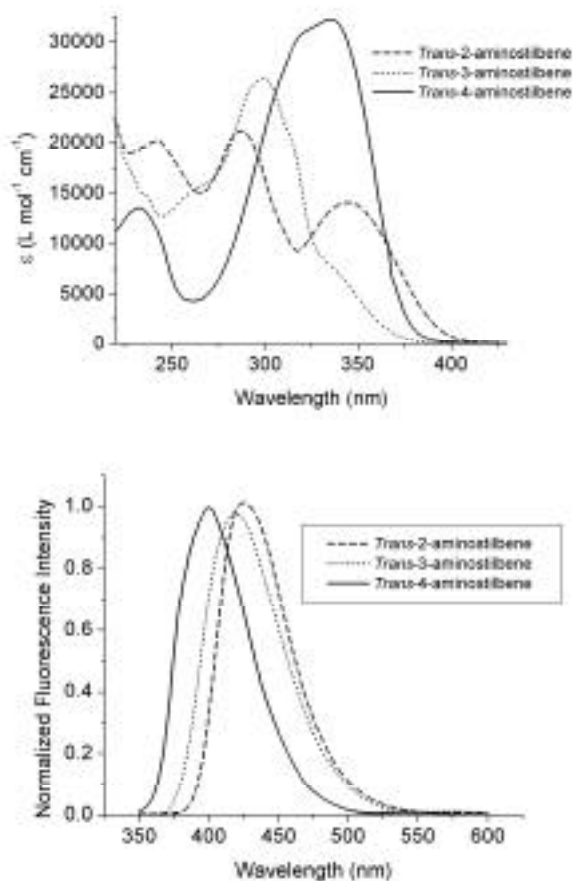


**Figure 1: Absorption spectra of the aminostilbenes in acetonitrile and fluorescence spectra in dibutylether**

In the case of *o*-4, two bands of similar intensity are observed, whereas for *m*-4 the spectrum appears to consist of two or more overlapping bands of different intensity. The absorption spectra of *m*-4 and *p*-4 show only slight solvatochromism (about 4 nm going from cyclohexane to acetonitrile) but the absorption spectra of *o*-4 show somewhat larger solvatochromism (12 nm going from cyclohexane to acetonitrile). By contrast, the fluorescence spectra of all three compounds show more pronounced solvatochromism. The fluorescence spectra of all three compounds show varying degree of vibronic structure in their fluorescence spectra in nonpolar solvent which disappears in medium polarity solvents such as dibutylether.

**Table 1.** Observed and Calculated Spectroscopic Parameters.

		Absorption max. ( $\lambda_{\text{max}} / \text{nm}$ ) <sup>a</sup>	Molar Absorptivity ( $\log \epsilon_{\text{max}}$ )	Fl. max. ( $\lambda_{\text{max}} / \text{nm}$ )	0,0 ( $\lambda_{\text{max}} / \text{nm}$ ) <sup>b</sup>	Oscillator strength ( $f$ ) <sup>c</sup>
<i>t</i> -S	hexane	294, (307, 321) <sup>d</sup>	4.45 <sup>d</sup>	347 <sup>e</sup>	326 <sup>e</sup>	0.75 <sup>f</sup>
	acetonitrile	294, (308, 320)	4.47, (4.46, 4.26)	347	325	0.76
<i>o</i> -4	hexane	286, 334	4.25, 4.11	407	373	0.23
	acetonitrile	291, 346	4.25, 4.08	445	398	0.23
<i>m</i> -4	hexane	298, (311, 329)	4.38, (4.28, 3.94)	387	356	0.12
	acetonitrile	300, (312, 332)	4.41, (4.30, 3.90)	446	384	0.12
<i>p</i> -4	hexane	316, (332)	4.50, (4.47)	380	354	0.86

acetonitrile	(318), 336	(4.49), 4.51	423	378	0.92
--------------	------------	--------------	-----	-----	------

<sup>a</sup>Shoulders in parenthesis. <sup>b</sup>Calculated by Berlman's method, reference ix. <sup>c</sup> $f = 4.3 \times 10^{-9}$   
 $\epsilon(\bar{\nu}) d\bar{\nu}$ . <sup>d</sup>From reference x, in heptane. <sup>e</sup>From reference xi, in methylpentane. <sup>f</sup>From  
reference 10.

The excited state dipole moments of the aminostilbenes, **4**, may be estimated by using the Lippert-Mataga equation (equation 1) where  $\epsilon$  is the solvent dielectric,  $n$  is the solvent refractive index,  $\mu_e$  and  $\mu_g$  are the excited state and ground state dipole moments respectively,  $a$  is solvent cavity assumed to be 5 Å,  $\nu_{\text{abs}}$  and  $\nu_{\text{flu}}$  are the absorption and fluorescence maximum in wavenumbers respectively.

$$\nu_{\text{abs}} - \nu_{\text{flu}} = \frac{-2\mu_e(\mu_e - \mu_g)}{hca^3} \frac{-1}{2\epsilon + 1} - \frac{n^2 - 1}{2n^2 + 1} \quad (1)$$

The estimated excited state dipole moments are in the order of 6-12 D for the three compounds indicating that they bear charge transfer character from the aniline ring to the styryl part of the molecule in the excited state. Based on the spectroscopy, it therefore appears that although **m-4** and **p-4** have similar degree of charge transfer in the excited state, **o-4** has a lower excited state dipole moment. It was stated earlier that **o-4** shows larger solvatochromic shifts in its absorption spectra, possibly due to specific solvation of its non-planar structure. This would in turn reduce the measured Stokes shift ( $\nu_{\text{abs}} - \nu_{\text{flu}}$ ) of **o-4** thereby reducing its excited state dipole (Table 2).

**Table 2.** Ground and Excited State Dipole Moments for the Aminostilbenes.

	$\mu_g / \text{D}^b$	$\mu_e / \text{D}^{a, c, d}$
<b>o-4</b>	1.5	6.0
<b>m-4</b>	1.5	11.9
<b>p-4</b>	2.1	10.2

<sup>a</sup>Calculated based on equation 1. <sup>b</sup>From reference xii.

<sup>c</sup>Assuming solvent cavity,  $a = 5$  Å. <sup>d</sup>95% confidence interval is  $\pm 1.0$  D.

On cooling solutions of **o-4** and **m-4** in 2-methyltetrahydrofuran (MTHF) from room temperature to 77 K, there are no significant changes in the fluorescence emission or excitation spectra. There are small (ca. 10 nm) red shifts observed on cooling due to changes in the dielectric<sup>xiii</sup> and refractive index of the solvent<sup>xiv</sup> and finally a blue shift below the glass transition temperature of MTHF (~ 120 K). This behavior is consistent with the notion that no large amplitude geometric relaxation occurs upon excitation of **o-4** and **m-4** in polar solvents such as MTHF. This led us to abandon the proposal of TICT state formation.

### **Photophysical data for the Aminostilbenes**

The quantum yields for fluorescence,  $f$ , of *trans*-stilbene and most of its para monosubstituted derivatives are usually quite low (< 0.1).<sup>ii</sup> Therefore it was surprising that the fluorescence quantum yields for **o-4** and **m-4** are > 0.75 in nonpolar solvents. The **p-4** analogue, by contrast, has a low fluorescence quantum yield in nonpolar solvent, similar to that for *trans*-stilbene (Table 3).<sup>i</sup> The fluorescence quantum yields are solvent dependent too, decreasing with increasing

solvent polarity. Another point of interest is that the singlet lifetimes of *o*-4 and *m*-4 are extraordinarily long. The singlet lifetimes of *o*-4 and *m*-4 are solvent dependent and increase with increasing solvent polarity. Singlet lifetimes of *trans*-stilbene are typically about 0.1 ns and most stilbene derivatives have singlet lifetimes < 2 ns.<sup>ii, 4</sup> The lifetimes of *o*-4 and *m*-4 are substantially longer, attaining a value of 11.7 ns for *m*-4 in acetonitrile solution, which is more than two orders of magnitude longer than the lifetime of *p*-4 in the same solvent.

The photoisomerization quantum yields of *p*-4 are similar to those of *trans*-stilbene. This is not a surprising observation given the similarity of all other photophysical data for *p*-4 and *trans*-stilbene (Table 3).<sup>iii</sup> In the case of *o*-4 and *m*-4, the quantum yields of photoisomerization are low, as expected based on the fluorescence quantum yield data. The photoisomerization quantum yields for *o*-4 and *m*-4 are solvent dependent and increase with increasing solvent polarity.

**Table 3.** Quantum Yields of Fluorescence ( $\phi_f$ ), Photoisomerization ( $\phi_i$ ), Singlet Lifetimes ( $\tau_s$ ) and Rate Constants of Fluorescence ( $k_f$ ).

		$\phi_f$	$\phi_i^a$	$\tau_s$ / ns	$k_f$ (expt.) / s <sup>-1</sup>	$k_f$ (calc) / s <sup>-1</sup> b
<i>t</i> -S	hexane	0.04 <sup>c</sup>	0.52 <sup>d</sup>	0.070 <sup>e</sup>	$6.0 \times 10^8$ <sup>c</sup>	$5.9 \times 10^8$ <sup>c</sup>
<i>o</i> -4	cyclohexane	0.88	0.04	3.7	$2.4 \times 10^8$	$1.4 \times 10^8$ <sup>g</sup>
	acetonitrile	0.69	0.12	5.4	$1.3 \times 10^8$	$1.1 \times 10^8$
<i>m</i> -4	cyclohexane	0.78	0.09	7.5	$1.0 \times 10^8$	$0.8 \times 10^8$ <sup>g</sup>
	acetonitrile	0.40	0.23	11.7	$0.3 \times 10^8$	$0.5 \times 10^8$
<i>p</i> -4	cyclohexane	0.05	0.49 <sup>f</sup>	~ 0.1	~ $5.0 \times 10^8$	$5.9 \times 10^8$ <sup>g</sup>
	acetonitrile	0.03	0.52	~ 0.1	~ $3.0 \times 10^8$	$4.6 \times 10^8$

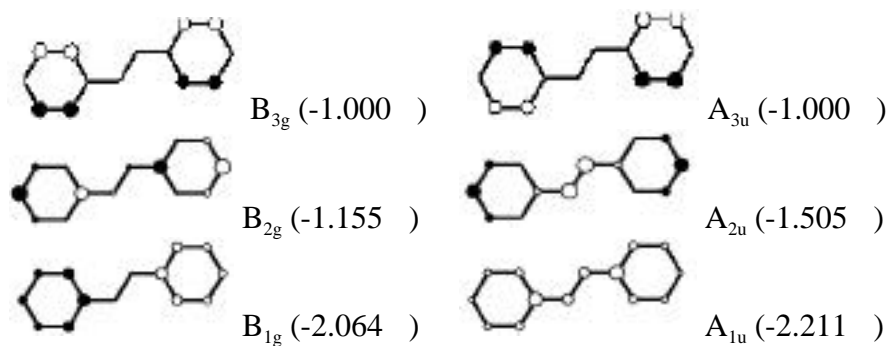
<sup>a</sup>Excitation at 313 nm. <sup>b</sup>Calculated by equation 3. <sup>c</sup>From reference xv. <sup>d</sup>In pentane, from reference xvi. <sup>e</sup>From reference xvii. <sup>f</sup>From reference iii. <sup>g</sup>In hexane solution.

### Barriers for Photoisomerization

The excited state of *trans*-stilbene decays mainly through two channels: fluorescence and activated photoisomerization along the singlet surface.<sup>i</sup> The barrier for singlet state isomerization is estimated to be 3.5 kcal/mol.<sup>ii</sup> Based on the similarity of the photophysical data for *p*-4 and stilbene, they are assumed to have similar barrier heights. Intersystem crossing for *trans*-stilbene occurs to an insignificant extent since the rate constants of fluorescence ( $5.9 \times 10^9$  s<sup>-1</sup>) and photoisomerization ( $\sim 10^{10}$  s<sup>-1</sup>) are much larger than that of intersystem crossing ( $\sim 4 \times 10^7$  s<sup>-1</sup>) at room temperature. Under these circumstances, if the barrier to photoisomerization is increased, fluorescence and intersystem crossing will gain importance. In the extreme case, when the barrier becomes large enough, fluorescence and intersystem crossing will be the two dominant pathways. In that case, any observed photoisomerization will occur from the triplet state. Since the decay channels are thermally unactivated, no temperature dependence is expected for any of the observable properties such as singlet lifetimes, fluorescence or photoisomerization quantum yields.

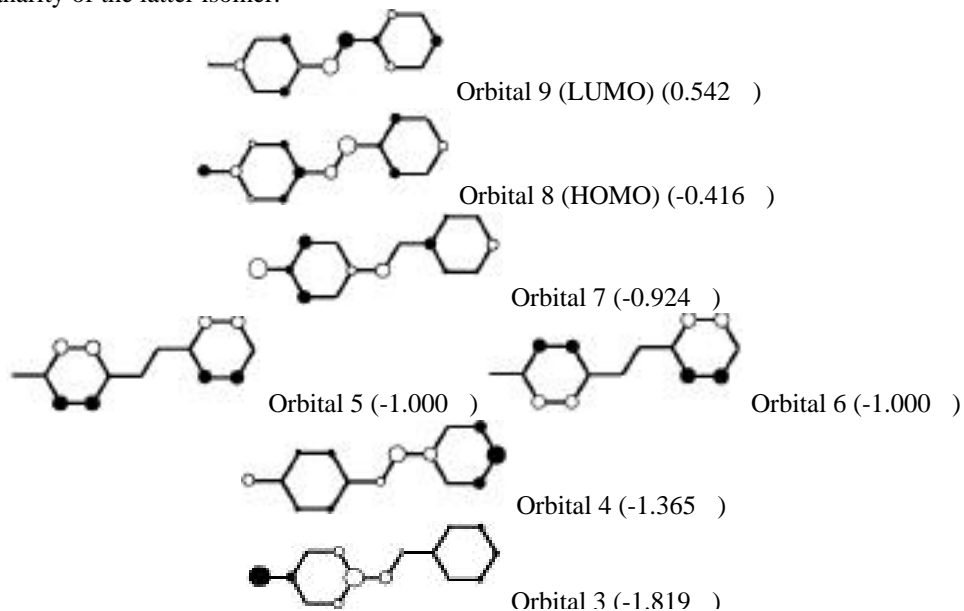
Measurement of the singlet lifetimes of *o*-4 or *m*-4 as a function of temperature in isopentane resulted in the observation of temperature independence of the singlet lifetimes (Figure 2). This suggests that the only channels of excited state decay are thermally unactivated: fluorescence and intersystem crossing.





**Figure 3:** Selected and \* Hückel orbitals of *trans*-stilbene ( $C_{2h}$  symmetry).

Selected Hückel orbitals of *trans*-stilbene are presented in Figure 3 for purposes of comparison with those of *p-4* which are shown in Figure 4. There is considerable similarity in the nodal properties of *trans*-stilbene orbitals and those of *p-4*. More specifically, orbitals 1, 2, 4, 5, 6, 8 and 9 of *p-4* correlate with orbitals  $A_{1u}$ ,  $B_{1g}$ ,  $A_{2u}$ ,  $B_{3g}$ ,  $A_{3u}$ ,  $A_{4u}$  and  $B_{4g}$  in *trans*-stilbene, respectively, whereas orbital 7 of *p-4* correlates with the  $B_{2g}$  orbital of *trans*-stilbene. The energy of orbital 7 (-0.924) of *p-4* is somewhat higher than that of the  $B_{2g}$  orbital (-1.155) in *trans*-stilbene and thus it lies above the pair of degenerate orbitals 5 and 6 of *p-4*. This is due to the interaction of the nitrogen p orbital with the  $B_{2g}$  orbital of *trans*-stilbene which results in the formation of orbitals 3 and 7 in *p-4* (Figure 5). It is interesting to note that although the nitrogen p orbital mixes with all orbitals to different extents, the largest coefficients are on orbitals 3 and 7 in *p-4* whereas orbitals 5 and 6 show no electron density on the nitrogen atom. This is due to the fact that in the corresponding  $B_{3g}$  and  $A_{3u}$  orbitals in *trans*-stilbene the carbon atoms to which they are attached have no electron density either, thereby precluding any interaction. It is also not surprising that the appearance of the orbital 7 is similar to that of the  $B_{2g}$  orbital in *trans*-stilbene rather than orbital 3, given the similarity in their energies (Figure 5). The amount of interaction between the nitrogen p orbital and the *trans*-stilbene orbitals is expected to decrease as the energy gap between the orbitals decreases. Therefore the higher energy \* orbitals show far less electron density on the nitrogen orbital than the orbitals. The charge transfer character displayed by the aminostilbenes as a result of \* excitation may be a result of this circumstance. The Hückel analysis can be extended to *m-4* and *o-4*, however it does not take into account the nonplanarity of the latter isomer.



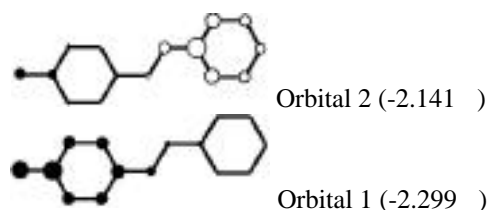


Figure 4: Selected and \* Hückel orbitals of *p-4*.

Whereas the Hückel analysis provides insights in to the origin of the red-shifted absorption and emission and increased polarity of the aminostilbenes compared to *trans*-stilbene in the excited state, it does not reveal the origin of the differences in the electronic spectra of the three isomeric aminostilbenes. To do so requires consideration of configuration interaction (CI), which in turn requires consideration of the local symmetry properties of the aminostilbenes.

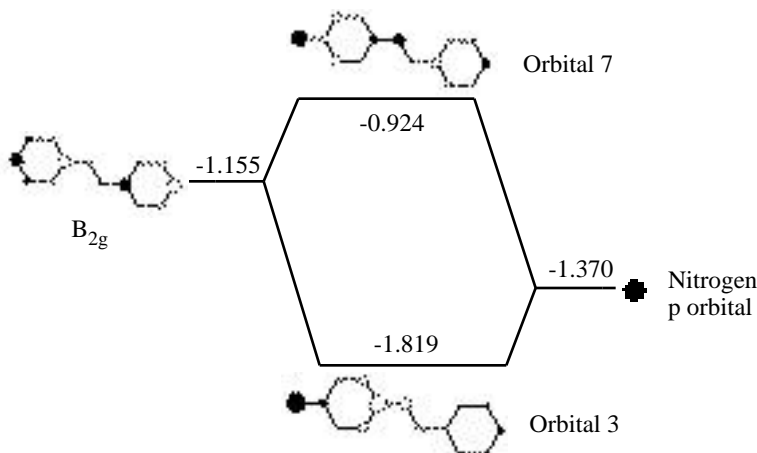


Figure 5: Orbital interaction diagram for orbitals 3 and 7 of *p-4*.

Based on orbital symmetry considerations, molecules with pseudo- $C_{2v}$  symmetry have transitions that can be classified as A or B type whereas molecules with lower symmetry such as pseudo- $C_s$  symmetry have only A type transitions (Figure 6).<sup>xx</sup> Transitions of different symmetry will not interact with each other and thus CI may be unimportant for some of the transitions of *trans*-stilbene and *p-4*. This is, in fact, the case for their lowest singlet states which are described by ZINDO<sup>xxi</sup> calculations as essentially pure HOMO → LUMO transitions with no configuration interaction. Since all of the transitions of *m-4* and *o-4* are of A symmetry, they are expected to be subject to CI. ZINDO calculations reveal the presence of two low energy \* transitions for *m-4* and *o-4*, both of which have extensive CI.

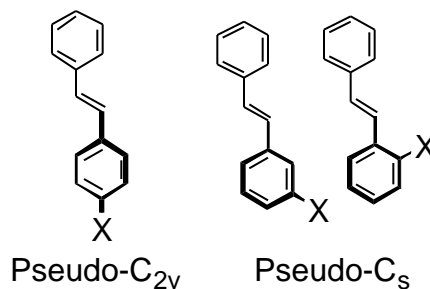


Figure 6: Local symmetry for the aminostilbenes.

Due to the presence of configuration interaction in the lowest excited states of *m-4* and *o-4*, the oscillator strength of the band is expected to decrease. Experimentally, this is found to be the case. The oscillator strength of the longest wavelength absorption band for *p-4* was estimated by straightforward integration of the molar absorptivity curve but in the case of *m-4* and *o-4*, the longest wavelength absorption band had to be approximated as a Gaussian curve and the oscillator strength computed by integration of the Gaussian curve (Figure 7).<sup>x</sup> In the case of *m-4* and *o-4*, the oscillator strength was found to be much smaller than that of *p-4*. One of the implications of smaller oscillator strengths is that a lower rate constant of fluorescence,  $k_f$ , is predicted using the Strickler-Berg relationship (equation 3).<sup>xxii</sup>

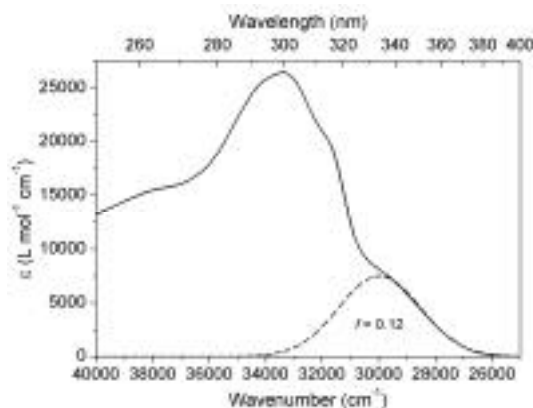


Figure 7: Strickler-Berg analysis for *m-4*.

It can be seen in Table 3 that the rate constants of fluorescence obtained experimentally agree quite well with those calculated from the Strickler-Berg relationship. Thus low fluorescence rate constants as well as the high barriers for singlet state photoisomerization are responsible for the long lifetimes *m-4* and *o-4*.

$$k_f = 2.889 \times 10^{-9} n^2 \frac{f(\bar{\nu}) d_{00}^-}{f(\bar{\nu})^{-3} d_{00}^-} \times \frac{(\bar{\nu}) d_{00}^-}{\bar{\nu}} \quad (3)$$

#### **Proposed Model to Explain the Large Excited Singlet Activation Barrier for *o-4* and *m-4***

We are now in a position to begin constructing a state energy diagram for the aminostilbenes. The ground state heats of formation for *trans*-stilbene and the three aminostilbenes obtained from semi-empirical AM1 calculations are similar. Evidently, the nonplanarity of *o-4* does not have a large effect on its heat of formation. The singlet energies reported in Table 1 are experimental values estimated from the crossing points of absorption and fluorescence spectra and are used to establish the energy of the singlet states in Figure 8.

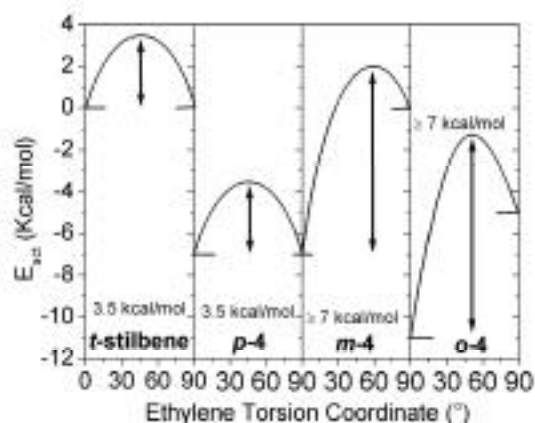


**Figure 8:** State Energy Diagram for the Aminostilbenes.

It may seem surprising that the energy of the excited  $S_1$  state of *m-4* is similar to that *p-4*, even though the amino group in *m-4* is not in resonance conjugation with the rest of the stilbene molecule, and that the energy of *o-4* is lower still. As noted in the preceding sections, CI can account for the lowering of the  $S_1$  energies. In fact, earlier theoretical calculations by Heilbronner and co-workers indicate that ortho disubstituted aromatic compounds should display a greater degree of CI and therefore a greater degree of  $S_1$  stabilization (cf. Figure 8).<sup>xxiii</sup>



**Figure 9:** Resonance forms for the  $S_1$  and  $P^*$  states of *p-4* and *m-4*.

In order to explain the large excited singlet activation barrier for *o-4* and *m-4*, it is necessary to compare the relative barriers to that of *trans*-stilbene. Since not much is known about the transition state leading to the twisted  $P^*$  state, its energies are inferentially based on the Hammond Postulate.<sup>xxiv</sup> Figure 8 shows a state energy diagram for all three compounds relative to *trans*-stilbene.

Experimentally we have found the barrier for singlet isomerization of *p-4* is similar to that of *trans*-stilbene. It has been shown by Saltiel and co-workers that in the case of *trans*-stilbene, the  $P^*$  state is approximately isoenergetic with the excited  $S_1$  state and that they are separated by a barrier of ca. 3.5 kcal/mole.<sup>xxv</sup> Thus we assume that the presence of the amino group in *p-4* can stabilize the  $P^*$  state as well as the  $S_1$  state. This is consistent with the resonance structures for the zwitterionic  $P^*$  shown in Figure 9. In the case of *m-4*, resonance stabilization of  $P^*$  cannot occur. Based on the Hammett parameters of para-amino ( $\rho^+ = -1.3$ ) vs. meta-amino ( $\rho_{\text{meta}} = -0.16$ ) the stabilizing effect of the amino group in the para position is almost absent in the meta position.<sup>xxvi</sup> Another insight is obtained from a computational study by Dewar and co-workers where it was found that the *meta*-aminobenzyl cation is destabilized relative to the *para*-aminobenzyl cation by 24 kcal/mol.<sup>xxvii</sup> Therefore it seems reasonable to assume that the  $P^*$  state is either non-stabilized or actually destabilized relative to the  $P^*$  state of *trans*-stilbene. This would account for an 7 kcal/mol activation barrier for *m-4* (Figure 8).

The case of *o-4* is complicated by its nonplanarity which results from nonbonded interaction between the amino and styryl groups (Figure 10). Semi-empirical AM1 calculations, indicate that the aniline styryl torsion angle is about 45-48° in the ground state (Figure 10) and 31° in the ethylene twisted  $P^*$  state. As a result, there is substantial inhibition of resonance stabilization of the zwitterionic  $P^*$  state as shown in Figure 11a.

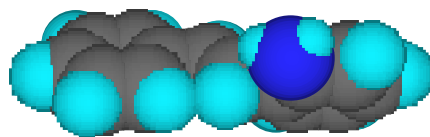


**Figure 10:** AM1 optimized  $S_1$  state of *o*-4.

Nakata et al have found, based on RHF/6-31  $G^*$  calculations, that resonance stabilization in benzyl cations obeys a  $\cos^2(\theta)$  dependence (Figure 11b).<sup>xxviii</sup> It is therefore expected that the stabilization of  $P^*$  in *o*-4 will be about 25% (2 kcal/mole) less than in *p*-4. Combining this value with the 4 kcal/mol additional stabilization of  $S_1$ , the energy of  $P^*$  is predicted to lie ca. 6 kcal/mol above that of  $S_1$ , in accord with the barrier height of > 7 kcal/mole estimated from experimental data (Figure 2).

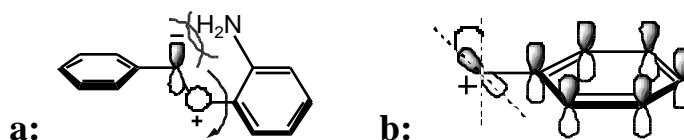


**Figure 11:** Loss of resonance energy in *o*-4 due to torsion.

## Conclusions

The present model serves to explain the unusual photophysics of the aminostilbenes. The electronic spectra of *para*-aminostilbene<sup>vii</sup> are red shifted in comparison to those of *trans*-stilbene,<sup>x,xi</sup> however its excited state behavior is similar to that of *trans*-stilbene in all respects. From this we conclude that the *para* amino substituent serves to stabilize both the  $S_1$  and  $P^*$  states to a comparable extent. In the case of the *meta*-aminostilbene and *ortho*-aminostilbene extensive configuration interaction results in more complex absorption spectra, lower singlet energies, and lower fluorescence rate constants in comparison to those for the *para* isomer. The  $P^*$  state of *meta*-aminostilbene is destabilized for electronic reasons whereas the  $P^*$  state of *ortho*-aminostilbene is destabilized for steric reasons. In both cases this leads to a large activation barrier on the singlet surface. As a result, photoisomerization arises via intersystem crossing to the triplet state followed by barrierless ethylene torsion. The long singlet lifetimes are a result of both the loss of the nonradiative singlet decay channel and the loss of oscillator strength of the  $S_0 \rightarrow S_1$  transition because of configuration interaction.

It needs to be stressed that these effects may only be observed in the presence of strong mesomeric groups such as the amino group which strongly stabilize the  $S_1$  state either by direct conjugation or by configuration interaction and destabilize the  $P^*$  state when they are in the *meta* position. Groups such as methyl are not mesomeric and therefore will not stabilize the  $S_1$  state whereas nitro groups stabilize the *para* and the *meta* position to equal extents based on their Hammett parameters.<sup>xxvi</sup> Hence the singlet state activation barrier in these cases is expected to remain low, resulting in behavior similar to that for *trans*-stilbene.<sup>ii</sup> These results indicate that the amino group may be unique in its ability to perturb the photochemical behavior of stilbene. An indication of the generality of the effect of a *meta* amino substituent on stilbene photochemistry is provided by the behavior of the disubstituted stilbenes **1a-3a**, which is qualitatively similar to that of the monosubstituted aminostilbenes. Comparison of our results with those of Lapouyade et al. for 3-nitro-4'-dimethylaminostilbene suggests that long singlet lifetimes require that the amine substituent be located in the *meta* position.<sup>iv</sup>

Finally, the reader who has persevered to this point may well wonder about existence of a meta or ortho-meta effect for *cis*-aminostilbenes. The answer should be appearing soon.

### Acknowledgements

We acknowledge Profs. Jack Saltiel and Siegfried Schneider for helpful discussions. Funding for this project was provided by NSF grant CHE-9734941.

- 
- <sup>i</sup> Saltiel, J.; Sun, Y.-P. *Photochromism, Molecules and Systems*; Durr, H.; Boas-Laurent, H.; Eds.; Elsevier: Amsterdam, 1990; p. 64 and references therein.
- <sup>ii</sup> Saltiel, J.; Charlton, J. L. *Rearrangements in Ground and Excited States*; de Mayo, P., ed.; Academic Press: New York, 1980; Vol. 3, p. 25.
- <sup>iii</sup> Güsten, H.; Klasinc, L. *Tetrahedron Letters* **1968**, 26, 3097.
- <sup>iv</sup> Lapouyade, R.; Kuhn, A.; Letard, J.-F.; Rettig, W. *Chem. Phys. Lett.* **1993**, 208, 48.
- <sup>v</sup> Lewis, F. D.; Yang, J.-S. *J. Am. Chem. Soc.* **1997**, 119, 3834.
- <sup>vi</sup> Zimmerman, H. E. *J. Phys. Chem. A.* **1998**, 102, 5616 and references therein.
- <sup>vii</sup> (a) Beale, R. N.; Roe, E. M. F. *J. Am. Chem. Soc.* **1952**, 74, 2302. (b) Jungmann, H.; Güsten, H.; Schulte-Frohlinde, D. *Chem. Ber.* **1968**, 101, 2690.
- <sup>viii</sup> Gegiou, D.; Muzkat, K. A.; Fischer, E. *J. Am. Chem. Soc.* **1968**, 90, 3907.
- <sup>ix</sup> Berlman, I. B. *Handbook of Fluorescent Spectra of Aromatic Molecules*, 2nd ed.; Academic Press: New York, 1971.
- <sup>x</sup> Jaffe, H. H.; Orchin, M. *Theory and Applications of Ultraviolet Spectroscopy*; John Wiley and Sons: New York, 1962.
- <sup>xi</sup> Dyck, R. H.; McClure, D. S. *J. Chem. Phys.* **1962**, 36, 2326.
- <sup>xii</sup> Everard, K. B.; Kumar, L.; Sutton, L. E. *J. Chem. Soc.* **1951**, 2807, 2812.
- <sup>xiii</sup> Furutsuka, T.; Imura, T.; Kojima, T.; Kawabe, K. *Tech. Rep. Osaka Univ.* **1974**, 367.
- <sup>xiv</sup> Timmermans, J. *Physico-Chemical Constants of Pure Organic Liquids*, Vol. 1; Elsevier: New York, 1950.
- <sup>xv</sup> Saltiel J.; Waller, A. S.; Sears, D. F., Jr.; Garrett, C. Z. *J. Phys. Chem.* **1993**, 97, 2516.
- <sup>xvi</sup> Waldeck, D. H. *Chem. Rev.* **1991**, 91, 415.
- <sup>xvii</sup> Kim, S. K.; Courtney, S. H.; Fleming, G. R. *Chem. Phys. Lett.* **1989**, 159, 543 and references therein.
- <sup>xviii</sup> Görner, H.; Schulte-Frohlinde, D. *J. Phys. Chem.* **1979**, 83, 3107.
- <sup>xix</sup> The Hückel orbitals were calculated using a HMO program developed by Prof. Arvi Rauk at the Department of Chemistry, University of Calgary, Canada. Website: <http://www.chem.ucalgary.ca/SHMO/>
- <sup>xx</sup> Cotton, F. A. *Chemical Applications of Group Theory*, 3<sup>rd</sup> ed.; John Wiley and Sons: New York, 1990.
- <sup>xxi</sup> Zerner, M. C.; Loew, G. H.; Kirchner, R. F.; Mueller-Westerhoff, U. T. *J. Am. Chem. Soc.* **1980**, 102, 589.
- <sup>xxii</sup> (a) Strickler, S. J.; Berg, R. A. *J. Chem. Phys.* **1962**, 37, 814. (b) Birks, J. B.; Dyson, D. J. *Proc. R. Soc. London, Ser. A* **1963**, 275, 135.
- <sup>xxiii</sup> (a) Grinter, R.; Heilbronner, E.; Godfrey, M.; Murrell, J. N. *Tetrahedron Letters* **1961**, 21 771. (b) Grinter, R.; Heilbronner, E. *Helv. Chem. Acta* **1962**, 45 2496.
- <sup>xxiv</sup> (a) Heilbronner, E. *J. Chem. Phys.* **1955**, 23, 224. (b) Heilbronner, E. *J. Chem. Phys.* **1956**, 24, 115.

*Equilibria of Organic Reactions*; Wiley: New York, 1963.

<sup>xxv</sup> Saltiel, J.; Waller, A. S.; Sears, D. F. Jr. *J. Am. Chem. Soc.* **1993**, *115*, 2453.

<sup>xxvi</sup> Brown, H. C.; Okamoto, Y. *J. Am. Chem. Soc.* **1958**, *80*, 4979.

<sup>xxvii</sup> Dewar, M. J. S.; Landman, D. *J. Am. Chem. Soc.* **1977**, *99*, 7439.

<sup>xxviii</sup> Nakata, K.; Fujio, M.; Saeki, Y.; Mishima, M.; Tsuno, Y.; Nishimoto, K. *J. Phys. Org. Chem.* **1996**, *9*, 57.